The Organization of Corticostriatal Connectivity in the Human Brain

The Organization of Corticostriatal Connectivity in the Human Brain

A dissertation presented

by

Eun Young Choi

to

The Division of Medical Sciences

in partial fulfillment of the requirements

for the degree of

Doctor of Philosophy

in the subject of

Neurobiology

Harvard University

Cambridge, Massachusetts

July 2013

Dissertation Advisor: Dr. Randy L. Buckner Eun Young Choi

The Organization of Corticostriatal Connectivity in the Human Brain

Abstract

Neurological and psychiatric disorders reveal that the basal ganglia subserve diverse functional domains, including movement, reward, and cognitive disorders (e.g., Parkinson's disease, addiction, schizophrenia). Monkey anatomical studies show that the striatum, the input structure of the basal ganglia, receives projections from nearly the entire cerebral cortex with a broad topography of motor, limbic, and association zones. However, until recently, non-invasive methods have not been available to conduct the complete mapping of the cortex to the striatum in humans. The development of functional connectivity magnetic resonance imaging (fcMRI) now allows the identification of functional connections in humans. The present dissertation reports two studies that first create a complete map of corticostriatal connectivity and then more closely examine striatal connectivity with association networks underlying cognition.

In Study 1, we first demonstrated the ability of fcMRI to detect corticostriatal connections by correctly identifying the inverted somatotopy in the posterior putamen identified with monkey anatomy. We then created a comprehensive striatal parcellation based on connectivity with pre-defined cortical networks. A coarse parcellation map showed coupling to motor, limbic, and association networks with an organization consistent with monkey anatomy. A fine-grained parcellation revealed more complex connectivity patterns, the majority of which consist of converging connections from distributed regions of association networks.

In Study 2, we further explored striatal connectivity with association networks underlying hierarchical cognitive control. A comparison of brain activity during task performance with an

fcMRI map of cortical networks revealed the participation of distinct association networks at different levels of cognitive control, suggesting the hierarchical functional organization of these networks. fcMRI revealed a rostro-caudal connectivity gradient between the caudate and hierarchically organized regions of lateral frontal cortex. While our fcMRI results were inconclusive, this connectivity may support hierarchical interactions between association networks.

Together, these studies provide a reference for the complete functional map of human corticostriatal connectivity, revealing that a majority of the striatum is coupled to association networks, including those underlying high-level cognition. This knowledge of the detailed topography of human corticostriatal connectivity will be important for understanding the basal ganglia's normal function and dysfunction in a wide range of brain disorders.

Table of Contents

Acknowledgements

To my trusted advisor and mentor for taking me under his guidance, his unfailing standard of excellence, and his equally unfailing patience and belief in me: Randy L. Buckner.

To the director of my program, the Program in Neuroscience, for his constant watchfulness and top concern for my scientific development and well-being: Richard T. Born.

To the other directors of my programs who helped me make key decisions during my training: Gary Yellen and Rachel I. Wilson (Program in Neuroscience) and Constance L. Cepko (Leder Human Biology and Translational Medicine Program).

To the members of my preliminary examination (P), dissertation advisory (A), and dissertation defense (D) committees: Richard T. Born (chair for P, A, D), Lisa M. Shin (P, A), William A. Carlezon (A), Daniel L. Schacter (A), John H. R. Maunsell (P), Margaret S. Livingstone (D), Joshua W. Buckholtz (D), and Suzanne N. Haber (D).

To my rotation professors who welcomed me into their laboratories: Kwang-Soo Kim, William A. Carlezon, Margaret S. Livingstone, and John A. Assad.

To the numerous professors who taught my mind-broadening classes.

To my collaborator and mentor for his extraordinary patience and generosity: David Badre.

To senior colleagues for their training, collaboration, mentorship, and friendship: Avram J. Holmes, B. T. Thomas Yeo, Itamar Kahn, Paul A. Ardayfio, and Justin T. Baker.

To other members of my laboratory throughout the years for invaluable scientific discussion, technical assistance, and professional and personal support: Leah Bakst, Joan Camprodón, Angela Castellanos, Jingjing Jenny Chen, Garth Coombs, Susanna Crowell, Hamdi Eryilmaz, Trey Hedden, Marisa O. Hollinshead, Fenna M. Krienen, Jimmy Li, Hesheng Liu, Sophia Mueller, Jamie Parker, Abid Qureshi, Anna Rieckmann, Mert Sabuncu, Jorge Sepulcre, Rebecca Shafee, Amitai Shenhav, Tanveer Talukdar, Koene R. A. Van Dijk, Kristina M. Visscher, Daisy D. Wang; and in particular, Jessica R. Andrews-Hanna and Justin L. Vincent.

To colleagues in other laboratories for enlivening scientific discussion and technical assistance and training: Christopher H. Chatham, Allison T. Knoll, John W. Muschamp, Tracie A. Paine, R. Nathan Spreng, Andri C. Tziortzi, Alice Y. Wang, ChoongWan Woo, Arash Yazdanbakhsh, and numerous others.

To the Harvard Neuroinformatics Research Group (Gabriele Fariello, Timothy O'Keefe, Victor Petrov), Center for Brain Science's Neuroimaging Core (Tammy Moran, Stephanie A. McMains, Ross W. Mair, W. Caroline West), Harvard FAS Research Computing Group (Jeffrey Chang), and the Martinos Help Desk (Sam Mehl, Paul Raines, Jonathan Kaiser) for excellent technical support.

To outstanding administrative support: Donna Gadbois, Karen Harmin, and Virginia Conquest.

To my loving family: my parents, Tae Sun Choi and Jae Suk Choi, and my sisters, Eunsun M. Choi and Eunhye D. Choi.

To dear friends who have become like family over the years: Yu-Ming Liou, Nina Vujovíc, Soyon Hong, Herbert Z. Wu, Kuo-hua Huang, Irene S. Kim, Joya Mukerji, Dream Team Depression (Jesse Kang, Amanda Leung, Paul A. Ardayfio), Sachith Dunatunga, and Garrett K. Drayna.

To my parents, Jae Suk Choi and Tae Sun Choi,
who understand the meaning of a long-term project.

Chapter 1:

Introduction

Patients suffering from diseases or stroke-induced lesions of the basal ganglia have long been observed by clinicians to have a medley of motor, emotional, and cognitive dysfunctions of varying degrees depending on the location of the affected region. Animal tract-tracing and electrophysiological studies have found anatomical loops connecting nearly the entire cerebral cortex with the basal ganglia and the thalamus, thus identifying the connections underlying these behavioral symptoms. At the same time, animal histology has shown a high degree of intermixing between connections in all nuclei of the basal ganglia and thalamus, suggesting that one of their functions is to integrate information from across the cortex to form complex, multi-modal behaviors.

Due to the invasiveness of these techniques, our anatomical knowledge is based on animal studies, which have provided great insight into motor and limbic connectivity, but may be limited for the more expansive and complex human association cortex supporting cognition. The recent development of neuroimaging now allows the direct, non-invasive study of humans. One of these methods, functional connectivity magnetic resonance imaging (fcMRI), has been demonstrated to identify functional connections in the human brain. Thus, in the present dissertation, fcMRI was used to investigate the organization of human cortico-basal ganglia-thalamic loops at the level of the striatum, which is the input structure of the basal ganglia and receives projections from nearly the entire cerebral cortex. In the two studies presented here, we sought to first comprehensively identify the organization of human corticostriatal connections and then to more closely examine the striatum's connectivity with human association networks. This introduction provides a summary of striatal anatomy, focusing on corticostriatal connectivity, and a consideration of the utility and limitations of fcMRI in investigating these connections.

Anatomy of the Striatum

The basal ganglia (*Lt:* collection of cells) are a set of subcortical structures that reside above the brainstem at the base of each cortical hemisphere. The basal ganglia consist of the striatum, pallidum (globus pallidus and ventral pallidum), substantia nigra in the brainstem, and the subthalamic nucleus. In monkeys, the basal ganglia receive topographic input from all cortical regions (with the exception of primary visual cortex), as well as subcortical regions including the thalamus, amygdala, hippocampus, and brainstem. The basal ganglia send output primarily to the thalamus, from which connections return to the cerebral cortex and brainstem. The functions of these connections are not completely understood, but it appears that the basal ganglia receive association, motor, and limbic information, integrate this information to form associations between features, actions, and outcomes, and then send out the integrated information to influence neural processing or trigger actions (Haber et al. 2011).

The striatum (*Lt:* striped, named for its striped appearance due to passing fibers) is the main input structure of the basal ganglia. The striatum is composed of three nuclei: the caudate (*Lt:* tail), putamen (*Lt:* husk), nucleus accumbens (short for *nucleus accumbens septi*, *Lt:* nucleus against wall), and the olfactory tubercle. The caudate and putamen are longitudinal structures lying in parallel to one another with the caudate located medially to the putamen. The caudate is C-shaped, following the curvature of the third ventricle, and is divided into a rostrally-located head, body, and caudally-located tail, which tapers and curves ventrally to below the putamen and then rostrally to form the bottom portion of the C-shape. The nucleus accumbens and olfactory tubercle, located below the caudate and putamen, span the rostral half of the striatum, ending approximately where the anterior commissure intercepts the striatum. The caudate and

putamen are almost completely separated by the internal capsule, a large white matter bundle, with the exception of cell bridges connecting the two sides. In lower animals, there is little to no separation of the caudate and putamen by the internal capsule. Hence, it is thought that the caudate and putamen were originally one complex and separated by the internal capsule over evolution (Haber et al. 2011).

The vast majority of neurons in the striatum are medium spiny projection neurons expressing GABA as their neurotransmitter. Nonetheless, the striatum has a heterogeneous cytoarchitecture revealed by stains of various substances. The dorsal striatum has clusters (called patches or striosomes) of neurons initially identified as acetylcholinesterase-poor regions in a matrix of acetylcholinesterase-rich neurons (Graybiel and Ragsdale 1978). Subsequent work has shown that these clusters also express a variety of other substances, such as dopamine receptors, opioid receptors, substance P, enkephalin, and calbindin (Graybiel 1990; Holt et al. 1997). The ventral striatum has a more complex organization without clear cluster boundaries and consistent correspondence in the expression patterns of various substances (Holt et al. 1997). The functional significance of this highly fractionated cytoarchitecture is not fully understood, but it may be related to the formation of integrated behaviors.

Corticostriatal Connectivity

The striatum, the main input structure of the basal ganglia, receives the vast majority of its inputs from the cerebral cortex, substantial inputs from the thalamus, and fewest inputs from the amygdala, piriform cortex, hippocampus, and brainstem (Haber et al. 2011). As the largest structure of the basal ganglia and the entry point for nearly all connections to the basal ganglia,

the striatum is ideal for comprehensively identifying cortico-basal ganglia-thalamic circuits. This section describes the development of our understanding of corticostriatal connectivity—an example of how technical advancement furthers scientific understanding.

The striatum as a motor structure

The striatum was originally thought to be a motor structure for several reasons. Due to its location between the brainstem and the cerebral cortex, very early theories surmised that the basal ganglia were a link between these two structures (Ferrier 1876). Its role in motor function was confirmed by animal studies in which lesion of the striatum caused contralateral paralysis and electrical stimulation lead to strong contralateral flexions of the body (Ferrier 1876). Furthermore, patients with congenital Wilson's disease, first described by Wilson (1912), showed "softening" primarily of the putamen and concurrent involuntary movements, extreme muscle flexion and stiffness, and tremor (along with an unexplained liver cirrhosis). More recent studies have used neuroimaging to identify the precise location of lesions and their accompanying effects (Bhatia and Marsden 1994). They have shown that putamen lesions lead almost always to movement disorders, most commonly dystonia, which is a condition in which the muscles are constantly flexed and cause twisting and repetitive movements or abnormal postures. In addition, Parkinson's and Huntington's disease, which have strong motor symptoms, arise from the degeneration of neurons in the substantia nigra pars compacta, a region that projects to the striatum, and in the striatum, respectively (Ehringer and Hornykiewicz 1960; Graveland et al. 1985).

The development of fiber degeneration tract tracing techniques allowed connections to be specifically identified. In this method, a lesion is placed in a region of interest, which causes the

degeneration of emanating axons. The cellular debris from the degeneration can be detected by various staining methods with varying degrees of sensitivity. In one of the first studies using the Marchi technique using osmium tetroxide, Wilson (1914) concluded that there was no cortical input to the striatum and that degeneration stained in the striatum was from fibers of passage. However, development of the Nauta technique using silver staining provided more sensitive detection, which allowed Glees (1944) to identify sensorimotor cortical input to the striatum in cats. Together, connectivity and striatal disruption studies provided evidence that the striatum is a motor structure.

The striatum receives widespread cortical input

Despite the view that the striatum is a motor structure, there were hints from patient cases that the striatum's function extends to other domains. Lesions of the caudate commonly lead to cognitive and emotional dysfunctions (Bhatia and Marsden 1994; Mendez et al. 1989). Cognitive and affective symptoms have been reported in patients with Parkinson's and Huntington's disease (Caine and Shoulson 1983; Raskin et al. 1990). Patients described by Wilson (1912) had, in addition to pronounced motor dysfunctions, progressive mental and emotional abnormalities, including childishness, proneness to laughter or annoyance, indecisiveness, and paranoia. The neuropsychiatric symptoms reported in striatal lesion cases are reminiscent of patient cases with lesions of the frontal lobe (Cummings 1993; Mesulam 1986), such as the famous case of Phineas Gage, who, upon the accidental destruction of his left dorsolateral prefrontal cortex, transformed from being rational and highly functioning to impulsive, irresponsible, and profane (Damasio et al. 1994). The similarity of symptoms due to striatal and frontal lesions suggested that the striatum has connections to association and limbic cortex, as well as motor cortex.

The more sensitive Nauta technique allowed for the detection of widespread cortical inputs to the striatum. Nauta and Whitlock (1956) identified inputs from the temporal cortex, identifying non-motor projections for the first time. A set of studies by Webster (1961, 1965) revealed that the striatum receives input from widespread areas of cortex in rats and cats. He further described an anterior-posterior and medial-lateral organization of the projections, the first description of the functional architecture of the striatum. These were followed by studies in monkeys that identified connections from the prefrontal cortex to the striatum (DeVito and Smith 1964; Johnson et al. 1968). The results from this approach culminated in an influential paper by Kemp and Powell (1970), who conducted a comprehensive study of cortical injections in monkeys. Based on their results, they proposed an influential model in which the cortex generally projects to the nearest striatal region along the rostro-caudal axis. Specifically, they found that frontal cortex projects to the rostral striatum, parietal and temporal cortex to ventral striatum, and occipital cortex to caudal striatum. This work, along with the finding that the basal ganglia projects to motor nuclei of the thalamus (Nauta and Mehler 1966), served as the basis for the funneling hypothesis proposed by Kemp and Powell (1971; Fig. 1.1*A*), modeled after the funneling hypothesis of the cerebellum (Evarts and Thach 1969). In this model, the basal ganglia receives widespread cortical input that is funneled into gradually smaller regions of the basal ganglia and the thalamus, which then send the output to motor structures to enact movement (Kemp and Powell 1971).

Cortical input to the striatum is longitudinal

The advent of autoradiography and horseradish peroxidase (HRP) tract tracing techniques revealed new details of corticostriatal connectivity that altered our understanding of the striatum.

This method injects radiolabeled amino acids or horseradish peroxidase (HRP) into the region of interest and provides increased specificity and detail in target regions over the fiber degeneration methods. Künzle (1975, 1977) was the first to use autoradiography to map the connections from the cortex to the striatum in monkeys. He discovered that the somatotopy of the motor cortex was preserved in the caudal putamen with an inverted topography (Künzle 1975). He also described for the first time that cortical projections terminate longitudinally (rostral to caudal) through the putamen, not solely to the nearest striatal region to the motor cortex (Künzle 1975). Goldman and Nauta (1977) also reported that projections from prefrontal cortex were longitudinal through the extent of the caudate. In a landmark paper, Selemon and Goldman-Rakic (1985) conducted a comprehensive study of cortical regions throughout association cortex. They found that association projections throughout the cortex terminate longitudinally in the striatum and that it is largely their medial-lateral topography that distinguishes them (Fig. 1.1*B*).

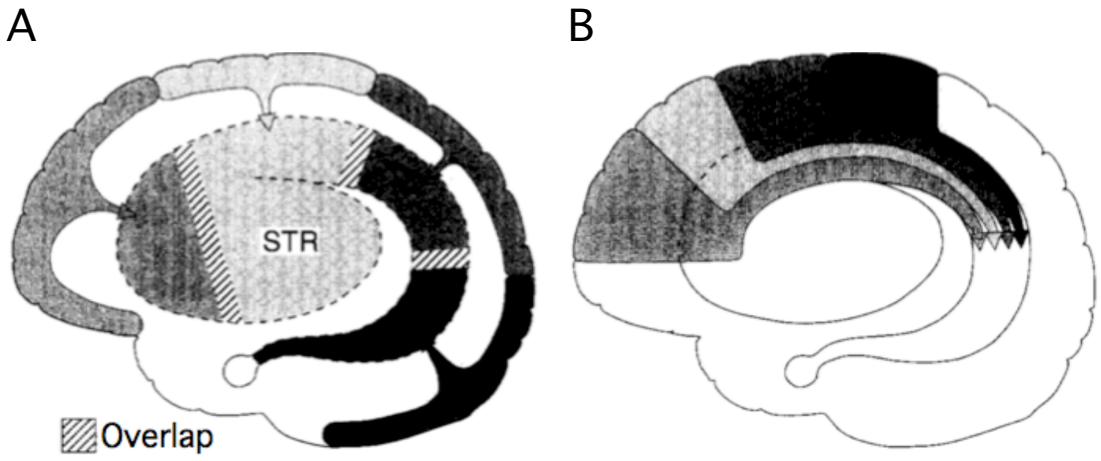

Figure 1.1 Two models of corticostriatal connectivity. (A) Based on lesion degeneration tract-tracing, cortical projections were thought to land in the nearest striatal region (Kemp and Powell 1970). (B) Autoradiography and horseradish peroxidase tract-tracing methods showing finer details revealed that cortical projections land longitudinally through the rostro-caudal extent of the striatum (Selemon and Goldman-Rakic 1985). STR: striatum. Figure modified from Parent and Hazrati (1995) with permission from Elsevier.

Heterogeneous patterning of input to the striatum

In addition to the longitudinal characteristic of cortical projections, Künzle (1975) and Goldman and Nauta (1977) noted a striking circular or elliptical patterning of the inputs to the striatum, reminiscent of the histologically defined striosomes described by Ragsdale, Graybiel, and others. Subsequent work has demonstrated that striosomes preferentially receive limbic input while the matrix preferentially receives sensorimotor and associative input (Gerfen 1984, 1992; see Crittenden and Graybiel 2011). Further work beyond the scope of neuroimaging is needed to understand the functional significance of this compartmentalization.

Functional map of corticostriatal projections

Further tract-tracing studies revealed greater details in the map of cortical projections in the striatum. In addition to the inverted somatotopy of motor cortical projections in the caudal putamen (Flaherty and Graybiel 1991; Künzle 1975), a second inverted somatotopy from the supplementary motor area was found more medially in the caudal putamen (Inase et al. 1996; Takada et al. 1998a). The body and tail of the caudate are dominated by association projections (Calzavara et al. 2007; Cavada and Goldman-Rakic 1991; Haber et al. 2006; Selemon and Goldman-Rakic 1985; Weber and Yin 1984; Yeterian and Pandya 1991). The rostral striatum has a markedly different pattern, with projections often spanning across the internal capsule into both the caudate and putamen, further supporting the idea that the caudate and putamen were originally one structure in evolution. The dorsolateral striatum receives projections from the frontal and supplementary eye fields (Calzavara et al. 2007; Parthasarathy et al. 1992; Stanton et al. 1988; Yeterian and Pandya 1991). The ventromedial striatum receives projections from the orbitofrontal cortex, piriform cortex, hippocampus, and amygdala (Ferry et al. 2000; Fudge et al.

2002, 2004; Haber et al. 1990; Heimer and Wilson 1975; Russchen et al. 1985; Yeterian and Pandya 1991). The territory in between the motor and limbic territories receives association projections (Calzavara et al. 2007; Cavada and Goldman-Rakic 1991; Haber et al. 2006; Selemon and Goldman-Rakic 1985; Weber and Yin 1984; Yeterian and Pandya 1991, 1993). Together, these projections have lead to the heuristic model of striatal functional connectivity as having a motor to association to limbic gradient of functional territories (Haber 2003; Parent 1990; Fig. 1.2), organized on a dorsolateral to ventromedial axis (Voorn et al. 2004).

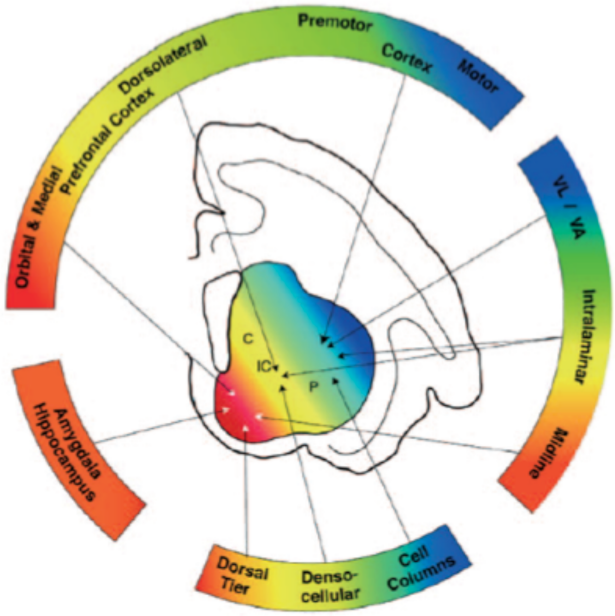

Figure 1.2 Heuristic model of striatal functional topography. Monkey tract-tracing studies reveal a general topography of cortical and subcortical connections, leading to the formation of this heuristic model consisting of a dorsolateral motor territory, a central association territory, and a ventromedial limbic territory. Tract-tracing results show additional details, such as the compartmentalization of connections and the presence of diffuse projections that cut across functional territories (Haber et al. 2006). C: caudate. P: putamen. IC: internal capsule. Adapted from Haber and Gdowski (2004) with permission from Elsevier.

Organization of association projections to the striatum

In a study to find organizational principles of corticostriatal projections, Yeterian and Van Hoesen (1978) discovered that reciprocally connected cortical regions (shown by prior studies) project to at least one common region in the striatum. Based on these results, Yeterian and Van Hoesen (1978) suggested the principle that interconnected cortical regions also share connections to the same regions in the striatum, much like a subcortical node of the network. Selemon and Goldman-Rakic (1985) further refined our knowledge by using double-labeling cases in which two cortical regions are injected within the same monkey to directly observe the relative organization of projections. They found that interconnected cortical regions may project to similar striatal regions, but the projections are interdigitated or intermixed and do not typically appear to overlap onto the same striatal neurons. Nonetheless, these projections may exert influence on the same milieu of neurons via interneurons.

The striatum participates in cortico-basal ganglia-thalamic circuits

Downstream of the striatum, there are connections with other basal ganglia structures that are critical to the functions of the basal ganglia. As striatal projection neurons are GABAergic, the striatum has an inhibitory effect on its targets, most notably the pallidum and substantia nigra. Briefly, striatal outputs to the pallidum and substantia nigra can be described by the model of direct and indirect pathways. The direct pathway consists of striatal inhibitory outputs to the internal segment of the globus pallidus (GPi) and the substantia nigra pars reticulata, which in turn reverse their tonic inhibition of the thalamus, which then send excitatory inputs to the cerebral cortex and brainstem. The indirect pathway consists of striatal inhibitory outputs to the external segment of the globus pallidus (GPe), which reverses its tonic inhibitory signal on the

GPi, thus allowing GPi to impose greater inhibition on the thalamus and reduce the chances of sending excitatory signals to thalamic targets. Thus, one model and popular heuristic of basal ganglia circuitry is that the direct and indirect pathways control the magnitude of the output of the basal ganglia (Albin et al. 1989; DeLong 1990). Others have also suggested that the direct pathway selects for the proper action while the indirect pathway inhibits improper actions (Mink 1996; Penney and Young 1983).

Parallel and integrated cortico-basal ganglia-thalamic circuits

The basal ganglia circuitry described above was first identified with the connections from the sensorimotor cortex. However, Heimer and Wilson (1975) reported the discovery of a limbic circuit with projections from the piriform cortex to the ventral striatum, and then to the ventral pallidum. Heimer (1978) later suggested that the ventral pallidum projects to the medial dorsal nucleus of the thalamus, which sends outputs to the prefrontal cortex. These discoveries suggested that there are multiple, potentially non-motor basal ganglia circuits in addition to the classic motor circuit. Similarly, DeLong and Georgopoulos (1981) suggested that there are segregated association and motor circuits based on tract-tracing studies showing the continued segregation of association and motor information in the globus pallidus and thalamus (Carpenter et al. 1976; Kim et al. 1976; Szabo 1962, 1967, 1970). In addition, electrophysiological recordings in the globus pallidus showed the preservation of the inverted somatotopy originating from the sensorimotor cortex (Alexander and DeLong 1985). These results lead to what has become the prevailing model of the basal ganglia, the segregated, parallel circuits model (Alexander et al. 1986; 1990; Fig. 1.3). Based on the maintained topography of connections through the basal ganglia, Alexander and colleagues suggested that there are at least five

segregated circuits, each consisting of a direct and an indirect pathway (DeLong 1990), that differ in functionality, but have a parallel organization of connections. Later, using trans-synaptic rabies viral tracers, Strick and colleagues confirmed the presence of distinct association and motor circuits (Kelly and Strick 2004; Middleton and Strick 1994, 2000, 2002).

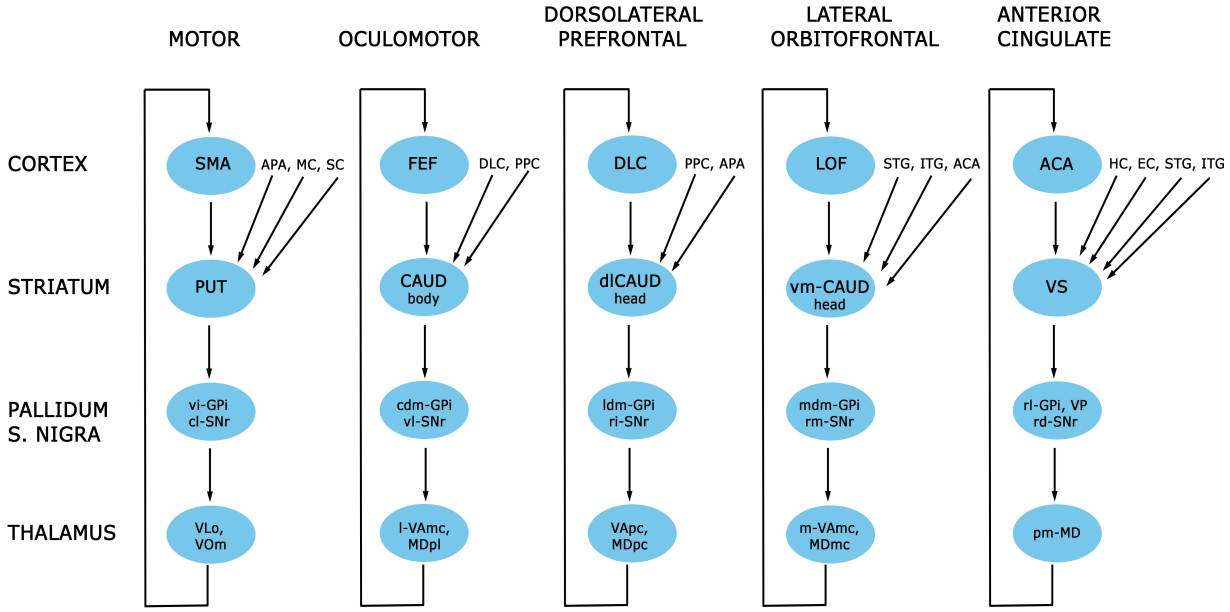

Figure 1.3 Parallel circuits model of the basal ganglia. Monkey tract-tracing studies suggest the presence of at least five distinct functional circuits with parallel connectivity, but involving separate regions of the cerebral cortex, basal ganglia, and thalamus. Each circuit also consists of thalamic projections to other cortical regions, forming open loops that provide a subcortical mechanism by which cortical regions can influence one another. Interaction between the circuits occurs through additional connections and integration at each level, not shown here. Adapted from Alexander et al. (1986) with permission from Annual Reviews, Inc.

While there is a distinct segregation of functional information, there is also evidence that integration occurs between the circuits, which would allow for the integrated behavior attributed to the basal ganglia. Integration between circuits may occur at each structure in the circuit by overlap between functional territories (Haber 2003). For example, Haber et al. (2006) showed that corticostriatal inputs from the frontal cortex have large territories of diffuse projections that

are much more extensive than their focal projections and that overlap one another. Chevalier and Deniau (1990) also suggested that while a general topography exists in the globus pallidus, the dendrites of pallidal neurons are long enough to receive inputs from multiple striatal functional outputs, thereby allowing for integration across functional domains. Integration may also occur by additional pathways from other structures. McFarland and Haber (2002) discovered that there are non-reciprocal as well as reciprocal corticothalamic connections. Haber et al. (2000) also discovered a set of spiraling pathways between the striatum and the substantia nigra pars compacta that suggest a flow of information from the ventral striatum to association striatum to motor striatum. In short, a combination of parallel and integrated circuits likely exists, which may give rise to the complex behaviors supported by the basal ganglia.

Neuroimaging of Human Corticostriatal Connectivity

Animal studies have taken us far in understanding the functional organization of the striatum. However, the question remains as to what the striatal functional organization is in humans, particularly for the association cortex, which is greatly expanded between humans and monkeys (Hill et al. 2010). The corticostriatal connectivity described above was obtained using invasive techniques in animals like tract-tracing and electrophysiology that cannot be done in humans. However, the advent of neuroimaging has made it possible to investigate human brain functions with tolerable risks.

Positron emission tomography (PET), which detects and localizes the decay of injected radiolabeled contrast agents, was the first neuroimaging method to be developed for brain research and provided the first demonstrations that neuroimaging can be used to localize human

brain functions (Fox et al. 1986; Fox et al. 1987). However, the invasiveness of the radiolabeled contrast agents in subjects limited its widespread use in research. In contrast, magnetic resonance imaging (MRI) can avoid invasive procedures by electromagnetically exciting the protons of water molecules abundantly present in tissue and measuring their energy emissions during relaxation (Lauterbur 1973). This property became the basis for the two methods available now to measure connectivity in humans: functional connectivity MRI (fcMRI), an off-shoot of functional MRI (fMRI), and diffusion MRI (dMRI). Since fcMRI is the tool used in the present studies, it will be discussed at greater length in the next section. The rest of this section will discuss dMRI in greater detail and its identification of human corticostriatal connectivity for the first time.

Diffusion magnetic resonance imaging

Experimental measurements of the diffusion coefficients of glycerol molecules with a diffusion sensitive MR sequence were first reported by Stejskal and Tanner in 1965. The idea of applying dMRI to spatially map living tissue was not conceived until nearly 20 years later by Le Bihan and others (Le Bihan and Breton 1985; Merboldt et al. 1985; Taylor and Bushell 1985). The method is based on the principle that a group of freely diffusing water molecules is on average displaced by the same amount in all directions (diffusion isotropy; Jones 2008). During imaging, the evenly distributed displacement of water molecules results in spin decoherence of their protons, leading to a decrease in MR signal (Jones 2008). Any obstructions in the free diffusion of the water molecules, like a cell membrane, lead to a greater displacement in certain directions, such as along the direction of an axon, and an increase in MR signal (Jones 2008). The early dMRI images were single diffusion-weighted images distinguishing white and gray

matter (Le Bihan and Breton 1985). The application of dMRI for tractography, called diffusion tensor imaging (DTI; Basser et al. 1994), was later developed based on the observation of diffusion anisotropy, or the dependence of the MR signal on the direction of the magnetic gradient during imaging (Moseley et al. 1990). In DTI, an object is imaged typically six times to probe by how much water molecules diffuse in six directions for each voxel. Measuring increased diffusion in a particular direction would indicate the presence of a white matter tract along that direction. This improved directional information thus allows white matter fibers to be traced in either a single pathway (deterministic tractography) or multiple pathways (probabilistic tractography) between a seed and a target region (Jones 2008).

The first mapping of corticostriatal connections in humans was shown using DTI (Lehéricy et al. 2004). Using large cortical seed regions covering the entire motor, premotor, prefrontal, or orbitofrontal cortex (which connected to the posterior putamen, posterior putamen, most of the anterior striatum, or ventral striatum, respectively), Lehéricy et al. for the first time showed distinct functional corticostriatal connections in humans, which agreed with monkey tract-tracing results. A reciprocal analysis using seed regions in the striatum showed a mixture of corticostriatal connections that was plausible based on monkey tract-tracing results. For example, a portion of the posterior putamen was connected at varying degrees amongst individual subjects to the ipsilateral supplementary motor area (SMA), and premotor, motor, and sensory cortices. A portion of the dorsal border of the anterior striatum, spanning the internal capsule and adjacent regions of putamen and caudate, was connected across all subjects to regions of the dorsal premotor cortex (Brodmann areas [BA] 8 and 6 and pre-SMA) and lateral prefrontal cortex (BA 9, 10, 45, 46, and 47), which have been seen in monkey tract-tracing studies (Parthasarathy et al. 1992; Selemon and Goldman-Rakic 1985). Leh et al. (2007) next examined corticostriatal

connections between the frontal cortex in greater detail. In addition to results agreeing with monkey anatomy using whole caudate and putamen seed regions, they conducted the first parcellation of the striatum, dividing the caudate based on differential connectivity to the dorsolateral prefrontal cortex and the ventrolateral prefrontal cortex and the putamen based on differential connectivity to the premotor cortex, motor cortex, and SMA. These results, too, were consistent with monkey tract-tracing. Draganski et al. (2008) provided the first comprehensive map of the striatum based on connectivity between the whole cerebral cortex to the whole striatum using probabilistic DTI to identify multiple cortical targets of a single striatal region. This analysis, which has similarities to our striatal parcellation approach in Study 1, color-coded each striatal voxel based on its connectivity profile to 23 cortical regions. The result was a striatal map showing a rostral-to-caudal gradient of connectivity from the medial and orbital prefrontal cortex to the dorsolateral frontal cortex and finally to the motor cortex. This study, like prior studies, agreed broadly with monkey tract-tracing.

Altogether, these dMRI studies provided the first evidence of human corticostriatal anatomical connections and showed that they have similar broad organizational patterns as those in the monkey, thereby allowing our theories of the basal ganglia based on animal work to be generally valid for humans. Subsequent dMRI studies have corroborated and elaborated upon these basic findings in the context of personality traits, striatal neurodegenerative disease, and aging (e.g., Cohen et al. 2009; Bohanna et al. 2011; Marrakchi-Kacem et al. 2013; Ystad et al. 2011). However, these original studies have a few important limitations. Firstly, their results do not show the longitudinal projections observed in monkey anatomy (Künzle 1975; Goldman and Nauta 1977). Instead, Draganski et al. (2008) and, later, Verstynen et al. (2012) show a rostral-to-caudal parallel correspondence in connections between the cortex and striatum, consistent

with the Kemp and Powell (1970) model of point-to-point connectivity. This seemingly discrepant finding, however, is not inconsistent with monkey tract-tracing results, which do show a general tendency for cortical regions to project most strongly to their nearest striatal regions (explaining why this organization was detected by Kemp and Powell with the less sensitive silver degeneration tract-tracing technique). But this point-to-point tendency exists within an overall longitudinal progression of connections through the striatum. These details may have been lost in the DTI studies due to the low sensitivity of the technique or thresholding over non-specific connections.

Secondly, these studies used large, discrete cortical seed regions that span across multiple Brodmann areas. Monkey anatomy shows that a given region of striatum has a high degree of heterogeneity, with inputs from multiple cortical regions located within the extent of these cortical seed regions. This is an issue that Draganski et al. (2008) began to address by using probabilistic DTI to identify multiple cortical targets from a given striatal region; however, they also used large cortical seed regions that reduce specificity. Both the need for identifying specific converging cortical inputs and observing longitudinal corticostriatal connections are addressed by studies using fcMRI, as described further below.

Functional Connectivity Magnetic Resonance Imaging

Like PET, contrast agents were initially used in fMRI to observe functional changes in the brain (Belliveau et al. 1991). However, the discovery of an endogenous contrast agent, deoxyhemoglobin (Ogawa et al. 1990b), allowed fMRI to be non-invasive and subsequently to become the dominant means of investigating human brain functions. As fMRI was explored and

analysis methods were developed, the serendipitous discovery of fcMRI, an analysis of a limited portion of the fMRI signal, provided a way to estimate functional connections in the human brain. The following section describes the basis for fcMRI, its strengths and limitations, and the insights it has provided into human corticostriatal connectivity.

The development of functional magnetic resonance imaging

Understanding fcMRI requires an understanding of the signal measured by fMRI. The fMRI signal is based on the phenomenon that protons radiate energy after excitation, a process that is sensitive to their immediate magnetic fields. Changes to the local magnetic fields affect how in-phase or out-of-phase a collection of excited spins of protons is, leading to an increase or decrease, respectively, in the overall energy radiated. In fMRI, the protons, primarily from water molecules, are initially polarized along a global magnetic field (provided by the magnet) and the changes in the local magnetic fields around protons are dependent on the concentration of deoxyhemoglobin (Ogawa et al. 1990b), a paramagnetic molecule (Pauling and Coryell 1936). Although neural activity recruits oxygen from hemoglobin, initially increasing the local concentration of deoxyhemoglobin (Ogawa et al. 1990b), vasodilation also occurs, bringing oxygenated blood into the area a few seconds later (Fox et al. 1986). This leads counterintuitively to a *decrease* in deoxyhemoglobin concentration and an *increase* in the fMRI signal (Bandettini et al. 1992; Kwong et al. 1992; Ogawa et al. 1992). Thus fMRI images show local increases in the fMRI signal to indirectly indicate neural activity. Much of the putative mechanism underlying the fMRI signal was determined by Ogawa and colleagues, who conducted the experiments showing that deoxyhemoglobin is the source of the image contrast in fMRI (Ogawa et al. 1990b), which they called the blood oxygenation level-dependent (BOLD)

contrast (Ogawa et al. 1990a).

These papers were followed a few years later by the first demonstrations of the ability of fMRI to map brain regions to function. Kwong et al. (1992) and Ogawa et al. (1992) independently showed that fMRI activity in the visual cortex was temporally correlated with visual stimulus onset and further mapped the retinotopy of visual cortex. Kwong et al. also showed that the MR signal was maximal when the visual stimulus (a checkerboard) flickered at 8 Hz, which has been shown by monkey electrophysiology studies to be the tuning frequency of primary visual cortex neurons. Bandettini et al. (1992) showed similar results for the somatomotor cortex. Thus it was demonstrated that the BOLD signal measured by fMRI could be used to localize functional activity in the human brain.

The discovery of functional connectivity magnetic resonance imaging

As the nature of the BOLD signal was investigated, it was found that in addition to task-evoked BOLD activity, there was also non-task-related oscillating activity present during both task performance and at rest, a state of no explicit task performance, which were presciently suggested by Ogawa and colleagues to be a possible means of mapping functional connections (Ogawa et al. 1993). Some of these oscillations in the BOLD signal were found to correlate with physiological rhythms, such as heart rate and respiration (Golanov et al. 1994). However, there was also seemingly spontaneous activity of an unknown source occurring at frequencies less than 0.1 Hz (Golanov et al. 1994) that persists during tasks, rest, sleep, and anesthesia (Fox and Raichle 2007). These spontaneous BOLD fluctuations were initially thought of as noise, but a seminal study by Biswal and colleagues demonstrated that they could identify the regions of the motor network by the temporal correlations of their spontaneous BOLD activity (Biswal et al.

1995). This unexpected discovery, while not a measure of direct connectivity like the tract tracers used in animals, offered a means by which functionally coupled regions connected by polysynaptic connections could be detected in the human brain. It was followed by the identification of other known systems, such as the visual network in monkeys (Vincent et al. 2007) and the hippocampal-parietal memory system in humans (Vincent et al. 2006), as well as exploration of less known systems, such as the default network (Greicius et al. 2003).

Strengths and limitations of fcMRI

The strength of fcMRI is its ability to detect functional connections across the whole human brain quickly, non-invasively, and in a non-demanding manner for subjects. As such, it has come to be used widely, leading to several new discoveries about the organization of the human brain. For example, the frontoparietal control network, thought to underlie executive functions, was discovered as a network (Vincent et al. 2008). The comprehensive identification of functional networks and their relative organization was also greatly accelerated, providing insight into the organization of the expanded human association cortex (Lee et al. 2012; Power et al. 2011; Yeo et al. 2011). In addition, the dysfunction of the frontoparietal control network in schizophrenia was recognized from a large patient cohort (Baker et al. in press).

The major limitation of fcMRI is the ambiguity in what it is detecting. On the one hand, it is clear that it reflects anatomical connections. fcMRI has detected somatotopies in the somatomotor cortex (Buckner et al. 2011), cerebellum (primary, secondary, and a previously unknown tertiary map; Buckner et al. 2011), and the putamen of the striatum (Choi et al. 2012) identified from monkey studies (Adrian 1943; Künzle 1975; Kelly and Strick 2003). A telling study by Krienen and Buckner (2009) showed the detection of disynaptic cortico-pontine-

cerebellar tracts identified from monkey polysynaptic rabies tracer experiments (Kelly and Strick 2004) that connect the motor cortex to the contralateral cerebellum, crossing at the pontine nucleus of the brainstem. Critically, lesion of the pontine nucleus was found to disrupt the functional connectivity between the cortex and contralateral cerebellum (Lu et al. 2011). Another lesion study showed that corpus callosotomy leads to the disruption of homotopic functional coupling between the left and right hemispheres (Johnston et al. 2008). A test of the upper range of specificity showed that fcMRI distinguishes between caudal V1 and ventral MT+ and between rostral V1 and dorsal MT+, which process information about the central and peripheral visual fields, respectively (Yeo et al. 2011). In addition, Yeo et al. (2011) demonstrated that the strength of the fcMRI correlation appears to reflect functional distance. In one of their analyses, they showed that the correlation strengths between regions of the dorsal "where" pathway (V1, MT+, LIP) and FEF placed these regions in a hierarchy that agreed with the well-characterized hierarchical organization identified in monkeys. Thus while all regions are correlated with one another, the correlation strength between two regions indicates their relative distance in this hierarchy. This example shows how fcMRI detects functional interactions arising from connections.

On the other hand, fcMRI has also given results that range from surprising but plausible to unsettling. Spontaneous BOLD fluctuations have been shown to vary across individuals (Mueller et al. 2013) and even within an individual depending on prior task performance (Stevens et al. 2010), current task performance (Shirer et al. 2012; Yeo and Krienen, unpublished data), mood (Harrison et al. 2008), state of wakefulness (Larson-Prior et al. 2011), and age (Andrews-Hanna et al. 2007); anatomy is a constant in comparison. In a particularly relevant example for the present studies, Yeo and colleagues observed that subjects performing a

semantic word classification task had an expanded frontoparietal control network as measured by fcMRI of data taken during task performance (Buckner et al. 2013). They found similar task-weighted shifts in the cortical parcellation using a comprehensive set of tasks, including visual, motor, auditory, and autobiographical tasks that recruit other networks (Krienen et al., unpublished observations).

Fortunately, there is one partial countermeasure to this issue, perhaps a reflection of the anatomical connections underlying functional activity. fcMRI provides remarkably stable and consistent results when averaging across subjects, which minimizes inter-subject differences and the random transient functional activity across subjects. As the number of subjects increases in a group mean fcMRI map, the correlation patterns change from being raggedy to very smooth and highly replicable. At rest, reliable and replicable results are obtained when averaging across roughly 30 subjects or more (personal observation). A decided example of the reliability of group mean data is seen in the trio of papers using fcMRI to comprehensively parcellate the cerebral cortex (Yeo et al. 2011), the cerebellum (Buckner et al. 2011), and, as will be described in Study 1, the striatum (Choi et al. 2012). In each of these studies, parcellations from two independent sets of 500 subjects each had a high percentage of agreement (cortex: 97.4%; striatum: 90.2% for the 7-network parcellation). Krienen and colleagues have also shown that cortical parcellations resembling the 1,000-subject cortical parcellations can be obtained from groups with as few as 14 subjects (Krienen et al., unpublished observation). Thus, we can obtain reliable, highly replicable results using fcMRI by averaging across multiple subjects, although more subjects may be necessary if the functional heterogeneity across subjects is greater (e.g., engaging in different tasks).

Thus it appears that fcMRI's sensitivity to functional interactions allows the

identification of functional connections in humans, but is also in a way too sensitive by detecting transient functional states. Therefore, perhaps the way to view fcMRI is that it is a powerful tool for comprehensively identifying functional interactions, which are made possible by anatomical connections, but requiring caution and awareness of the functional state of the subject. Buckner et al. (2013) conclude that "fcMRI is best used as a tool for generating hypotheses about brain organization that will require further study with external methods."

fcMRI also suffers from certain limitations shared by all fMRI methods. While the temporal lag in the hemodynamic response is not an issue, spatial resolution is particularly significant for a small structure like the striatum. In the present studies, fMRI data were acquired in 3 mm voxels using a 3 Tesla scanner. The spatial resolution is further diminished by the imperfect normalization of individual subject brains to standard atlas space, as well as the application of Gaussian smoothing (full width at half maximum = 6 mm) to boost the signal to noise ratio. Thus, we are not capable of observing the microarchitecture described above that is so striking about the striatum, nor the tail of the caudate, which nearly all fMRI studies leave unexamined. Gaussian smoothing and partial volume averaging (the splitting up of a signal source into multiple voxels) also confound whether overlap in correlations, for example at the boundaries of the parcellation networks shown in Study 1, are truly due to biological overlap or a blending of signals from adjacent sources, a major confound in both of the present studies. As an imaging method, fcMRI is sensitive to head motion and physiological rhythms. As a method measuring BOLD contrast, it is important to keep the vasculature in mind (Blinder et al. 2013). Finally, as a correlational method, we are unable to determine directionality between correlated regions.

In short, the strengths of fcMRI come from non-invasively providing a comprehensive

snapshot of the brain's functional connections, allowing for the study of large-scale organizational patterns in humans. However, fcMRI's sensitivity to functional interactions is a double-edged sword and requires consideration of the subject's functional state. These caveats given, the rest of this section discusses the results provided by fcMRI regarding human corticostriatal connectivity.

Insights into human corticostriatal connectivity using fcMRI

The earlier section on dMRI reported the broad agreement of the human dMRI corticostriatal connectivity with monkey tract-tracing results, but with the limitation that large, discrete cortical regions were used in their analyses, hindering the detection of specific converging cortical inputs, and the caveat that the studies did not report longitudinal connections through the striatum. fcMRI provides an alternate method of assessing functional connectivity that provides complementary information addressing these issues. Two fcMRI studies have provided our prior basic knowledge of the corticostriatal functional connections in humans. Di Martino et al. (2008) were the first to use fcMRI to demonstrate the functional connections from select regions of the striatum to the whole cerebral cortex. Using seed regions determined from a meta-analysis of fMRI and PET studies with striatal activation (Postuma and Dagher 2006), Di Martino et al. showed three distinct cortical fcMRI maps with correlations in the orbitofrontal cortex from anterior ventral striatal seed regions; the medial frontal, posterior cingulate, and parietal cortices from an anterior dorsal caudate seed region; and the dorsal cingulate cortex, premotor cortex, and temporoparietal junction from putamen seed regions. Barnes et al. (2010) converged on a similar three maps from a more comprehensive approach. They created a parcellation of the striatum by clustering striatal voxels into three divisions according to their

whole brain correlation patterns—an approach similar to ours in Study 1, but with key differences (see Study 1 for further discussion). As with dMRI, a number of other studies examining the effects of various conditions, like psychiatric diseases (Harrison et al. 2009; Tu et al. 2011), age (Ystad et al. 2011), and drug applications (Kelly et al. 2009), have corroborated these three general corticostriatal fcMRI maps.

Several clear issues here are a need to move beyond three generalized corticostriatal maps, to explore the resolution limits of the technique in the striatum, and to gain a more detailed mapping of corticostriatal connectivity. These issues are directly addressed by the first study. There is also another pressing issue here, the need for a rigorous comparison of the fcMRI results with anatomy. In contrast to the "top-down" approach of the vast majority of monkey corticostriatal tract-tracing studies (also adopted by the human dMRI corticostriatal connectivity studies), which placed injections in cortical regions and examined their striatal projections, these studies (with the exception of Barnes et al. 2010) had a "bottom-up" approach of seeding striatal regions and examining cortex-wide correlations, precluding a side-by-side comparison of monkey anatomy and human fcMRI. Undoubtedly, the greater feasibility of placing tracer injections in the monkey cortex and seeding the structurally smaller striatum using fcMRI had a role in determining this. Study 1 also addresses this gap in knowledge by comparing striatal correlations from specific cortical regions side-by-side with striatal projections from our best guess of homologous monkey regions. These and other motivations for the present studies are discussed below.

Motivation for the Present Studies

As discussed in the previous section, prior to undertaking Study 1, there was a need for a detailed, comprehensive map of corticostriatal connectivity in humans and a thorough comparison with monkey tract-tracing results. Study 1 addresses these issues by creating a complete and detailed functional parcellation of the striatum based on correlations with *a priori* cortical networks. More specifically, in a conceptually identical process used to parcellate the cerebellum in a companion study (Buckner et al. 2011), the striatum was parcellated by assigning each striatal voxel to its most strongly correlated cortical network from a set of 7 or 17 cortical networks identified independently by Yeo et al. (2011). Study 1 also compares fcMRI correlations with monkey tract-tracing from specific cortical regions with at least a fair homology between monkeys and humans and at least two corroborating monkey projection patterns from injections in two independent laboratories.

The approach of parcellating the striatum based on cortical networks is a novel one that departs from nearly all prior fcMRI and DTI studies, which used large, discrete cortical seed regions. Support for our approach comes from monkey studies, which have suggested that regions that are interconnected project to overlapping terminal fields in the striatum (Yeterian and Van Hoesen 1978; Selemon and Goldman-Rakic 1985). This suggests that each striatal region in association territory is coupled to whole networks, not single regions. Prior fcMRI studies also indicate a similar organization exists in humans, showing that a striatal seed region in the dorsal caudate or putamen has functional coupling to distributed regions of the cortex (Barnes et al. 2010; Di Martino et al. 2008). Thus, in Study 1, we examined how striatal regions are functionally connected to *a priori* cortical networks from a set of 7 cortical networks chosen

for the clustering stability of the parcellation and resemblance to known functional networks (Fig. 1.4), or from a set of 17 cortical networks chosen for its relative clustering stability and its finer grained information useful for exploration (Yeo et al. 2011). This approach was successful in the cerebellum, creating parcellations that correctly identified the primary and secondary motor divisions and the association division between them, as identified by monkey polysynaptic tract-tracing (Buckner et al. 2011). In light of increasing evidence that behavioral functions arise from the interaction of multiple brain regions, we hoped that this approach would shed light into the striatum's interactions with cortical networks.

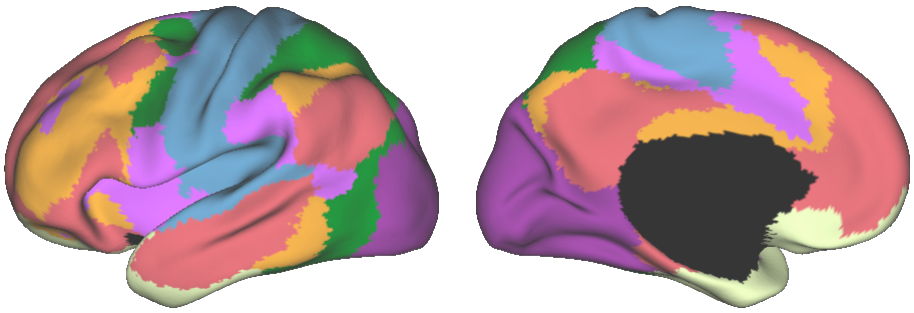

Figure 1.4 Seven-network parcellation of the human cerebral cortex. Two striatal parcellation maps were created by assigning each striatal voxel to its most strongly correlated cortical network in a 7- or 17-network cortical parcellation model. The 7-network cortical model, shown here, was created independently from the striatal results from a dataset of 1,000 healthy young adults. Each of the 7 colors represents a separate network. This model, created by a data-driven clustering algorithm, shows sensory and association networks that resemble known functional and anatomical networks.

The second study takes advantage of our ability to map human functional connections to address our relatively little knowledge about the basal ganglia's role in human cognition. One important cognitive function is cognitive control, or the ability to apply thought and action towards goals, plans, or intentions (Badre and D'Esposito 2009). In Study 2, we examined the functional connectivity underlying hierarchical cognitive control, which is the use of higher and lower order control for tasks of varying difficulty. Patient lesion studies (Milner 1963) and

neuroimaging studies of memory (Buckner 2003) and rule usage (Badre and D'Esposito 2007; Koechlin et al. 2003) have identified a caudal-to-rostral gradient of lateral frontal cortex regions involved in easier and more concrete to harder and more abstract cognitive control. These regions are thought to be hierarchically organized such that higher order regions influence the activity of lower order regions, rather than simply a gradient of independent regions. A patient lesion study (Badre et al. 2009) provided evidence for this by showing that localized lesions along the lateral frontal cortex prevent the ability to complete hierarchical rule usage tasks corresponding to and above, but not below, the level of the lesion location (Badre et al. 2009).

The activity of this functional hierarchy during hierarchical cognitive control raises two questions that are addressed in Study 2. The first question asks what the link is between the functional hierarchy and the organization of association networks. In contrast to the functional hierarchy, which is localized to the lateral frontal cortex, association networks have been suggested based on monkey anatomy to consist of interconnected regions distributed throughout association cortex with no clear hierarchy (Goldman-Rakic 1988). This organization suggests that there are distributed regions involved in a cognitive function, rather than the functional hierarchy of localized regions involved in hierarchical cognitive control. How are both observations true? In Study 2, we compared fMRI activity during task performance with an fcMRI map of cortical networks to investigate this apparent conflict.

The second question in Study 2 asks, how does the functional hierarchy arise; what is the connectivity underlying it? One possible way may be through cortico-basal ganglia-thalamic circuits. The striatum's receipt of projections from nearly the entire cerebral cortex and their putative participation in parallel cortico-basal ganglia-thalamic circuits (Alexander et al. 1986, 1990) suggest that there are circuits specific to each order of the hierarchy. Given the high

degree of overlap that also occurs in the striatum (Haber et al. 2006), these circuits may interact in the striatum to give rise to the functional hierarchy of the lateral frontal cortex. This possibility was investigated by examining the patterns of functional connectivity from the hierarchical regions of lateral frontal cortex for an organization that is suggestive of hierarchical interaction.

After more than a century of valuable animal work, neuroimaging has ushered in a new era in which humans can be directly studied. However, like any other technique, neuroimaging has its limitations and should be studied in conjunction with animal work, not outdate it. Together, the present studies comprehensively map human corticostriatal connectivity, relying upon prior animal work, and provide additional insight into the connectivity underlying human cognitive functions. The next chapters present each study in greater detail, followed by a general discussion of the findings.

Chapter 2:

Choi, E.Y., Yeo, B.T.T., and Buckner, R.L. (2012).

The Organization of the Human Striatum Estimated by Intrinsic Functional Connectivity.

***J. Neurophysiology*, 108(8): 2242-2263.**

Summary

The striatum is connected to the cerebral cortex through multiple anatomical loops that process sensory, limbic, and heteromodal information. Tract-tracing studies in the monkey reveal that these corticostriatal connections form stereotyped patterns in the striatum. Here the organization of the striatum was explored in the human using resting-state functional connectivity MRI (fcMRI). Data from 1,000 subjects were registered using nonlinear deformation of the striatum in combination with surface-based alignment of the cerebral cortex. fcMRI maps derived from seed regions placed in the foot and tongue representations of the motor cortex yielded the expected inverted somatotopy in the putamen. fcMRI maps derived from the supplementary motor area were located medially to the primary motor representation, also consistent with anatomical studies. The topography of the complete striatum was estimated and replicated by assigning each voxel in the striatum to its most strongly correlated cortical network in two independent groups of 500 subjects. The results revealed at least five cortical zones in the striatum linked to sensorimotor, premotor, limbic, and two association networks with a topography globally consistent with monkey anatomical studies. The majority of the human striatum was coupled to cortical association networks. Examining these association networks further revealed details that fractionated the five major networks. The resulting estimates of striatal organization provide a reference for exploring how the striatum contributes to processing motor, limbic, and heteromodal information through multiple large-scale corticostriatal circuits.

Introduction

Animal studies and human patient cases demonstrate that the basal ganglia are involved in diverse functional domains including movement, cognition, and reward (Alexander et al. 1986; DeLong and Georgopoulos 1981; Haber and Gdowski 2004; MacLean 1972). Providing an anatomical basis for functional diversity, tract-tracing studies show that the basal ganglia are connected to distributed regions of the cerebral cortex through multiple, partially parallel anatomical loops (Alexander et al. 1986, 1990). Each loop includes projections from the cerebral cortex, through the basal ganglia, to the thalamus, and back to the cerebral cortex. Cortical efferents to the striatum (the main input nucleus of the basal ganglia) form distinct patterns depending on their cortical origin. The posterior putamen and the dorsolateral anterior putamen receive projections from motor and motor association cortex, the central anterior striatum from cognitive regions including prefrontal cortex, and the ventral anterior striatum from regions associated with the limbic system, in particular medial and orbital frontal cortex (Haber et al. 1994; Parent 1990). More complex projection patterns are also observed that do not fit neatly into a tripartite heuristic, including interdigitated projection zones (Selemon and Goldman-Rakic 1985). Nonetheless, corticostriatal projections in the monkey broadly differentiate motor, cognitive, and affective systems, suggesting a basis for functional specialization within the basal ganglia. Characterizing the detailed topography of corticostriatal projections in the human is thus important for understanding basal ganglia function and how motor and neuropsychiatric disorders arise from its dysfunction.

Organization of the Striatum in the Human

Corticostriatal projections in the human have been explored using non-invasive neuroimaging methods including intrinsic functional connectivity (Barnes et al. 2010; Di Martino et al. 2008; Zhang et al. 2008), diffusion tensor imaging (DTI; Draganski et al. 2008; Leh et al. 2007; Lehéricy et al. 2004), T1-weighted voxel-based morphometry (VBM; Cohen et al. 2008), and meta-analysis of corticostriatal co-activation in task-based functional studies (Postuma and Dagher 2006). Consistent with estimates of striatal organization in the monkey, these studies reveal broad topographic patterns that differentiate motor, cognitive, and affective zones of the striatum. For example, using DTI, Lehéricy et al. (2004) examined white-matter tracts arising from seed regions placed within the striatum. The posterior putamen gave rise to fiber tracts that travelled through the corona radiata to the motor and adjacent premotor cortices, the anterior striatum targeted the prefrontal cortex and pre-supplementary motor area (pre-SMA), and the ventral striatum revealed tracts associated with the orbital frontal and temporal cortices. Draganski et al. (2008) mapped the detailed voxel connectivity profiles of each point in the human striatum to 23 regions distributed throughout the ipsilateral cerebral hemisphere. The estimated topography demonstrated the tripartite division. More detailed analysis also revealed a functional gradient within the striatum as suggested by Haber (2003) based on animal tracing studies.

Intrinsic functional connectivity MRI (fcMRI; Biswal et al. 1995) has recently emerged as a complementary tool to map the organization of corticostriatal circuits. The basis and limitations of fcMRI are discussed in our companion papers (Buckner et al. 2011; Yeo et al. 2011) and elsewhere (Buckner 2010; Fornito and Bullmore 2010; Fox and Raichle 2007; Power et al. 2010; Van Dijk et al. 2010). fcMRI detects low-frequency correlations between regions of

the brain. The correlations are constrained by polysynaptic anatomical connectivity (although other factors also contribute to functional coupling) such that two regions that are anatomically connected will tend to show stronger functional coupling measured at rest. Thus, it is possible to map striatal organization by examining the functional coupling patterns between the striatum and the cerebral cortex.

Di Martino et al. (2008) were among the first to systematically explore striatal organization using fcMRI. By examining the cerebral coupling patterns from six seed regions placed throughout the striatum, they demonstrated clear functional subdivisions. However, the patterns of cortical coupling did not simply involve discrete regions of cortex. Rather, individual striatal regions were coupled to widespread cortical targets. For example, the seed region placed in the right dorsal caudate was functionally correlated with bilateral regions of the dorsolateral prefrontal cortex, anterior cingulate, posterior cingulate, and the inferior parietal lobule (e.g., see their Fig. 3).

In a recent fcMRI exploration of the striatum, Barnes et al. (2010) employed graph analytic techniques. Using a procedure conceptually similar to the DTI work of Draganski et al. (2008), the profile of functional connectivity for each striatal voxel was analyzed to identify clusters of voxels with similar cortical connectivity patterns. They found that at least three clusters of striatal voxels could be grouped together based on their similar coupling patterns to distinct, distributed cortical networks (forming modules). Thus, both the analyses of Di Martino et al. (2008) and Barnes et al. (2010), while consistent with distinctions between motor, cognitive, and affective systems, also suggest that striatal functional coupling is not localized to discrete portions of a specific lobe or cortical region. Rather, striatal regions are functionally coupled to distributed regions throughout the cerebral cortex.

Current Study

The present paper builds upon these prior studies using an approach that follows from our recent companion papers (Buckner et al. 2011; Yeo et al. 2011). We previously identified functionally coupled networks across the cerebral cortex (Yeo et al. 2011; see also Power et al. 2011) that provided a basis for mapping the cerebellum (Buckner et al. 2011). Here each striatal voxel was mapped to its most correlated cortical network, thereby comprehensively mapping the striatum in reference to cerebral networks. In this regard, the present strategy differs from prior studies of the striatum that target specific anatomically defined cortical targets (e.g., dorsolateral prefrontal cortex). The goals of this paper are (1) to provide reference maps that are a current best estimate of the organization of the human striatum as measured by functional connectivity, (2) to compare human striatal functional connectivity to monkey anatomical connectivity, and (3) to explore whether there are any global patterns that provide insight into corticostriatal circuit organization in the human.

Results

Functional Connectivity Reveals the Somatomotor Topography of the Striatum

Anatomical tract-tracing (Flaherty and Graybiel 1993; Künzle 1975) and electrophysiological studies (Alexander and DeLong 1985) have shown that the primary motor cortex projects to the putamen with an inverted topography. Figure 2.1*A* shows a representative tract-tracing case (Flaherty and Graybiel 1993) of the foot and tongue in the monkey putamen. The same inverted topography was seen in the human striatum using an fMRI motor task conducted in our companion paper (Buckner et al. 2011; Fig. 2.1*B*) in which subjects moved their feet or tongues. Functional connectivity revealed the inverted motor topography (Fig. 2.1*B*; discovery sample). fcMRI maps of seed regions placed in the striatal foot and tongue representations (Table 2.1) show that cerebral correlations are specific to their respective motor cortex representations (Fig. 2.1*C*; replication sample). These results demonstrate that functional connectivity identifies the expected inverted somatomotor topography in the striatum.

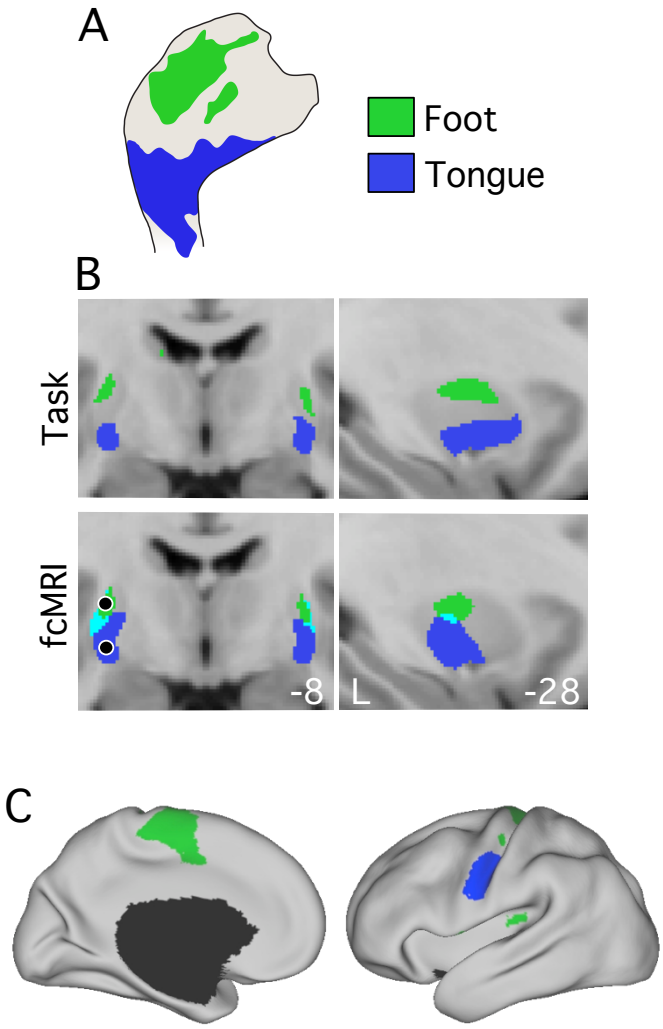

Figure 2.1 Functional connectivity reveals the inverted somatomotor topography within the posterior putamen that is comparable to monkey anatomy and task-evoked estimates. (A) A representative case is shown of the inverted somatomotor topography in the monkey putamen revealed by tracer injections in the foot (green) or tongue (blue) representation of the primary motor cortex. Adapted from Flaherty and Graybiel (1993; see Table 2.3 under Motor Foot). (B) Coronal sections (left column, y = -8) and left sagittal sections (right column, x = -28) display the inverted somatomotor topography in the task-evoked (top panel) and functional connectivity (bottom panel) data. Green color indicates foot representation; blue color indicates tongue representation. The functional connectivity images were produced from the replication sample (n = 500) using seed regions in the foot- and tongue-specific motor cortex representations from the task-evoked data. (C) Functional connectivity from the foot- and tongue-specific representations in the putamen (seed regions shown in bottom panel of B) show specific correlations with the foot and tongue regions of the motor cortex. A threshold was used of 0.4 for the task data, z(r) > 0.04 for the striatal fcMRI data, and z(r) > 0.07 for the cortical fcMRI data. Seed region coordinates are reported in Table 2.1. Monkey corticostriatal projection tracings shown here and in later figures were redrawn for conformity. Original tracings showed terminal labeling; redrawings included both dense and diffuse projections. Original tracings of the right striatum were flipped in the redrawings for conformity.

Table 2.1 Locations of Seed Regions Used to Assess Specificity of Somatomotor and Ventral Attention Networks

Cerebral Cortex	Left Hemi Coordinates
$M1_F$ (foot)	-6, -26, 76
$M1_H$ (hand)	-41, -20, 62
$M1_T$ (tongue)	-55, -4, 26
SMA	-3, -5, 59
Striatum	
Motor Foot	-29, -9, 8
Motor Hand	-30, -7, 2
Motor Tongue	-29, -9, -5
SMA	-24, -7, 7
Ventral striatum (default zone)	-28, -9, -10

Notes: Coordinates represent x,y,z in the atlas space of the Montreal Neurological Institute (MNI). Motor task fMRI together with probabilistic histological maps of areas 2 and 4 (Fischl et al. 2008; Geyer et al. 1996; Grefkes et al. 2001) were used to identify foot, hand, and tongue regions of the motor cortex ($M1_F$, $M1_H$, $M1_T$) in the left hemisphere. A probabilistic histological map of area 6 (Geyer 2004) and a comparison of monkey and human motor tasks (Picard and Strick 1996) were used to identify the supplementary motor area (SMA) in the left hemisphere. All striatal seed regions were selected in regions with strong and specific correlations from their respective cortical functional connectivity maps. The ventral striatum seed region was placed in a relatively high confidence region of the default network zone in the posterior ventral striatum.

Functional Connectivity Reveals the Lateral-Medial Division of the Primary Motor and Supplementary Motor Cortices in the Striatum

Figure 2.2*A* shows a representative case of a double-injection in the hand regions of the ipsilateral primary motor cortex (M1) and SMA in one monkey (Takada et al. 1998a). The tracing shows that the SMA preferentially projects medially and the primary motor cortex projects laterally to one another in the monkey putamen (for ipsilateral areas). Seed regions in the estimated human homolog of SMA and the hand-specific region of the motor cortex (Table 2.1) correlate preferentially to the medial and lateral putamen, respectively (Fig. 2.2*B*; discovery sample). Cortical fcMRI maps derived from seed regions in the striatal motor and SMA

representations (Table 2.1) showed preferential correlations to the primary motor cortex and SMA, respectively (Fig. 2.2*C*; replication sample). The SMA correlations, however, were not specific, possibly due to signal bleeding between the putamen and the adjacent cortex, which we will discuss further below.

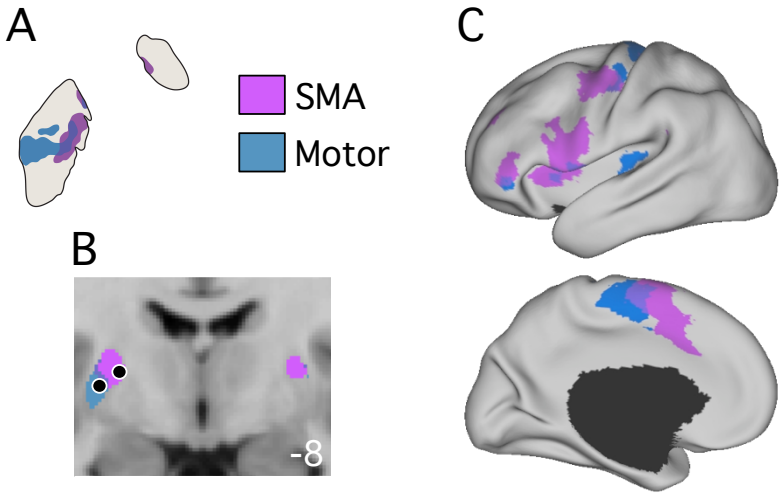

Figure 2.2 Functional connectivity reveals the lateral-medial topography of the primary motor and supplementary motor cortices within the putamen that is comparable to monkey anatomy. (A) A representative case is shown of the lateral-medial topography of the primary motor cortex and SMA in the monkey putamen revealed by tracer injections in the motor (blue) and SMA (purple) forelimb representations. Adapted from Takada et al. (1998a; see Table 2.3 under SMA). (B) A coronal section (y = -8) displays the lateral-medial topography in the functional connectivity data produced from the replication sample (n = 500) using seed regions of the task-evoked motor hand representation and the estimated human SMA homolog. Thresholds of z(r) > 0.04 and 0.09 were applied for the motor hand and estimated SMA striatal fcMRI maps. (C) Functional connectivity maps from the motor- and SMA-specific striatal seed regions (regions shown in B) illustrate their preferential correlations with primary motor cortex and SMA. A threshold of z(r) > 0.07 was applied. Seed region coordinates are reported in Table 2.1. Note that there is also correlation with insular regions that fall near to the striatum. We suspect that these are residual artifacts of limited resolution that are not fully handled by our methods (see text).

Functional Connectivity Reveals a Complete Functional Map of the Striatum

The reasonable agreement between the monkey anatomical studies and functional connectivity for motor cortex suggested that functional connectivity could be used to map the

striatum comprehensively. Our mapping strategy entailed assigning each striatal voxel to its most strongly correlated cortical network (see Methods) in the 7- and 17-network cortical parcellations, as identified by Yeo et al. (2011). Figure 2.3 shows the high degree of reliability (7-network: 90.2%; 17-network: 87.2% overlapping voxels) of this method in two independent sets of 500 subjects (discovery and replication) for both parcellations. Disagreement between the discovery and replication samples tended to be between neighboring networks, especially within association cortex (e.g., 81.1% of the voxel disagreements for regions falling within the default network (red) in the discovery sample were classified to the frontoparietal control network (orange) in the replication sample). Figures 2.4 and 2.5 display best estimates of the 7- and 17-network parcellations using all 1,000 subjects. Figure 2.6 shows the confidence estimates of the parcellations.

Several observations emerged from these parcellations. First, the 7-network striatal parcellation (Fig. 2.4) showed that 5 of the 7 networks are strongly represented in the striatum: motor (blue), ventral attention (violet), frontoparietal control (orange), default (red), and limbic (cream) networks. There was a small representation of the dorsal attention (green) network in the right posterior ventral putamen and virtually no representation of the visual (purple) network. The 17-network parcellation (Fig. 2.5) appeared to be a fractionation of the 7-network parcellation with a similar pattern, but with finer-grain information about functional divisions within a network. One notable exception to this is the pink network at around $y = 12$, which is a region susceptible to cortical signal bleeding as we will discuss below.

Second, the assignments of the motor (blue) network and ventral attention (violet) network, which includes premotor areas, in the 7-network parcellation agreed with the cerebral cortex fcMRI analyses shown in Figures 2.1 and 2.2. The posterior putamen was assigned to the motor

Figure 2.3 Reliability of human striatal maps based on functional connectivity. Each voxel in the striatum is assigned a color corresponding to its most strongly correlated cerebral network according to the legends below of the 7- (left) and 17-network (right) cortical parcellations (from Yeo et al. 2011). The 7- and 17-network parcellations were each produced in the discovery sample *(n* = 500) and replicated in the replication sample (*n* = 500). For example, the blue regions of the striatum include those voxels that are more strongly correlated with the blue cerebral network (involving somatosensory and motor cortices) than any other network. Note that the discovery and replication maps are highly similar (voxel overlap was 90.2% and 87.2% for the 7- and 17-network estimates, respectively).

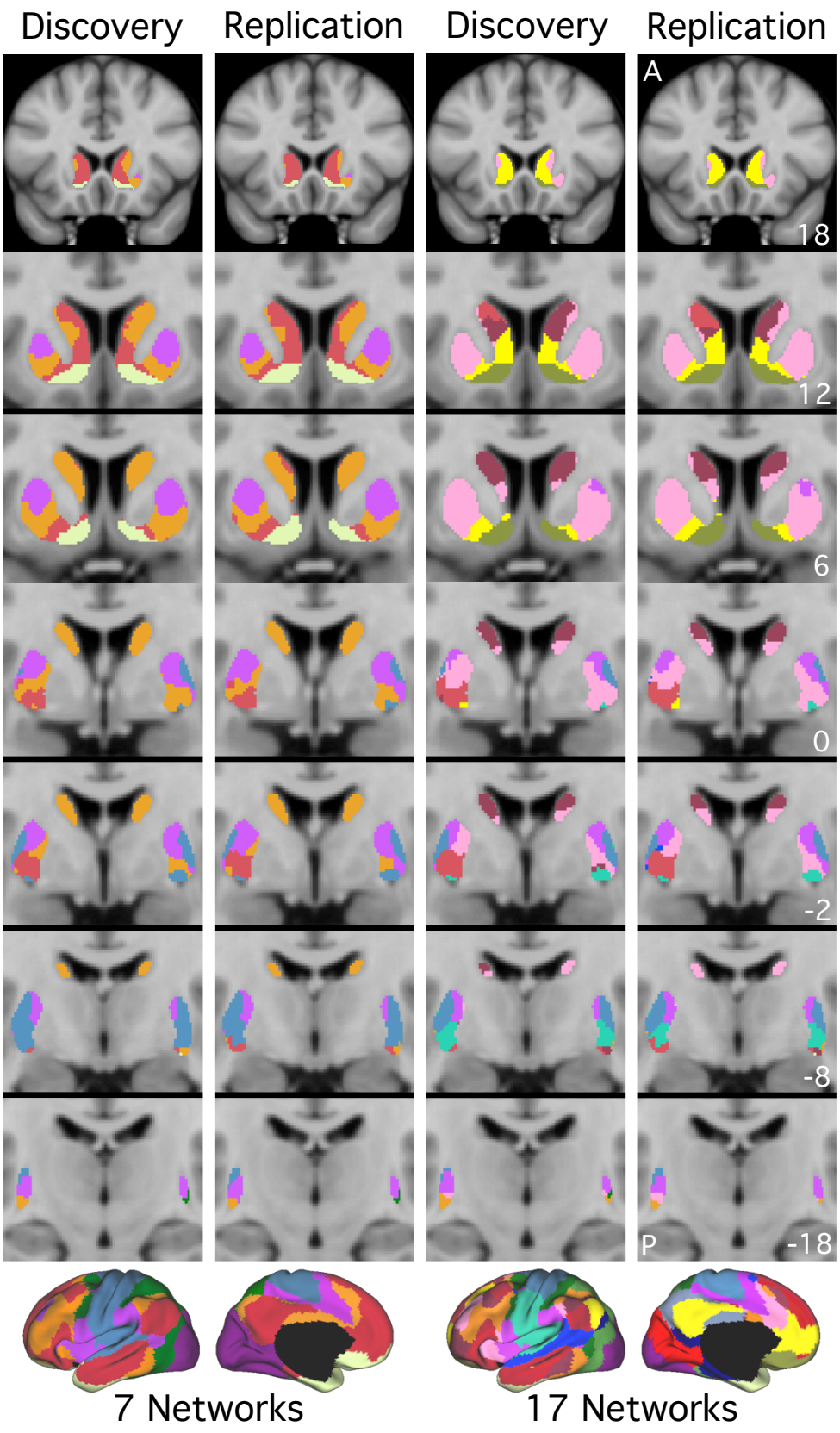

Figure 2.3 (Continued)

Figure 2.4 A map of the human striatum based on functional connectivity to 7 major networks in the cerebrum. Each voxel in the striatum is assigned a color corresponding to its most strongly correlated cerebral network in the 7-network cortical parcellation shown in the bottom legend (from Yeo et al. 2011). The full sample of 1,000 subjects was used to create a best estimate of the map. The sections display coronal (left), sagittal (middle), and transverse (right) images. A = anterior, P = posterior, M = medial, L = lateral, S = superior, and I = inferior. The slice coordinate in the MNI atlas space is located at the bottom right of each panel.

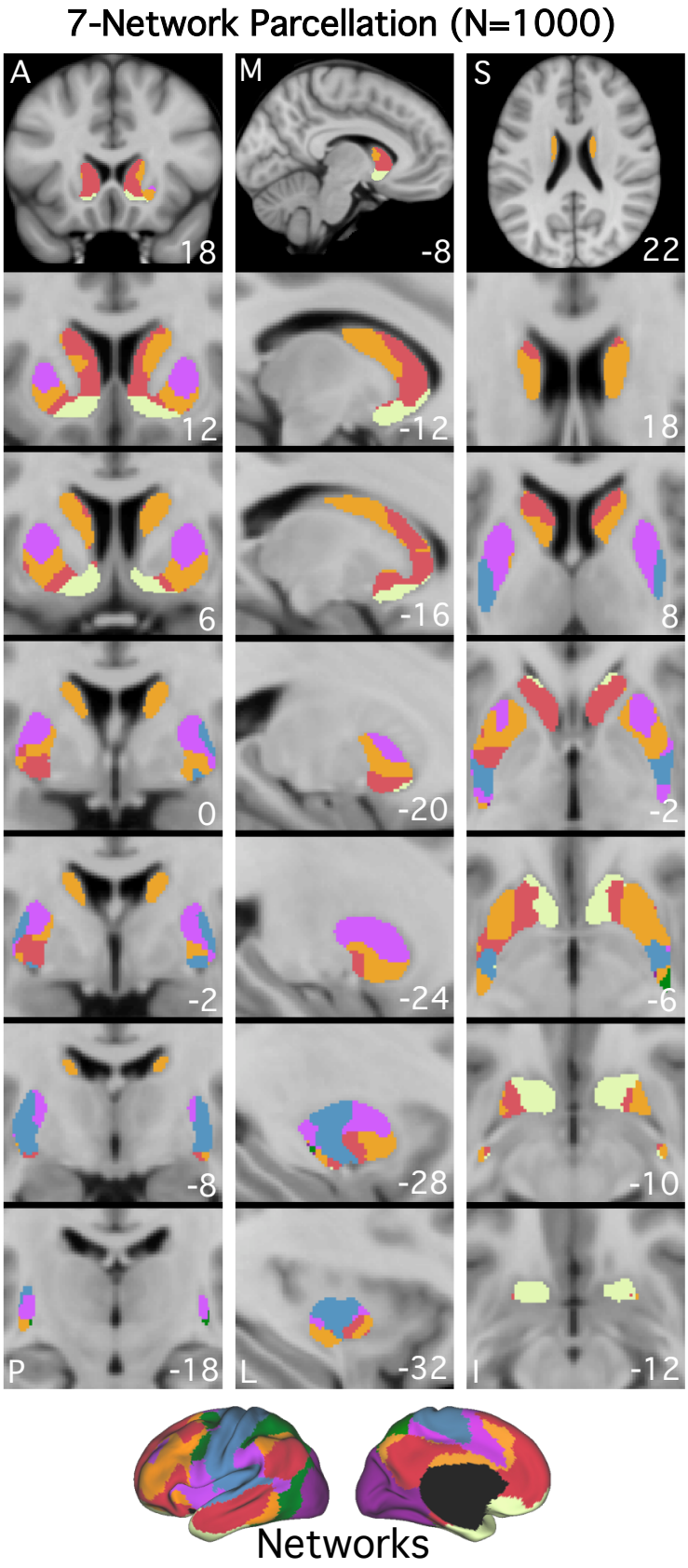

Figure 2.4 (Continued)

Figure 2.5 A fine-parcellated map of the human striatum based on functional connectivity to 17-networks in the cerebrum. The format and use of abbreviations are the same as in Figure 2.4 but in this instance in relation to a finer cerebral parcellation involving 17-networks (from Yeo et al. 2011). These data are from the full sample of 1,000 subjects. Note that this method identifies the correct locations of the foot (blue) and tongue (aqua) regions in the posterior putamen. As will be discussed in the text, some features of the parcellation are uncertain, as illustrated by the asterisk in the putamen (labeled as the pink network).

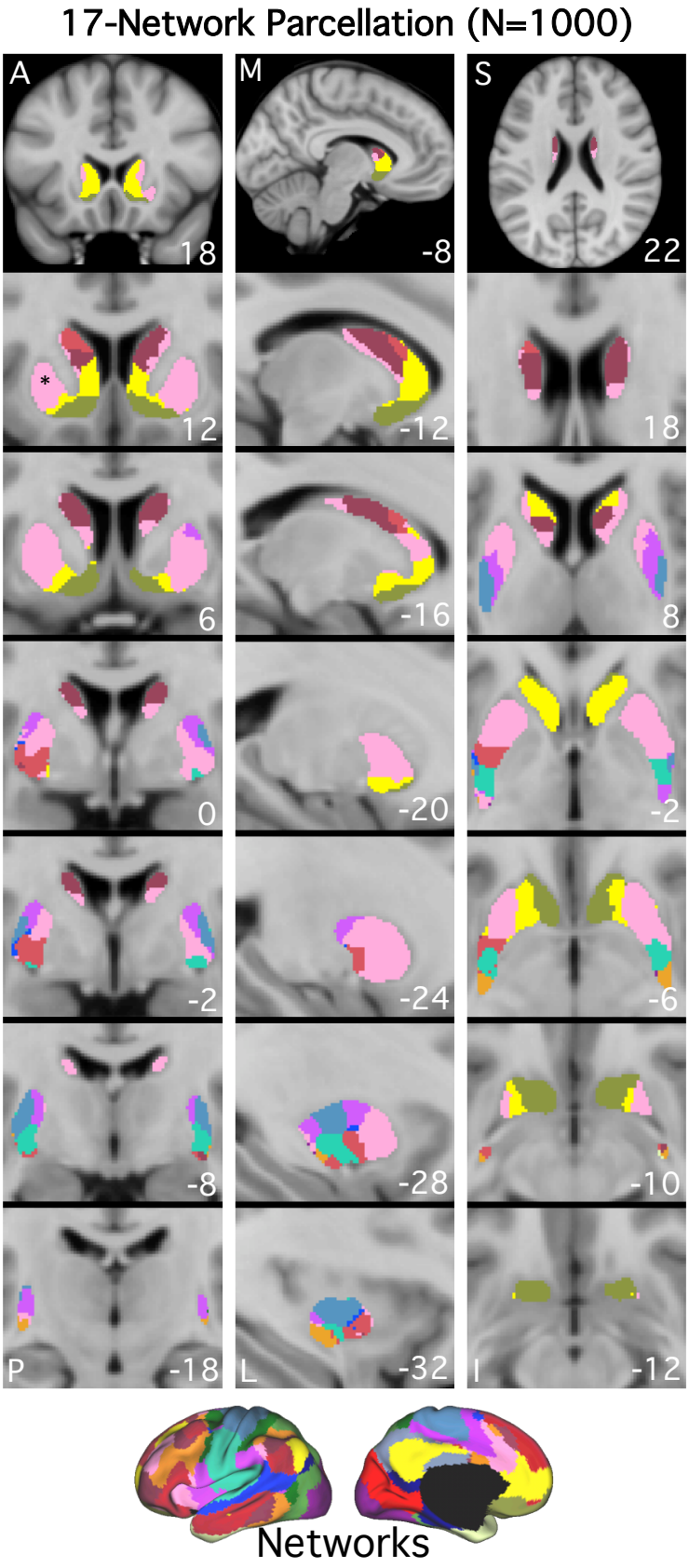

Figure 2.5 (Continued)

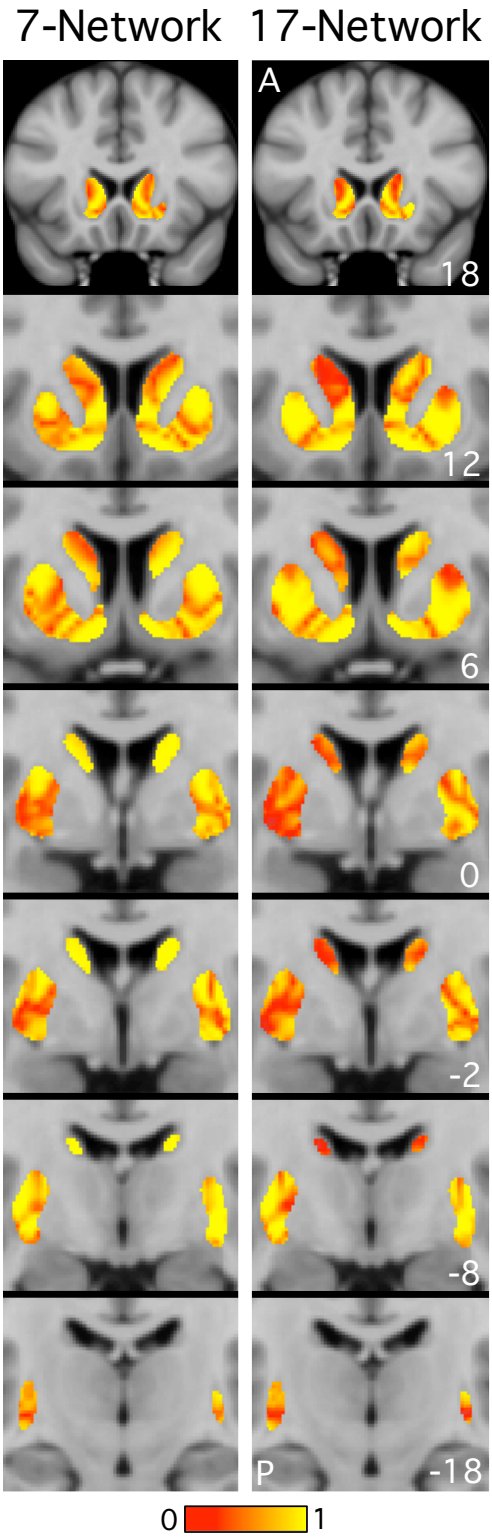

Figure 2.6 Confidence of the parcellation estimates. Confidence values for each voxel of the striatum with respect to its assigned network versus second-choice network are displayed for the 7- (left column) and 17-network (right column) estimates from 1,000 subjects. Network boundaries are generally associated with lower confidence values.

network laterally and the ventral attention network medially. Furthermore, the motor representation in both the motor cortex and striatum fractionated into dorsal foot (blue) and ventral tongue (aqua) parcellations in the 17-network model, consistent with the inverted somatotopy seen in monkey anatomy. These results suggest that the parcellation method recovers the topographic arrangements of motor subdivisions.

Third, the parcellations broadly agree with prior models of the striatum that propose gradients of connectivity. The 7-network parcellation shows that corticostriatal circuits, in particular the association circuits, couple to zones of the striatum that extend along its longitudinal extent, consistent with anatomical studies (Yeterian and Van Hoesen 1978; Selemon and Goldman-Rakic 1985). There is also a dorsolateral to ventromedial organization (Haber et al. 1994; Parent 1990; Parent and Hazrati 1995). We will expand on these organizational properties in the Discussion.

Fourth, the parcellation parallels monkey anatomical projections in the posterior ventral striatum. In addition to projections to the ventral putamen from the tongue region of the motor cortex, monkey anatomy reveals projections to the posterior-most portion of the ventral striatum from association and limbic cortices (there are also projections from subcortical structures, such as the amygdala [Russchen et al. 1985; Fudge et al. 2002, 2004], but we will not address them here). Figure 2.7 shows the 7-network parcellation of the posterior ventral striatum and the corresponding fcMRI maps, showing that the posterior ventral striatum is functionally coupled to the motor and, further ventrally, the association cortical networks.

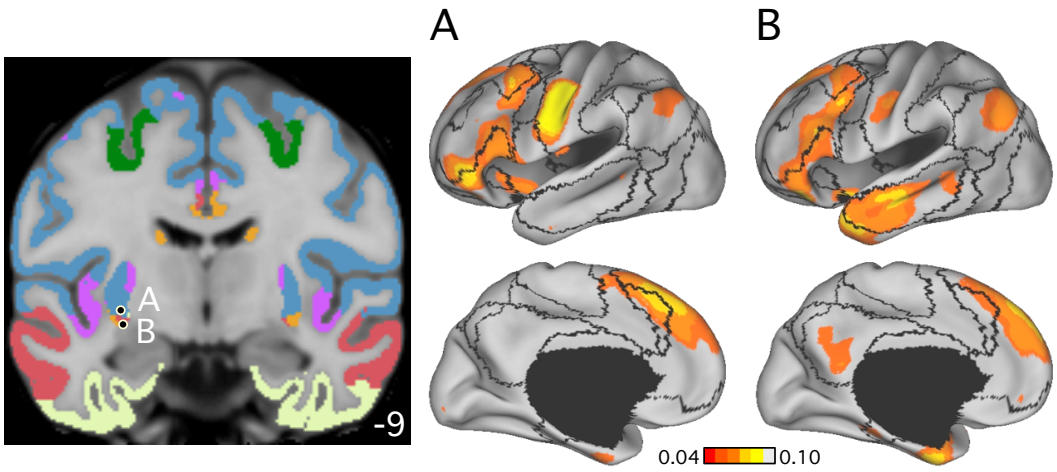

Figure 2.7 Distinct regions of the posterior ventral striatum are coupled to motor and association cortical networks. Seed regions placed in the motor (A) and default (B) network assignments of the left posterior ventral striatum in the 7-network parcellation reveal correlation with the motor and default cortical networks, respectively, in the replication sample (n = 500). The 7-network cortical parcellation is also displayed to show that these corticostriatal fcMRI correlations are minimally influenced by signal bleeding from the adjacent cortex.

Quantitative Measurement of Association and Limbic Corticostriatal Circuits Demonstrates Specificity

The previous analyses illustrated that the functional connectivity of the motor cortex and SMA within the striatum is correctly localized in the 7- and 17-network striatal parcellations. We next sought to determine how well the parcellations captured seed-based functional connectivity estimates. Figure 2.8 shows the cortical fcMRI maps (replication sample) resulting from seed regions placed in high confidence regions of the frontoparietal control, default, and limbic divisions of the 7-network striatal parcellation (discovery sample; Table 2.2). These fcMRI maps revealed distinct correlation maps that largely agreed with the parcellation. For example, a region located in the central caudate head (region A) was correlated to cortical regions in the frontoparietal control network, including the dorsolateral prefrontal cortex and the inferior parietal lobule (Fig. 2.8*A*). In contrast, a more ventral region (region B) was correlated to cortical regions linked to the default network, including the posterior cingulate cortex and medial

prefrontal cortex (Fig. 2.8*B*). We note, however, that the cortical correlations did not always fall neatly within their assigned cortical networks: the correlations in some locations spilled across boundaries into neighboring networks or did not cover the entire assigned network. The latter patterns may be due to the resolution limitations or the presence of subnetworks, as we will explore later.

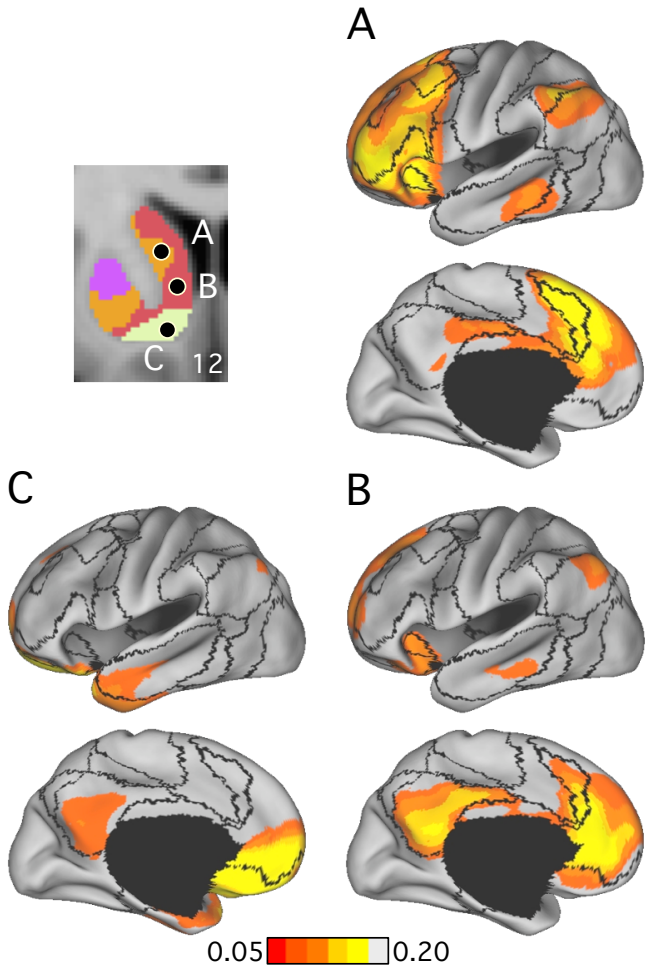

Figure 2.8 Evidence for preferential patterns of corticostriatal functional connectivity involving association and limbic networks. Left hemisphere cortical functional connectivity maps derived from the replication sample (n = 500) are shown for seed regions placed in high confidence regions of the striatum from the discovery sample (n = 500) for the (A) frontoparietal control, (B) default, and (C) limbic networks. Seed regions are shown in the center image (Table 2.2). Separate regions of the striatum are correlated with distinct cerebral networks underlying cognitive and limbic function.

Table 2.2 Locations of Seed Regions Used to Quantify Specificity of Association and Limbic Networks

Cerebral Cortex	Left Hemi Coordinates
aMT+	-51, -64, -2
FEF	-26, -6, 48
$IPS3_m$	-31, -48, 46
PCC	-3, -49, 25
PF_v	-55, -38, 33
PFC_{da}	-31, 39, 30
PFC_{dp}	-44, 15, 48
PFC_{la}	-41, 55, 4
PFC_m	-7, 46, -2
PFC_{mp}	-5, 22, 47
PGa	-52, -50, 49
PGc	-42, -61, 31
PrC_v	-50, 6, 30
PrCO	-35, 7, 5
scg25	-4, 17, -8
6_{am}	-4, 9, 47
Striatum	
Frontoparietal Control Network	-12, 10, 8
Default Network	-8, 10, 1
Limbic Network	-10, 11, -9

Notes: Left hemisphere cerebral cortical seed regions were obtained from Yeo et al. (2011) except precentral opercular (PrCO), anterior medial BA6 (6_{am}), ventral area PF (PFv), and central area PG (PGc), which were selected from the discovery dataset to cover remaining key cortical regions and named based on probabilistic histological maps of nearby areas (Caspers et al. 2006; Geyer 2004). Striatal seed regions were selected from the frontoparietal control, default, and limbic networks based on the discovery dataset using the confidence map as a guide.

In order to quantitatively characterize the specificity of these corticostriatal coupling patterns, we computed the correlations of the 3 striatal seed regions with cortical seed regions distributed throughout the cerebral cortex (Table 2.2). The results, plotted in polar form (Fig. 2.9), revealed 3 distinct functional connectivity patterns in which striatal seed regions were preferentially correlated to the cortical seed regions of their respective networks.

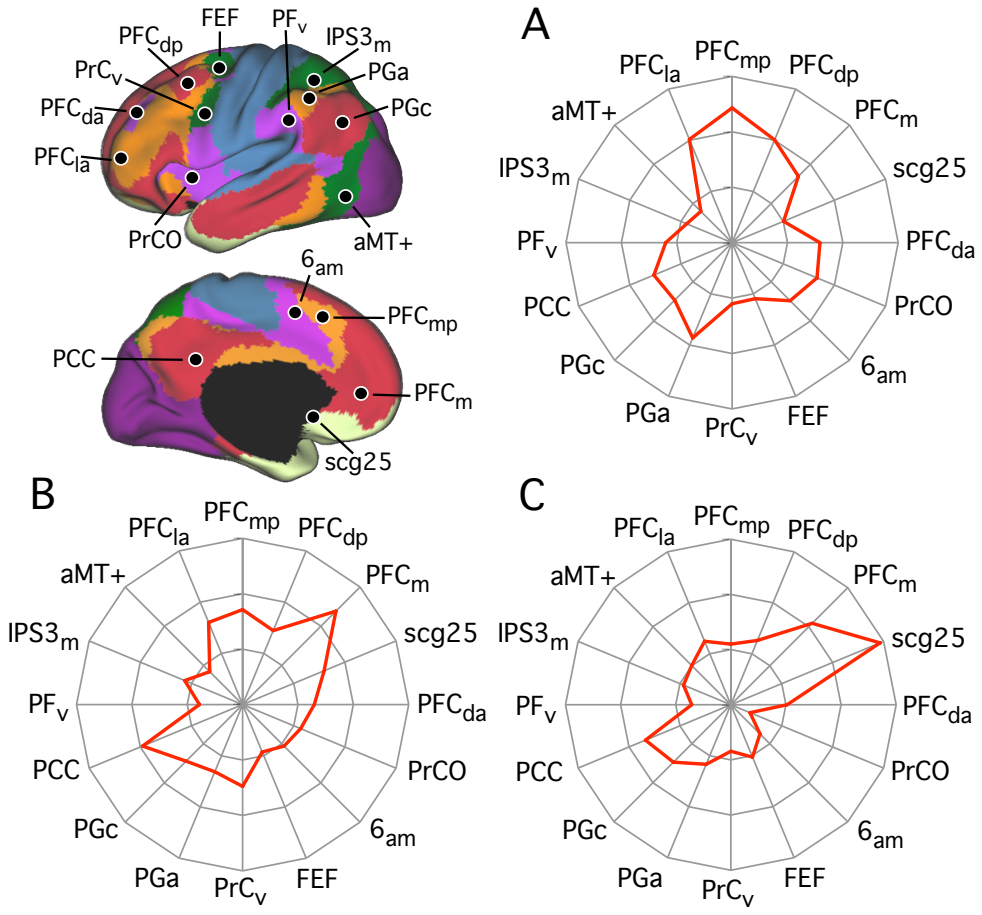

Figure 2.9 Quantitative evaluation of the specificity of corticostriatal circuits involving association and limbic networks. (A-C) The three polar plots display the functional connectivity correlation values derived from the replication sample (n = 500) for each of the striatal seed regions (Table 2.2) from Figure 2.8 with cortical seed regions placed in distributed regions of cortical networks, shown in the center image. Polar scale ranges from r = -0.25 (center) to r = 0.35 (outer boundary) in 0.2-step increments. Each polar plot has a distinct connectivity profile.

Cortical Signal Bleeding

Due to the proximity of the insula to the striatum, we suspected that there might be bleeding of cortical signal into the striatum. Signal bleeding has previously been observed between proximal structures, such as the visual cortex and the cerebellum (Buckner et al. 2011) and the sensorimotor and auditory cortices (Yeo et al. 2011). In the former case, regressing out the visual cortex signal from the cerebellum revealed correlations to the motor cortex, as

predicted by monkey anatomical tract-tracing studies (Buckner et al. 2011). In the striatum, prior to regressing out the cortical signal, the majority of the putamen was assigned to the ventral attention network (violet) located adjacently in the insula (Fig. 2.10, *A* and *E*). This is most likely due to the strong correlations between the insula and the putamen as shown by an fcMRI map of a seed region in the ventral attention network of the insula (Fig. 2.10, *B* and *F*; see Methods for seed region coordinate). To correct for the signal bleeding, we regressed out the cortical signal within 8 or 9 mm of the striatum (see Methods). This regression removed most of the correlations in the posterior putamen (Fig. 2.10*D*), leading to the assignment of the posterior putamen to the motor network (Fig. 2.10*C*), as predicted by monkey anatomy. In the anterior putamen, regressing out the proximal cortical signal reduced these correlations (Fig. 2.10*H*) and revealed the assignment of the central and ventral anterior putamen to the frontoparietal control and default networks (Fig. 2.10*G*), which also agrees with monkey anatomical tract-tracing studies (Fig. 2.12, 2.13, and 2.14).

We also examined an alternative regression method (Fig. 2.11) that removed the signal from only the neighboring cortical voxels (within 9 mm) of each striatal voxel, thus regressing out a unique signal for each striatal voxel. This revealed a parcellation (Fig. 2.11*B*) with slight shifts in network boundaries in these regions of uncertainty, but largely qualitatively similar to the first regression model (Fig. 2.11*A*).

These regression methods revealed that the putamen is susceptible to signal bleeding from the adjacent cerebral cortex. In contrast, the network assignments in the caudate remain qualitatively unchanged between the no regression and regression methods. We are therefore least confident of the results in the putamen and will focus on the more certain caudate results in the remainder of this paper.

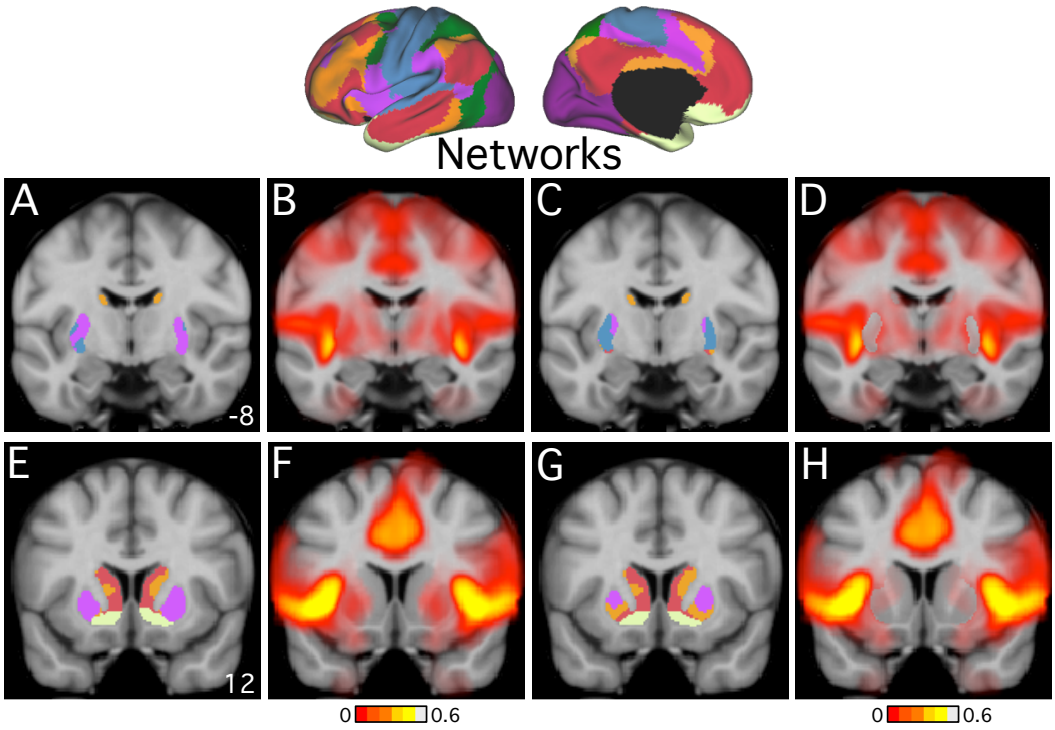

Figure 2.10 Regression of cortical signal from the striatum. The effects of regressing out the adjacent cortical signal from the striatum are shown using the full sample of 1,000 subjects. The top panel shows the posterior striatum (y = -8) and the bottom panel shows the anterior striatum (y = 12). The first two columns show the 7-network parcellation (A, E) and an fcMRI map of a proximal insula seed region (B, F) with no cortical signal regression from the striatum (see Methods for seed region coordinate). The third and fourth columns show the 7-network parcellation (C, G) and fcMRI maps of the same seed region (D, H) with regression of cortical signal from the striatum (not applied to cortex). The 7-network cortical parcellation is also displayed to show potential sources of signal contamination from the adjacent cortex. Note how the parcellations are dominated by the network labeled by violet (which includes the adjacent insula). When regression is applied, a more plausible parcellation results. The contrast between the functional connectivity patterns within the striatum before (e.g., F) and after (e.g., H) regression of adjacent cortical signal illustrates that bleeding of signal from cortex to striatum is mitigated but not fully removed. Signal bleeding minimally affects the major portions of the caudate and ventral striatum. Parcellation estimates within the putamen are less certain. The fcMRI maps plot correlation values ranging from z(r) = 0 to 0.6.

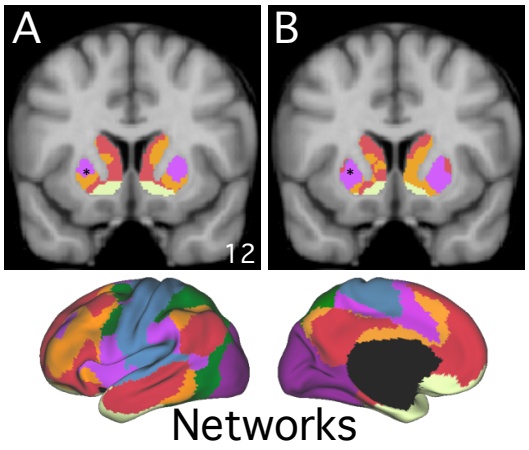

Figure 2.11 Alternative regression method for removing cortical signal from the striatum. The 7-network parcellation results are shown for the anterior striatum (y = 12) using the regression method applied in this paper (A; see Methods and Fig. 2.10) in which the signal from a unitary cortical mask is regressed from all striatal voxels. An alternative regression method is shown where for each striatal voxel the signal of neighboring cortical voxels within 9 mm is regressed out (B). Asterisk indicates the region of low confidence similar to Figure 2.5. The full sample of 1,000 subjects was used.

Functional Connectivity of the Striatum in Relation to Monkey Anatomic Connectivity with Association Cortex

Since the association and limbic networks include cerebral regions that are expanded in humans relative to monkeys (Hill et al. 2010; Van Essen and Dierker 2007), it is difficult to be certain about homologies. There are nonetheless several cases of replicated anatomical projection patterns (at least two corroborating injection patterns from two independent laboratories) with suspected human homologies (Table 2.3). Figure 2.12 shows comparisons for three association and limbic regions, as well as two motor regions as reference. Fig 2.12*A* shows the seed regions in the dorsolateral prefrontal cortex (PFC_{lp}), medial prefrontal cortex (PFC_{md}), and scg25, as well as the motor hand cortex ($M1_H$) and the SMA from Figure 2.2. Figure 2.12*B* shows representative injection cases from approximately homologous regions in the monkey, while Figure 2.12*C* shows human functional connectivity patterns in the replication sample.

Table 2.3 Seed Regions and Studies Used to Compare Human Functional Connectivity and Monkey Anatomy

Cortical Region	Left Hemi Human Coordinates	Monkey Injection Site	Replicated Monkey Anatomical Studies
Motor Foot	-6, -26, 76	Motor Hindlimb	Case 72-451, Künzle 1975
			Cases 32L, 37L, **40**, Flaherty and Graybiel 1993
			Case 31R, Flaherty and Graybiel 1994
Motor Hand	-41, -20, 62	Motor Forelimb	Cases **Rhesus Monkey**, Cynomolgus Monkey, Liles and Updyke 1985
			Case 42, Flaherty and Graybiel 1993
			Cases O, M, Inase et al. 1996
			Case **Ta**, Takada et al. 1998a
			Case Si, Takada et al. 1998b
			Case CMA7, Takada et al. 2001
Motor Tongue	-55, -4, 26	Motor Face or Mouth	Case 72-448, Künzle 1975
			Case **40**, Flaherty and Graybiel 1993
SMA	-3, -5, 59	SMA Forelimb	Cases O, M, Inase et al. 1996
			Cases **Ta**, It Takada et al. 1998a
			Case Tk, Takada et al. 1998b
			Case **San**, Inase et al. 1999
			Cases CMA5, CMA6, Takada et al. 2001
PCC	-3, -49, 25	PCC or Rsp	Case SM-85, Powell 1978 Anat Rec
			Case **1**, Baleydier and Mauguiere 1980
PFC_a	-8, 69, 7	Area 10	Case 4, Yeterian and Pandya 1991
			Case Area 15B, Eblen and Graybiel 1995
			Cases OM36, **OM38**, Ferry et al. 2000
PFC_{lp}	-45, 29, 32	Areas 9 or 46	Case **1**, Selemon and Goldman-Rakic 1985
			Cases 5, **6**, Yeterian and Pandya 1991
			Case 131, Calzavara et. 2007
PFC_{md}	-11, 45, 6	Area 32	Case **2**, Yeterian and Pandya 1991
			Case **OM35**, Ferry et al. 2000
PFC_{mp}	-5, 22, 47	Area 9m	Case **5**, Selemon and Goldman-Rakic 1985
			Case 78, Calzavara et al. 2007
PGa	-52, -50, 49	Area 7	Case 1B, Yeterian and Van Hoesen 1978
			Case **11**, Selemon and Goldman-Rakic 1985
			Case 5, Cavada and Goldman-Rakic 1991
PGc	-42, -61, 31	Area 7a/Opt	Case **2**, Cavada and Goldman-Rakic 1991
			Cases 19, 22, Yeterian and Pandya 1993
scg25	-4, 17, -8	scg25	Case OM32, Ferry et al. 2000
			Fig. 2, Haber et al. 2006
STS	-55, -10, -16	Anterior Superior Temporal Gyrus	Fig. 2, Yeterian and Van Hoesen 1978
			Case 4, Van Hoesen et al. 1981
			Case **12**, Selemon and Goldman-Rakic 1985
			Case 5, Yeterian and Pandya 1998

Table 2.3 (Continued)
Notes: These cortical regions were selected for having a suspected homology between monkey and human and having at least two replicated monkey tract-tracing injection cases from independent laboratories. Human seed region coordinates were selected using a variety of methods, including human histological probability maps and human motor fMRI tasks. Cases listed in bold type were adapted with permission for use in Figures 2.1, 2.2, 2.12, 2.13, and 2.14. See Methods and figure legends for further details.

The monkey dorsolateral prefrontal cortex injection (PFC_{lp}) was in the dorsal bank of the principal sulcus and shows a central band of connectivity across the putamen and caudate (Fig. 2.12, third column). The corroborating independent observation of this injection pattern is shown in Figure 2.13*B* (first column). This pattern of connectivity in the central band of the putamen and caudate is seen in the corresponding striatal fcMRI map of the dorsolateral prefrontal cortex in the human, as well as in the 7-network parcellation, which assigns this region to the frontoparietal control (orange) network. The anatomy for the PFC_{md}, from an injection of area 32, shows a dorsoventral pattern of connectivity that is particularly strong in the medial edge of the caudate (Fig. 2.12*B*, fourth column). The corroborating independent observation of this medial caudate pattern is seen in the anatomical tracing for PFC_{md} in Figure 2.14*B* (fourth column). The functional connectivity of the estimated human homolog shows a similar dorsoventral pattern covering the ventral caudate and the dorsal edge of the medial caudate assigned to the default network (red) in the 7-network parcellation. Finally, both the anatomy arising from an area 25 injection in the monkey and the functional connectivity for scg25 showed a pattern covering the nucleus accumbens (Fig. 2.12, fifth column), which is assigned to the limbic (cream) network in the 7-network parcellation. These selected cases suggest that functional connectivity is capable of identifying association and limbic, as well as motor-related, corticostriatal circuits.

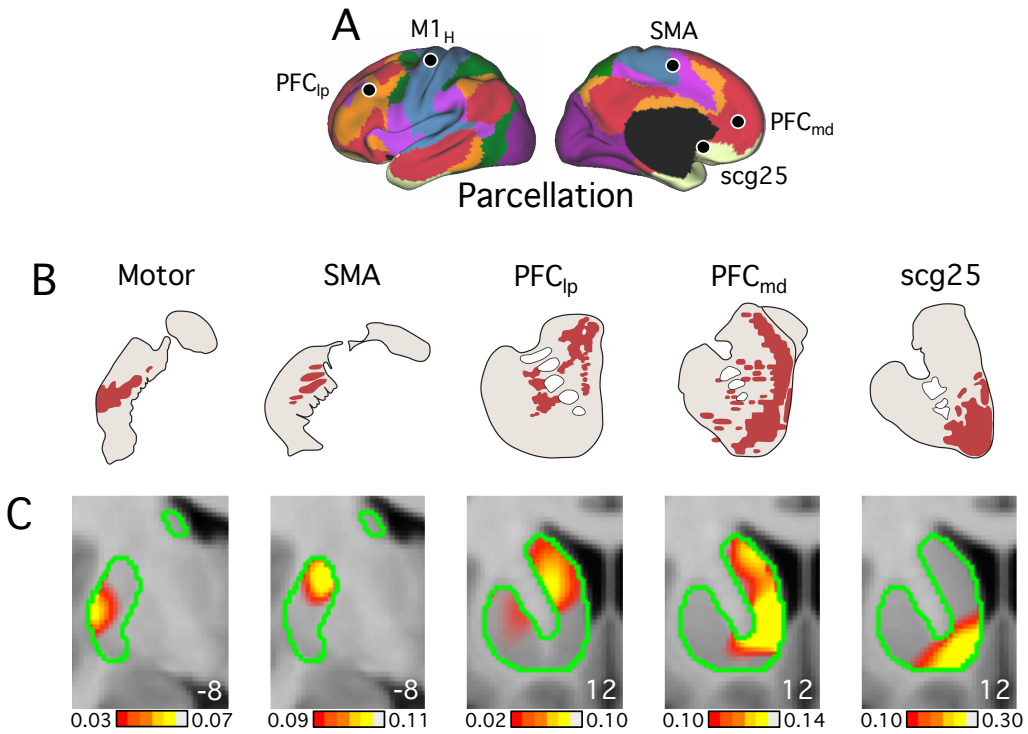

Figure 2.12 Functional connectivity reveals the distinct topography of motor, association, and limbic networks. (A) Five regions with replicated monkey tract-tracings and putative human homologs were selected for comparison: dorsolateral prefrontal cortex (PFC_{lp}), medial prefrontal cortex (PFC_{md}), estimated subgenual cingulate area 25 (scg25), motor cortex, and SMA. All estimated homologies here and in subsequent figures are uncertain but reasonable approximations based on the available literature. (B) A representative anatomical tract-tracing case for each region is shown. Cases illustrated are listed in Table 2.3. (C) Coronal slices show the corresponding functional connectivity generated from the replication sample (n = 500) using the seed regions depicted in A. Slice atlas coordinates are displayed in the lower right. Note the similarity of the patterns between the anatomy and functional connectivity, as well as their correspondence with the motor (blue), ventral attention (violet), frontoparietal control (orange), default (red), and limbic (cream) parcellations in the 7-network parcellation. Anatomical tract-tracing cases were adapted for conformity as described in Fig. 2.1 from the following: Motor (Liles and Updyke 1985) and SMA (Inase et al. 1999), PFC_{lp} (Selemon and Goldman-Rakic 1985) and scg25 (Haber et al. 2006), and PFC_{md} (Ferry et al. 2000). Original tracings from Ferry et al. (2000; PFC_{md} and Fig. 2.14 PFCa) showed the density of axonal synaptic boutons. The redrawing for PFC_{md} included only the overlapping circles in the original tracing.

Functional Connectivity of Association Cortex in Relation to Monkey Anatomy

Previous studies have suggested that anatomically connected cortical areas may project to similar regions of the striatum (Yeterian and Van Hoesen 1978), with complex patterns of

overlap and interdigitation (Selemon and Goldman-Rakic 1985). In Figures 2.13 and 2.14, we explored the possible convergence of correlation patterns within the striatum. In Figure 2.13 we examined 3 distributed cortical regions (Fig. 2.13*A*) that fell within the frontoparietal control network (orange): PFC_{lp}, PGa, and PFC_{mp} (Table 2.3). The fcMRI maps of these 3 cortical regions showed correlations in the dorsal anterior caudate (Fig. 2.13*C*), suggesting that functionally related cortical regions are associated with similar regions in the striatum. While there are limitations in comparing tracings between monkeys, anatomic cases in the dorsal bank of the principle sulcus, LIP, and area 9m, respectively, all show projections to the dorsal anterior caudate (Fig. 2.13*B*).

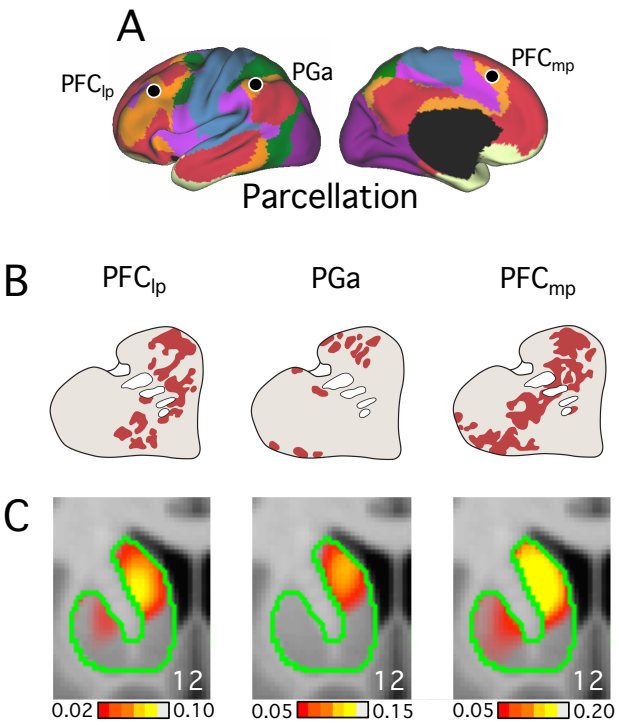

Figure 2.13 Functional connectivity reveals that distributed cortical regions within the frontoparietal control network couple to similar zones of the striatum. (A) PFC_{lp}, anterior area PG (PGa), and dorsomedial prefrontal cortex (PFC_{mp}) were chosen as distributed cortical regions within the frontoparietal control network in order to compare human functional connectivity with monkey anatomy within a single network. (B) A representative anatomical tract-tracing case for each region is shown. Cases illustrated are listed in Table 2.3. (C) Coronal slices show the corresponding functional connectivity generated from the replication sample (*n* =

Figure 2.13 (Continued)
500) using the seed regions depicted in A. Slice atlas coordinates are displayed in the lower right. Note the broad similarity of the patterns both across the regions and between the monkey anatomy and human functional connectivity. Anatomical tract-tracing cases were adapted as described in Fig. 4 from Selemon and Goldman-Rakic 1985.

In Figure 2.14, we compared five cortical regions within the default network (red): the superior temporal sulcus (STS), PGc, PCC, PFC_{md}, and PFC_a (Fig. 2.14*A*; Table 2.3). Injections within putative homologs in the monkey showed a pattern covering the medial edge of the caudate in the anterior half of the striatum for the STS, mPFC, and PFC_a (Fig. 2.14*B*), a pattern that was also seen in the functional connectivity in the human (Fig 2.14*C*). Of note, the STS is a region of expansion between the human and the monkey (Hill et al. 2010), which may explain why the region of the human temporal lobe that shows the medial caudate pattern of connectivity does not extend to the anterior portion of the superior temporal pole, as it is in the monkey. The functional connectivity maps of the PGc and PCC also showed a medial caudate pattern, but unlike the other regions, the corresponding monkey injection pattern covered only the dorsomedial edge of the caudate. These anatomical patterns were also seen by Yeterian and Pandya (1993) for the PGc and Powell (1978) for the PCC (see Table 2.3). We do not understand yet the reasons for this discrepancy. Overall, from these limited cases, these observations support the idea that distributed regions of a functional cortical network are associated with similar regions in the striatum.

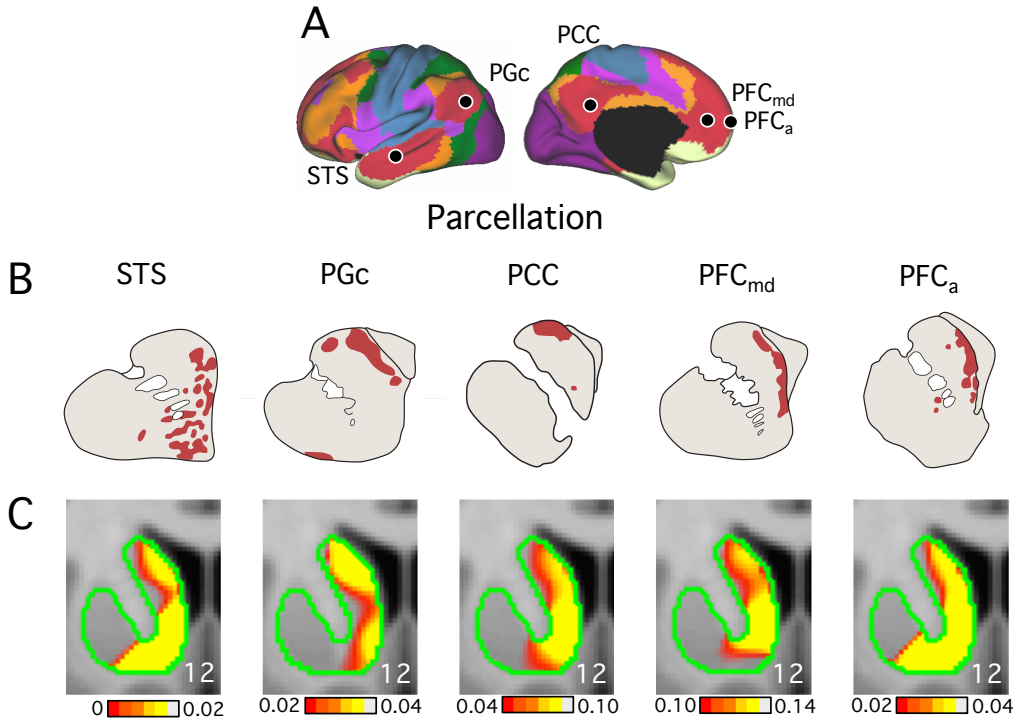

Figure 2.14 Functional connectivity reveals that distributed cortical regions within the default network couple to similar zones of the striatum. (A) Five regions, the superior temporal sulcus (STS), the central portion of area PG (PGc), posterior cingulate cortex (PCC), PFC_{md}, and PFC_a in the frontal pole, with replicated monkey tract-tracings and putative human homologs were selected to compare functional connectivity with monkey anatomy within the default network (red). Cases illustrated are adapted from cases in Table 2.3. (B) A representative anatomical tract-tracing case for each region is shown. (C) Coronal slices show the corresponding functional connectivity generated from the replication sample (n = 500) using the seed regions depicted in A. Slice atlas coordinates are displayed in the lower right. Note the general similarity of the patterns both across the regions and between the monkey anatomy and human functional connectivity. However, several discrepancies are also notable including the differences between PGc and PCC and STS. Anatomical tract-tracing cases were adapted as described in Figs. 2.1 and 2.12 from the following: STS (Selemon and Goldman-Rakic 1985), PGc (Cavada and Goldman-Rakic 1991), PCC (Baleydier and Mauguiere 1980) from Oxford University Press, and PFC_{md} (Yeterian and Pandya 1991) and PFCa (Ferry et al. 2000).

The Striatum Is Further Divided According to Correlations with More Specific Distributed Cortical Networks

Beyond what can be gleaned from monkey-human comparisons, a detailed analysis of the human striatum reveals a complex organization that may reflect the presence of multiple large-scale circuits. This feature is best illustrated by examining the 17-network parcellation, which

generally appears to be a fractionation of the coarser 7-network striatal parcellation. For example, the default network (red) of the 7-network parcellation fractionates into two association networks in the 17-network parcellation. To determine the specificity of this coupling (labeled as red and yellow), we placed seed regions in distributed cortical regions of the two separate association networks in the 17-network model. These consisted of seed regions in the lateral and medial frontal cortex, the PCC, and the parietal cortex (Fig. 2.15; Table 2.4). Functional connectivity maps of these seed regions from the replication sample revealed that the cortical regions in the first association network (red) were preferentially correlated to the dorsal caudate (Fig. 2.15*A*), while the cortical regions in the second association network (yellow) were preferentially correlated to the ventral caudate (Fig. 2.15*B*). The specificity of these correlations suggests that subnetworks (e.g., the red and yellow association networks of the 17-network cortical parcellation) might form distinct circuits with the striatum.

Table 2.4 Locations of Seed Regions Used for Functional Connectivity of Distributed Cortical Networks

Cerebral Cortex	Left Hemi Coordinates
PCC	-3, -49, 25
PFC_m	-7, 46, -2
PFC_{dp}	-44, 15, 48
PFC_v	-55, 24, 13
PGa_v	-54, -54, 35
PGp_{dp}	-43, -70, 43

Notes: Left hemisphere cerebral cortical seed regions were obtained from Yeo et al (2011) except for anterior ventral area PG (PGa_v) and the dorsal posterior portion of posterior area PG (PGp_{dp}), which were selected from the cortical regions in the yellow association network in the 17-network parcellation of the discovery dataset. They were named based on probabilistic histological maps of nearby areas (Caspers et al. 2006; Geyer 2004).

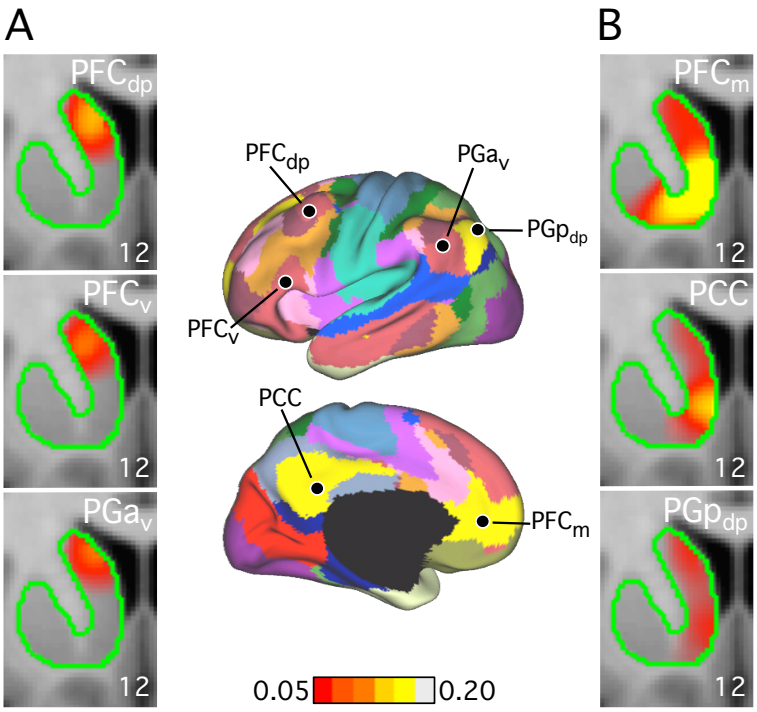

Figure 2.15 Functional connectivity reveals that interdigitated cerebral association networks couple to nearby but preferentially distinct zones of the striatum. Two association networks that each comprises of distributed regions within the cortex (labeled red and yellow) in the 17-network parcellation were selected to examine fine-grained features of corticostriatal organization. The center image shows three seed regions distributed across the brain for each network (Table 2.4). Functional connectivity was computed using the replication sample (n = 500). (A) The functional connectivity of PFC_{dp}, PFC_{v} and PGa_{v} from the red association network converge on similar zones of dorsal caudate head (shown in coronal slice y = 12). (B) By contrast, the functional connectivity of PGp_{dp}, PCC, and PFC_{m} from the yellow association network converge upon similar zones of the ventral caudate head. Note that spatially juxtaposed cerebral regions (e.g., PG_{av} and PGp_{dp}) coupled to distinct striatal zones consistent with their belonging to separate large-scale cerebral networks.

Discussion

This study characterized the functional organization of the human striatum based on intrinsic functional connectivity to the cerebral cortex. We confirmed the motor zones of the posterior putamen and observed the inverted somatomotor topography in agreement with monkey anatomy. Our results also agree with prior models that divide the striatum into broad functional territories of reward, cognition, and motor function. With the use of detailed analyses of cerebral networks provided by our companion paper (Yeo et al. 2011), we constructed a fine-grained functional map of the complete striatum. Results revealed that the majority of the human striatum's subdivisions are linked to cerebral networks involving distributed regions of association cortex. While gradients dividing striatal zones among reward, cognitive, and motor functions are broadly correct, details of striatal organization present a more complex organization that may parallel the complex interdigitation of large-scale association networks in the cerebral cortex and their projections to overlapping zones within the striatum. In the following sections, we discuss these points in greater detail, as well as caveats and limitations of these striatal parcellation maps.

The Striatum Is Coupled to Multiple, Distinct Functional Networks in the Cerebral Cortex

Examining the full striatal parcellation suggested that the striatum is coupled to multiple functional networks within the cerebral cortex. At the broadest level, the parcellation is consistent with models of striatal organization based on monkey tract-tracing studies (Haber et al. 1994; Parent 1990; see also Fig. 2.12): motor-related subdivisions localized to the posterior putamen (blue in Fig. 2.4), a limbic-related subdivision localized to the ventral striatum (cream

in Fig. 2.4), and an extensive central band of territory spanning the anterior caudate and putamen linked to association cortex (orange and red in Fig. 2.4). Tracing studies of the output pathways of the basal ganglia show that they maintain the broad functional segregation of the input pathways to the striatum (Alexander et al. 1986; Middleton and Strick 2002; Strick et al. 1995). Human DTI studies have illustrated a convergent pattern: a dorsal to ventral gradient of connections in the anterior striatum from the dorsal PFC to the orbital frontal cortex, and an anterior to posterior gradient of association to motor cortical connections in the putamen (Bohanna et al. 2011; Cohen et al. 2008; Draganski et al. 2008; Leh et al. 2007; Lehéricy et al. 2004). The present striatal parcellations provide further information with a comprehensive view of the functional architecture of the striatum. For example, the striatal parcellations revealed that the majority of the striatum is dedicated to association cortex (e.g., the frontoparietal control and default network regions). Unlike the motor and ventral attention network zones in the striatum that are localized in the putamen, the striatal association zones span the entire longitudinal extent of the striatum and claim territories in both the caudate and putamen. This may reflect the limited extent of the motor network versus the parallel, distributed association networks that dominate the human cerebral cortex.

Despite the similarity of the parcellations to the monkey anatomy for motor, limbic, and association networks (Figs. 2.12-2.14), there were a few discrepancies for the dorsal attention and visual networks in the 7-network parcellation. The dorsal attention network (green) was present in a region in the right posterior ventral putamen (Fig. 2.4, coronal slice y = -18 and axial slice z = -6). A relaxed striatal mask showed that the posterior caudate was also assigned to the dorsal attention network. These parcellation assignments agree with monkey anatomical projections from FEF and SEF, regions that participate in the dorsal attention network. However,

there are also projections from FEF and SEF to the anterior dorsal caudate, often also into the internal capsule and the medial dorsal putamen, which were not seen in the parcellation (Stanton et al. 1988 Cases PER, GNA, and TRB; Künzle and Akert 1977 Case 73-228; Yeterian and Pandya 1991 Case 9; Parthasarathy et al. 1992 Cases M1, M2, M3, M5; Calzavara et al. 2007 Cases 478, 96, and 184). Examination of the fcMRI correlations from regions in the dorsal attention network revealed that the absence of these networks in the parcellation was due to relatively low-level striatal correlations that did not survive the winner-take-all strategy when creating the parcellation. For example, the fcMRI map of estimated human FEF showed weak correlations to the anterior dorsal striatum, which were not represented in the parcellation, but correlations to the posterior ventral putamen were sufficiently strong enough to be represented in the parcellation.

There was also an absence of the visual network (purple) in the 7-network parcellation. A relaxed striatal mask showed a few voxels assigned to the visual network in primarily bilateral posterior ventral putamen and the tail of the caudate, as well as the anterior-most portion of the head of caudate. Examining the underlying fcMRI correlations from striate and extrastriate cortices yielded unexpected results. The fcMRI map of V1 showed weak correlations throughout the striatum, while the maps of extrastriate cortex, including from the estimated human MT+ complex, showed virtually no correlation in the striatum (except for weak correlations in the posterior putamen from seed regions in V3 and V4). This is in direct contrast to monkey anatomical tract-tracings that detected corticostriatal projections from extrastriate cortex, but not V1 (Maunsell and Van Essen 1983; Saint-Cyr et al. 1990; Ungerleider et al. 1984). The correlations seen from V1 may be due to signal bleeding from correlations in the lateral

geniculate nucleus and pulvinar of the thalamus. However, at present, we do not have an explanation for the absence of correlation from extrastriate cortex.

Distinct Striatal Zones Are Preferentially Coupled to Separate Networks Within Association Cortex

In order to interpret our results for association cortex, we qualitatively compared the human results to the available tract-tracing studies in the monkey (Table 2.3). As a heuristic display of correspondence, Figure 2.12 shows major zones of the human striatum identified with fcMRI as compared to examples from reproduced patterns in the monkey literature. Several of these striatal subdivisions linked to association cortex were explored in detail. One caveat to note is that the striatum is characterized by interdigitated projection zones (Selemon and Goldman-Rakic 1985). At the level of our resolution, this overlap may limit what we can reveal with fcMRI. Nonetheless, several observed patterns suggested that the majority of the human striatum may be linked to distinct large-scale cerebral association networks and further that distinct zones of the striatum are coupled to the distributed regions that comprise each large-scale network.

The central caudate head extending into the medial putamen. One often-observed pattern in the monkey literature arises from tracer injections in the dorsolateral prefrontal cortex. Injections in areas 9 and 46 typically project strongly to the caudate head extending into the medial putamen. The caudate projections continue throughout the body and tail but largely spare the most medial aspects of the caudate (Calzavara et al. 2007; Haber et al. 2006; Selemon and Goldman-Rakic 1985; Yeterian and Pandya 1991). Figure 2.12 illustrates that a dorsolateral prefrontal seed region (PFC_{lp}) couples to a central zone of the human striatum that can be distinguished from the coupling pattern of a medial prefrontal cortex seed region (PFC_{md}) that

covers the medial wall of the caudate. The striatal zone coupled to dorsolateral prefrontal region PFC_{lp} is associated with the frontoparietal control network (orange network in Fig. 2.4). The dorsolateral prefrontal cortex has previously been associated with a similar band of territory across the caudate and putamen using DTI (Draganski et al. 2008; Leh et al. 2007; Lehéricy et al. 2004) and VBM (Cohen et al. 2008), suggesting that this robust pattern can be observed using multiple techniques.

Of further interest, the striatal zone linked to the frontoparietal control network may receive projections from parietal association cortex. Much like injections of prefrontal areas 9 and 46, injections at or near parietal area 7 include projections through the caudate (Cavada and Goldman-Rakic 1991; Yeterian and Van Hoesen 1978; Yeterian and Pandya 1993). Figure 2.13 illustrates that cortical association regions distributed throughout the frontoparietal control network, including parietal association cortex (PG_a), have similar functional coupling patterns in the striatum.

Medial head of the caudate extending along the medial wall. In contrast to the central anterior striatum that couples with the frontoparietal control network (Fig. 2.12; PFC_{lp}), the medial wall of the anterior caudate shows specific coupling with the medial prefrontal cortex (Fig. 2.12; PFC_{md}), a region assigned to the default network in the 7-network parcellation. This pattern was also seen with VBM (Cohen et al. 2008). As with the frontoparietal control network, distributed cortical seed regions within the default network, including parietal region PGc, each show a coupling pattern that involves the medial head of the caudate, in most cases along the dorsoventral extent of the medial wall (Fig. 2.14).

Neighboring striatal zones couple to different association networks. In addition to the single injection case studies presented in Figures 2.12, 2.13, and 2.14 illustrating the coupling of

striatal zones to distributed cortical networks, several studies have examined differing corticostriatal projection patterns in adjacent striatal zones. Through a series of double-labeling cases, Selemon and Goldman-Rakic (1985) showed that dorsolateral prefrontal cortical projections terminate in the central portion of the caudate head extending into the medial putamen (their case 16; highly similar to case PFC_{lp} illustrated in the present Fig. 2.13). By contrast, orbital frontal projections terminated along the medial wall in a pattern more similar to those observed for the medial prefrontal injections illustrated in Figure 2.14 (PFC_{md} and PFC_{a}). Thus, the medial head of the caudate is linked more with medial and orbital frontal regions than are the central zones of the caudate. All of these projections extend through the anterior-to-posterior axis of the striatum with the medial-to-lateral pattern best visualized in the head of the caudate.

Cavada and Goldman-Rakic (1991) further report a telling set of tracing injections that contrast 7a/Opt with 7ip within parietal association cortex. An injection at or near 7a/Opt displayed overlapping, but medially located projections to those from 7ip in the dorsal caudate head, paralleling the human parcellation boundary between the default network and the frontoparietal control network. We suspect that the injections of 7a/Opt fall within the monkey homolog of the default network: the posterior portion of 7a that comprises Opt in the monkey is connected to the parahippocampal gyrus and posterior cingulate, and minimally so with distant sensory and motor regions (e.g., Andersen et al. 1990 Case 5; Barnes and Pandya 1992 Cases 1 and 2; Cavada and Goldman-Rakic 1989 Case 2; Mesulam et al. 1977 Case 1). However, while the 7a/Opt projections to the striatum fall medial to those arising from 7ip, they do not extend down the medial wall (e.g., also see Yeterian and Pandya 1993 Case 22) as seen from injections in other posteriorly located (putative) homologs of the default network in monkeys (Fig. 2.14,

PGc and PCC). Nonetheless, there is a medial-to-lateral gradient for parietal regions that, like prefrontal cortex, roughly divides the anterior caudate between the estimated anatomy of the default network and frontoparietal control network.

This medial-to-lateral distinction divides the striatum based on large-scale networks that each possess prefrontal and parietal components. Selemon and Goldman-Rakic (1985, their Fig. 15; 1988, their Fig. 2) suggested that projections from the posterior parietal cortex and dorsolateral prefrontal cortex are located preferentially in separate regions of the striatum. Despite the apparent discrepancy with our data, it is possible that these two models of organization are consistent if one considers the overlap between the posterior parietal and dorsolateral prefrontal projections (Selemon and Goldman-Rakic 1985, their Fig. 9) and the possibility that these injections cover different association networks, each with their distinct striatal projection zones.

Striatal zones distinguish juxtaposed cerebral association networks. The above discussion highlights evidence that distinct large-scale networks of association cortex are coupled to adjacent but distinct zones of the striatum. This principle can be further extended. Using the fine-parcellated segmentation of the cerebral cortex as a guide, distributed regions that fall within anatomically adjacent (but functionally distinct) networks were shown to have subtly different coupling patterns in the striatum. Figure 2.15 displays an example. Two sets of regions are plotted that each fall within a separate distributed large-scale association network. While these two sets of regions show overlapping functional coupling patterns within the striatum, a consistent difference emerges with one network preferentially coupled to the dorsal medial head of the caudate (Fig. 2.15*A*) and the second network preferentially coupled to the ventral medial head of the caudate (Fig. 2.15*B*). This difference in preferential coupling extends to the

juxtaposed parietal regions PGa_v and PGp_{dp}. It is also of interest that the regions of the default network most closely associated with limbic structures (PCC, PFC_m, and PGp_{dp}) are linked to striatal zones that fall between the nucleus accumbens and striatal zones linked to the dorsolateral prefrontal cortex (the central caudate head). These findings reinforce the idea that distinct large-scale networks, which comprise the majority of the human cerebral mantle, are coupled to distinct zones of the striatum. Moreover, the widely distributed regions within each cerebral network show similar functional coupling within the striatum.

Basis of Striatal Coupling to Distributed Cerebral Regions

Evidence from studies examining retrograde tracer injections in the striatum anticipates the results we illustrate in the human. Arikuni and Kubota (1986) showed that retrograde injections into the ventromedial caudate of the monkey striatum lead to tracer uptake distributed in the OFC, lateral frontal lobe, and temporal lobe (parietal and medial frontal cortices were not reported). In the cat, Rosell and Gimenez-Amaya (1999) showed that retrograde injections in the dorsal anterior caudate result in labeled neurons in distributed frontal, parietal, and temporal cortices. In a comprehensive set of tracings in the rat, McGeorge and Faull (1989) showed that retrograde injections in the striatum lead to tracer uptake in distributed regions of the neocortex, mesocortex, and allocortex. We show here in humans that functional connectivity from a single striatal seed region produces a distributed pattern of cortical correlations (Fig. 2.8). DTI studies have also shown that seed regions of the striatum have distributed connections with the cerebral cortex (Draganski et al. 2008; Leh et al. 2007). These combined observations suggest that the striatum is functionally integrated with distributed cortical networks. We cannot, however, observe the microstructural organization and connectivity of these correlations.

Previous studies in the monkey shed insight into the details of convergent projection patterns in the striatum. Yeterian and Van Hoesen (1978) proposed that cortical regions connected to one another share projection zones in the striatum. Selemon and Goldman-Rakic (1985) refined this observation using double-labeled cases. In their seminal study, they revealed that projections from parietal and frontal cortex only partially overlapped and, when overlap was present, an interdigitated pattern emerged, suggesting that projections between prefrontal and parietal regions do not commonly project to the same striatal neurons. The present results cannot resolve this level of anatomic detail, but the consistent and robust functional coupling patterns observed between distributed cortical regions and common striatal zones raises again the possibility that striatal zones may in some way integrate connections from widely distributed cortical regions. Our results provide a clue that may help understand prior results. As illustrated in Figure 2.15, nearby cerebral regions can participate in distinct cerebral networks and couple to separate striatal zones. The adjacency of these cortical networks and their striatal targets may partially explain the limited overlap observed by Selemon and Goldman-Rakic in their double-labeled cases. Although these injections were confirmed to be in anatomically connected cortical regions, they each tended to cover a large territory that might include multiple areas with diverse connectivity profiles. Thus partial overlap in the striatum may result when the injections into frontal and parietal regions sample distinct combinations of cerebral networks.

Caveats and Limitations

It is important to note that measuring functional connectivity is not the same as measuring anatomic connectivity, thus limiting the conclusions that can be drawn from our work (previously discussed in Buckner et al. 2011, Yeo et al. 2011). Limitations include the inability

to determine the directionality of the connectivity and to interpret our striatal parcellations as rigid representations of anatomic connectivity. It is intriguing how well human striatal functional connectivity corresponds to gross topographic patterns from monkey anatomic tracings. Nonetheless, we feel confident that there will be discrepancies and boundary conditions to this correspondence because functional connectivity is constrained but not fully dictated by anatomic connectivity.

A major limitation of the present work is resolution, which prevents the observation of striatal microstructure, including the overlap or interdigitation of connections in striosomes and matrisomes. In addition, in a structure with observed interdigitation of projections, our winner-take-all strategy may be misleading in regions with a high heterogeneity of connections. For these reasons, we recommend viewing the parcellations with the aid of the confidence maps, as well as examining the underlying functional connectivity for any particular region of interest. The strength of these parcellation maps is that they give a comprehensive view of the functional territories of the striatum; however, their utility is limited for certain questions.

Resolution also impacted our results in a way that is particularly problematic for the striatum. The striatum is near to the cerebral cortex, in particular the putamen and the insula, resulting in signal bleeding across the cortical-striatal boundary that can be partially, but not entirely, mitigated (Figs. 2.10 and 2.11). We suspect that the pink network assignment in the anterior putamen of the 17-network parcellation (Fig. 2.5) is a result of signal bleeding from the adjacent insula. For this reason, we are least confident about the details of our parcellations around the dorsal putamen. High resolution functional imaging (e.g., ~1 mm) in individual subjects at high field may circumvent this issue in future studies.

A further limitation of our work is that we only mapped the striatal coupling to the

cerebral cortex. There are strong projections to the striatum from subcortical structures, which we have not considered here, such as the amygdala (Fudge et al. 2002, 2004; Russchen et al. 1985) and the cerebellum via the thalamus (Hoshi et al. 2005). We refer interested readers to another study examining the functional connectivity of the amygdala to the striatum (Roy et al. 2009).

Conclusions

Specific striatal zones are functionally coupled to distinct cerebral networks. As seen by prior studies, the posterior putamen is dedicated to motor function and the nucleus accumbens to limbic function. The remaining majority of the striatum is connected to parallel, distributed association networks that may underlie contributions of the striatum to higher cognitive functions.

Experimental Procedures

Overview

The present study consists of three analyses. First, the feasibility of mapping specific corticostriatal circuits using fcMRI was explored by examining the correlations between the motor cortex and the striatum, for which there are strong predictions from monkey tract-tracing studies.

Having observed that fcMRI can reveal motor-related topographical properties of the striatum, we next comprehensively mapped the functional connectivity between the striatum and the entire cerebral cortex. This was done by assigning each striatal voxel to its most strongly correlated cortical network in 500 subjects (discovery sample) and replicating the topography in an independent sample of 500 subjects (replication sample). The cortical networks were defined by a clustering method developed in our companion paper (Yeo et al. 2011) that parcellates the cerebral cortex into networks of regions that have similar profiles of corticocortical functional connectivity. After demonstrating the reliability of the maps, all 1,000 subjects were used to provide a best estimate of the striatal topography based on a coarse (7-network) and fine (17-network) parcellation of the cerebral cortex.

In the third analysis, we explored striatal networks in greater detail. We assessed the parcellations using a quantitative analysis of corticostriatal specificity and qualitative comparisons of how well seed-based cortical fcMRI maps agreed with monkey anatomical studies. We compared the human functional connectivity estimates to monkey anatomical cases located across the motor, association, and limbic networks. We also compared cases within the same association networks. Finally, we examined subdivisions of the association networks in the

17-network parcellation of the striatum in greater detail to explore finer distinctions suggested by the functional connectivity analysis. For all analyses, seed regions were identified in the discovery sample or an outside source such as an fMRI task, and functional connectivity was quantified in the independent replication sample to avoid bias.

Participants

One thousand paid participants ages 18 to 35 were clinically normal, English speaking young adults with normal or corrected-to-normal vision. The subjects are the same individuals as reported in Yeo et al. (2011) and Buckner et al. (2011). Subjects were excluded if their slice-based fMRI signal-to-noise ratio (SNR) was low (< 100; Van Dijk et al. 2012), artifacts were detected in the MR data, their self-reported health information indicated a history of neurological or psychiatric illness, or they were taking psychoactive medications. The subjects were imaged during eyes open rest (EOR) and divided into two samples (each n = 500) matched for age and gender: discovery (mean age = 21.3 yr, 42.6% male) and replication (mean age = 21.3 yr, 42.8% male) samples. Participants provided written informed consent in accordance with guidelines set by institutional review boards of Harvard University or Partners Healthcare.

MRI Data Acquisition

All data were collected on matched 3T Tim Trio scanners (Siemens, Erlangen, Germany) using the vendor-supplied 12-channel phased-array head coil. The functional imaging data were acquired using a gradient-echo echo-planar imaging (EPI) sequence sensitive to blood oxygenation level-dependent (BOLD) contrast (Kwong et al. 1992; Ogawa et al. 1992). Whole-brain coverage was achieved with 47 3mm-slices aligned to the anterior-commissure posterior-

commissure (AC-PC) plane using automated alignment (van der Kouwe et al. 2005). Structural data included a high-resolution multiecho T1-weighted magnetization-prepared gradient-echo image (multiecho MP-RAGE; van der Kouwe et al. 2008). Functional imaging parameters were: TR = 3000 ms, TE = 30 ms, flip angle = 85º, 3 x 3 x 3-mm voxels, FOV = 216 and 47 slices. Structural scan (multiecho MP-RAGE) parameters were: TR = 2200 ms, TI = 1100ms, TE = 1.54ms for image 1 to 7.01 ms for image 4, FA = 7º, 1.2 x 1.2 x 1.2-mm and FOV = 230. During the functional scans, subjects were instructed to stay still, stay awake, and keep their eyes open. Resting-state data acquisition is described in detail in Yeo et al. (2011).

Functional MRI Data Preprocessing

fMRI data were preprocessed as described in Yeo et al. (2011). Briefly, the first four volumes of each run were discarded, slice-acquisition-dependent time shifts were compensated per volume using SPM2 (Wellcome Department of Cognitive Neurology, London, UK), and head motion was corrected using rigid body translation and rotation using FMRIB Software Library (FSL; Jenkinson et al. 2002; Smith et al. 2004). The data underwent further preprocessing specific to functional connectivity analysis, including low-pass temporal filtering, head-motion regression, whole-brain signal regression, and ventricular and white matter signal regression (Van Dijk et al. 2010).

Structural MRI Data Preprocessing and Functional-Structural Data Alignment

Structural data preprocessing and functional-structural data alignment were the same as described in Yeo et al. (2011) and Buckner et al. (2011). The structural data were processed using automated algorithms provided in the FreeSurfer version 4.5.0 software package

(http://surfer.nmr.mgh.harvard.edu), which reconstructed a surface mesh representation of the cortex from each individual subject's structural image and registered each subject to a common spherical coordinate system (Dale et al. 1999; Fischl et al. 1999a, 1999b, 2001; Ségonne et al. 2004, 2007). See Yeo et al. (2011) for details.

The structural and functional images were aligned (Fig. 2.16; similar to Buckner et al. 2011, their Fig. 1, *A* and *B*) using boundary-based registration (Greve and Fischl 2009) available from the FsFast software package (http://surfer.nmr.mgh.harvard.edu/fswiki/FsFast). The resting-state BOLD fMRI data were then aligned to the common spherical coordinate system via sampling from the middle of the cortical ribbon in a single interpolation step (similar to Buckner et al. 2011, their Fig. 1, *A, B, C,* and *E*). Consistent with prior methods (Buckner et al. 2011; Yeo et al. 2011), a 6-mm full-width half-maximum (FWHM) smoothing kernel was applied to the fMRI data in the surface space and the data were downsampled to a 4-mm mesh. Examination of the non-smoothed data revealed noisier but qualitatively similar parcellations as those from the smoothed data.

Hybrid Surface- and Volume-Based Alignment

The cerebral cortex was modeled as a two-dimensional surface to respect its topology and registered to a common spherical coordinate system, as described above. The striatum was modeled as a volume and aligned using a non-linear volumetric registration algorithm in a process analogous to that done for the cerebellum in Buckner et al. (2011; see their Fig. 1, *B* and *D*). For each subject, the structural volume was jointly deformed to a probabilistic template and segmented into one of multiple brain structures (Fischl et al. 2002; 2004; see Buckner et al. 2011 for more details). The resulting deformation field, together with the correspondence between the

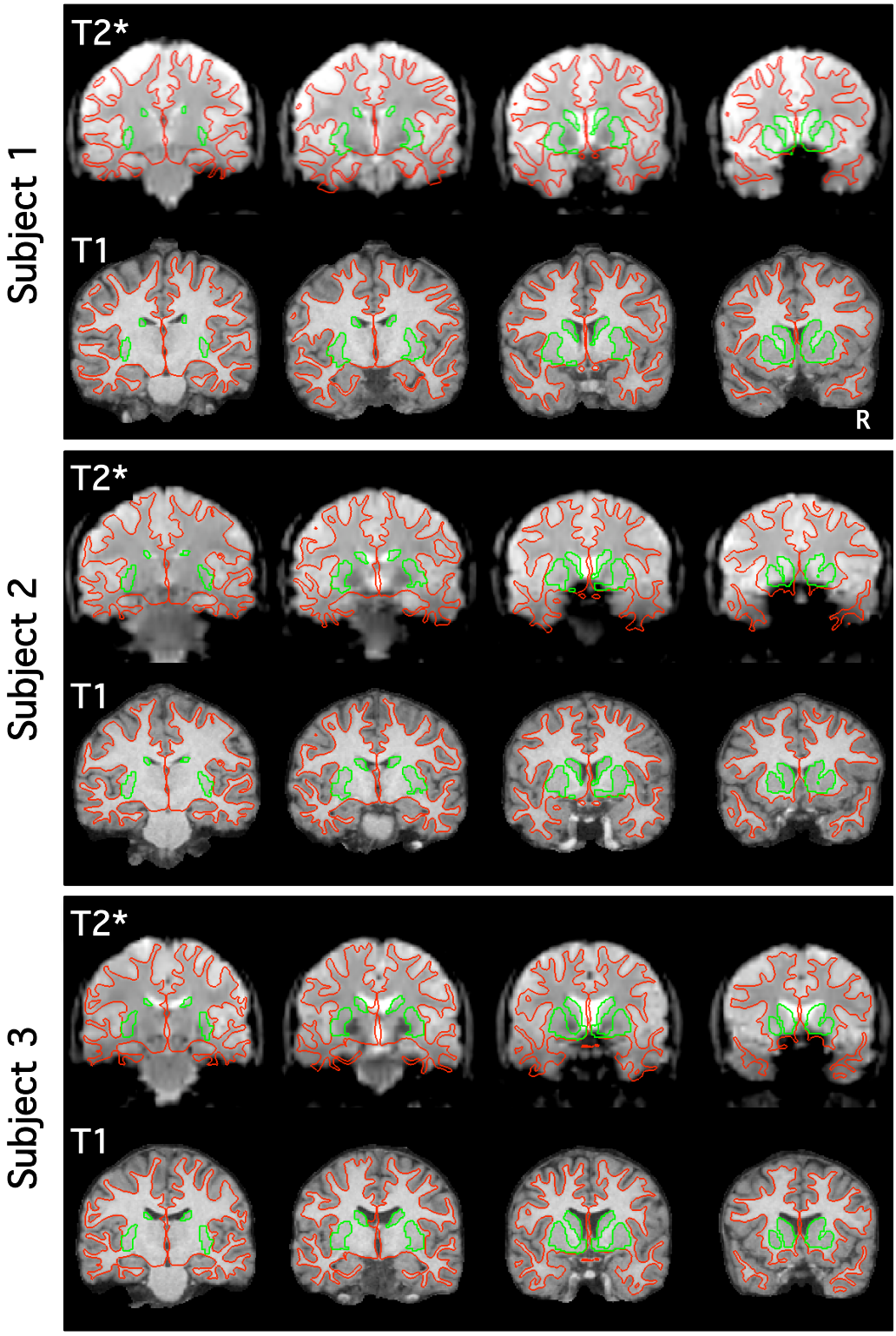

Figure 2.16 Examples of within-subject surface and volume extraction. Examples of the extracted cerebral cortex surface and striatal boundaries are shown for three typical subjects within their native space. The red line delineates the estimated boundary of the cerebral cortical surface between the gray and white matter. The green line shows the estimated edge of the

Figure 2.16 (Continued)
striatum tailored to each individual subject's T1-weighted image. The green line is superimposed on the T2* images to illustrate deviations in the BOLD data. Imperfections are apparent in the BOLD data, particularly in the ventral striatum, which lies near to the signal dropout region of the orbital frontal cortex.

structural-functional data alignment discussed above, was used to transform the subject's fMRI data into the common FreeSurfer nonlinear volumetric space. The normalized volumetric fMRI data within the striatum (defined using a FreeSurfer template mask of the striatum; we note that the tail of the caudate is not included in this mask) were smoothed with a 6-mm FWHM smoothing kernel. The use of this nonlinear deformation resulted in improved intersubject anatomical alignment (Fig. 2.17) as compared to a linear transformation. The normalized FreeSurfer nonlinear volumetric data were transformed into FSL Montreal Neurological Institute (MNI) space (similar to Buckner et al. 2011, their Fig. 1, *D* and *E*) using the spatial correspondence established by running the FSL MNI152 template (Fonov et al. 2011) through the FreeSurfer pipeline.

Quality Control

Registered functional and structural data were visually inspected for proper registration. Figure 2.16 shows good correspondence between the T1 and T2* registration within the native space for three typical subjects (similar to Buckner et al. 2011, Fig. 1, *A* and *B*). Intersubject volumetric registration was also inspected for proper alignment of the striatum across subjects (similar to Buckner et al. 2011, Fig. 1, *B* and *D*). Figure 2.17 illustrates this with normalized T1 images for three typical subjects.

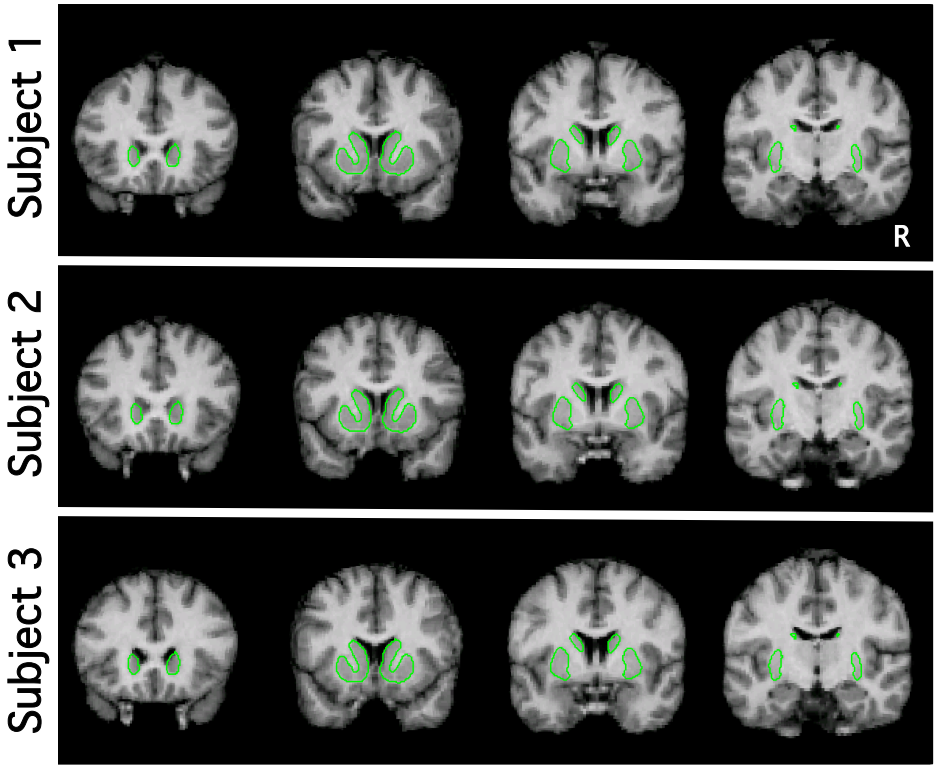

Figure 2.17 Examples of between-subject striatal alignment. Volumetric images are shown for the registered structural data from three typical subjects. The green line represents the striatal edge estimated from the group structural template and is superimposed identically across the subjects to illustrate each individual's registration to the group template. Each subject's striatum is well registered in relation to the template. Close examination reveals subtle differences between subjects reflecting alignment errors on the order of a few millimeters.

Mapping Between Surface- and Volume-Based Coordinates and Visualization

Spatial correspondence between the FreeSurfer surface and volumetric coordinate systems was established by averaging over 1,000 subjects the composition of the transformation from each subject's native space to the FreeSurfer surface space and the transformation from the FreeSurfer nonlinear volumetric space. Using the spatial correspondence between FSL MNI152 space and FreeSurfer nonlinear volumetric space, we were able to estimate MNI atlas coordinates (Evans et al. 1993; Fonov et al. 2011). All analyses were performed in FreeSurfer surface and volumetric spaces and displayed in MNI atlas space for the volume and the left and right inflated PALS cortical surfaces using Caret software (Van Essen 2005) for the surface.

Regression of Adjacent Cerebral Cortex Signal when Analyzing the Striatum

The physical proximity of the striatum to the insula and orbital frontal cortices resulted in the blurring of fMRI signal at the cortical-striatal boundary, particularly between the putamen and insula. In order to eliminate the cortical signal, we regressed out the mean signal of the cortical voxels that were within 4.0 (8 mm) or 4.5 (9 mm) voxels from the left or right putamen, respectively (see Buckner et al. 2011 for use of this general approach for the cerebellum). The distances were asymmetric to allow for approximately equal numbers of left and right cortical voxels to contribute to the regression. The regression took place on the individual subject level: the fMRI signal within the left and right cortical regression masks were averaged and regressed out from the smoothed fMRI data within the striatum.

Signal-to-Noise Ratio (SNR) Maps

Temporal SNR of the motion corrected fMRI time series was computed for each voxel in the subject's native volumetric space by averaging the signal intensity across the whole run and dividing it by the standard deviation over time. The SNR was averaged across runs within subject when multiple runs were available. The SNR was then averaged across the 1,000 subjects from the core dataset and displayed in the volume to visualize the SNR of the striatum (Fig. 2.18). SNR was good throughout most of the striatum; signal dropout occurred primarily in and around the ventral striatum / nucleus accumbens. Another issue to keep in mind is that there may be insufficient power to accurately characterize striatal regions that are coupled to cerebral regions with low SNR, such as the orbital frontal cortex (see Fig. 3 of Yeo et al. 2011).

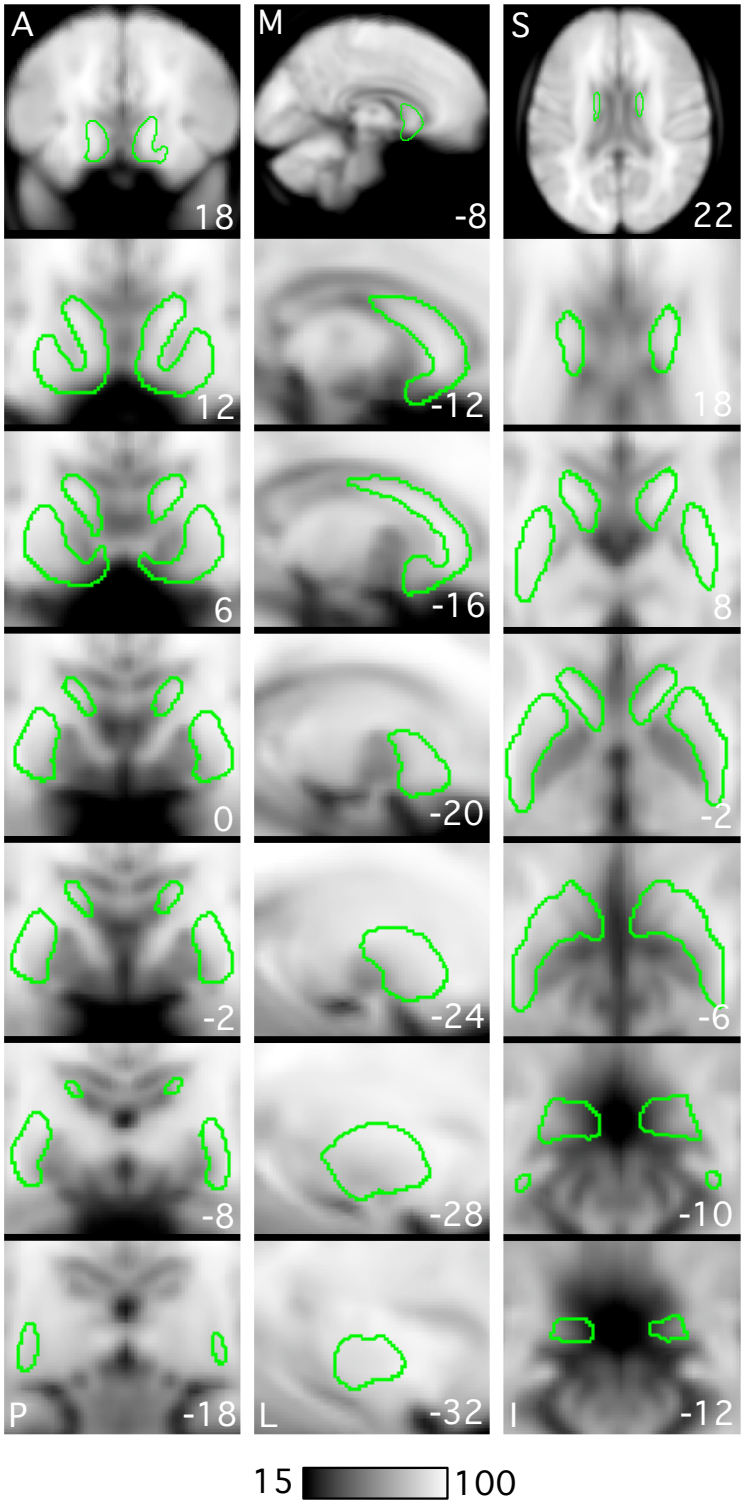

Figure 2.18 Signal-to-noise ratio (SNR) maps of the functional data from the full sample (*N* = 1,000). The mean estimate of the BOLD fMRI data SNR is illustrated for coronal (left), sagittal (middle), and transverse (right) images. The sagittal sections are of the left hemisphere. A = anterior, P = posterior, M = medial, L = lateral, S = superior, and I = inferior. The slice coordinate in the MNI atlas space is located at the bottom right of each panel. The estimate of the

Figure 2.18 (Continued)
striatal edge from the group template is illustrated in green (similar to Figure 2.17). Note the generally high and uniform SNR except for regions of ventral striatum.

Striatum Parcellation and Confidence Maps

Unlike the cerebellum, which has relatively specific functional connectivity correlations to cerebral networks, the striatum has less specific correlations that in some places spill across cortical network boundaries (see Fig. 2.8 for illustration), which may be due to the higher impact of signal blurring on the structurally smaller striatum. For this reason, using the method employed for the cerebellum parcellation (Buckner et al. 2011) leads to striatal voxel assignments that, upon examining the underlying functional connectivity, do not reflect the strongest correlations of that voxel. For example, voxels in the ventral putamen (y = -10) were assigned to the default network because of extensive low-level correlations to regions of the default network, even though the strongest correlations resided in the motor network. In order to create parcellations representing the most strongly correlated network, we chose an alternative method of parcellation for the striatum. For each striatal voxel, the top 25 most correlated cortical vertices were selected and the network with the most vertices belonging to it became the assigned network for the striatal voxel. For example, within the top 25 cortical vertices for a striatal voxel, if 13 resided in one network and 12 in another, that striatal voxel would be assigned to the first network. 25 was selected as the number of top cortical vertices to use because this led to parcellations that most accurately reflected the strongest underlying correlations. This approach mostly affected the ventral putamen at around y = -10, with a portion of the striatal voxels switching from default (red) to motor (blue) assignment. Since striatal voxels varied on how well they belonged to their assigned networks, a confidence map was calculated in which the fraction of the top 25 correlated cortical vertices belonging to the

assigned network was computed for each striatal voxel (e.g., in the above example of a striatal voxel with 13 vertices in the first choice network and 12 vertices in the second choice network, the confidence value = 13/25 = 0.52).

Seed Region Correlation Estimates Between the Striatum and Cerebrum

Striatal fcMRI maps for specific cerebral seed regions were obtained by computing the Pearson's product moment correlation between the surface region's preprocessed resting fMRI time course and the time courses of striatal voxels. Each cerebral seed region included a single surface vertex (~4 x 4 mm) but should be considered spatially more extensive because of spatial smoothing. Conversely, a correlation map from each striatal seed region was obtained by computing the correlation between the voxel's time course and the time courses of all vertices on the cerebral cortical surface. Striatal seed regions were restricted to a single voxel (2 x 2 x 2 mm) and affected by spatial smoothing. To obtain group-averaged correlation *z*-maps, the correlation maps of individual subjects were converted to individual subject *z*-maps using Fisher's *r*-to-*z* transformation and then averaged across all subjects in the group. The Fisher's *r*-to-*z* transformation increases normality of the distribution of correlations in the sample. For subjects with multiple runs, the individual subject *z*-maps were first averaged within the subject before submitting to the group average. An inverse Fisher's *r*-to-*z* transformation was then applied to the group-averaged correlation *z*-map, yielding a group-averaged correlation map.

Selecting Regions for Functional Connectivity Analysis

The striatal fcMRI maps of the foot and tongue representations (Fig. 2.1*B*) were created using cerebral seed regions corresponding to the foot and tongue representations in the motor

cortex based on an fMRI motor task as described by Buckner et al. (2011). The foot and tongue single voxel striatal seed regions (Fig. 2.1*B*) were chosen from these maps from regions that had strong and minimally overlapping foot and tongue correlations. These seed regions were used to create cortical fcMRI maps from the foot and tongue representations in the striatum (Fig. 2.1*C*). Seed region coordinates are reported in Table 2.1.

The striatal fcMRI maps of the SMA and motor hand representations (Fig. 2.2*B*) were created using cerebral seed regions corresponding to the SMA and the hand representation in the motor cortex based on an fMRI motor task from Buckner et al. (2011). The hand region of the motor cortex was chosen to approximately match the monkey anatomical cases shown (Fig. 2.2*A*), in which injections were made in the forelimb regions of the ipsilateral primary motor cortex and SMA of the monkey. The selection of the SMA seed region was guided by the probabilistic histological map of BA6 created from 10 human subjects (Fischl et al. 2008; Geyer 2004). The seed region was selected to be posterior to the anterior commissure, which is suggested by Picard and Strick (1996) to be a rough anatomical boundary line between the pre-SMA and SMA. Single voxel striatal seed regions (Fig. 2.2*B*) were selected within the striatal fcMRI maps derived from the cerebral SMA and the motor hand seed regions and used to create cortical fcMRI maps (Fig. 2.2*C*).

In Figure 2.7, seed region A in the motor zone (blue) was the same as the striatal tongue seed region used in Figure 2.1. Seed region B was selected to be in a relatively high confidence region of the default network zone (red) of the posterior ventral striatum.

The striatal seed regions in Figure 2.8 are representative of their respective networks and selected from high confidence regions (Table 2.2). The cerebral seed regions in Figure 2.9 were selected to consist of multiple seed regions each from the default (red), frontoparietal control

(orange), ventral attention (violet), and dorsal attention (green) networks, with two or three anterior (frontal) and one or two posterior seed regions, as well as one seed region from the limbic network (cream; Table 2.2). The cerebral seed regions in Figure 2.15 (Table 2.4) were placed in distributed regions of the association networks of the 17-network parcellation labeled in red and yellow. Seed regions from Yeo et al. (2011) were used for aMT+, $IPS3_m$, PFC_{la}, PFC_{da}, PFC_{dp}, PCC, PFC_m, PFC_{mp}, PFC_v, PGa, $PrC_{v,}$ and FEF. The remaining seed regions were selected to cover other key cerebral regions. PF_v, PGa_v, PGc, PGp_{dp}, PrCO, and 6_{am} were labeled based on probabilistic histological maps of nearby areas (Caspers et al. 2006; Fischl et al. 2008; Geyer 2004). Seed region scg25, which lies in the limbic (cream-colored) cortical network, was based on the peak scg25 coordinate from a GingerALE meta-analysis of fMRI studies (Fitzgerald et al. 2008) that compared depressed patients versus healthy controls in emotion tasks, such as responding to happy or sad faces. Coordinates reported in the Talairach and Tournoux (1988) coordinate system (2.62, 15.17, -3.42) were converted to FSL MNI152 space (-4, 17, -8; Lancaster et al. 2007).

The comparisons in Figures 2.12, 2.13, and 2.14 were selected as regions for which an approximate comparison could be made between monkey anatomical projections and human functional connectivity. Each region had at least two agreeing monkey tract-tracing cases from independent laboratories (Table 2.3). Our procedure for selecting regions is imperfect because of difficulties in assessing homologies and defining specific areal boundaries, especially in association cortex. Nonetheless, comparisons allowed us to make a qualitative assessment of whether broad organizational properties of the striatum in the monkey parallel those observed in the human.

In Figure 2.12, the motor and SMA anatomical tracing estimates were from injections in

the forelimb regions of the monkey motor cortex (Liles and Updyke 1985 Case Rhesus Monkey) and SMA (Inase et al. 1999 Case San). The corresponding human motor hand and SMA seed regions were the same as those used in Figure 2.2. The PFC_{lp} anatomical tracing estimate was from an injection in the dorsal bank of the principal sulcus (Yeterian and Pandya 1991 Case 6). The corresponding human PFC_{lp} seed region (from Yeo et al. 2011) was located in the middle frontal gyrus and placed centrally to minimize the possibility of being in areas 10 or 8 (Petrides and Pandya 1999). The PFC_{md} anatomical tracing estimate was from area 32 (Ferry et al. 2000 Case OM35). The corresponding human PFC_{md} seed region was placed at or near area 32, just anterior to the genu of the cingulate gyrus. The exact homology of these human and monkey area 32 regions is uncertain because of the expansion of the medial prefrontal cortex in the human and a putative anterior-posterior shift of macaque area 32 (Öngür et al. 2003; see also Buckner et al. 2008). This approximation may be sufficient at our resolution as the region just rostral to the anterior cingulate as well as the zone encompassing a portion of the subgenual anterior cingulate fall within the same functional connectivity network (Yeo et al. 2011). The scg25 anatomical tracing estimate was from an injection in area 25 (Haber et al. 2006). The corresponding human seed region was the same as the one described in the previous paragraph for seed region scg25.

In Figure 2.13, seed regions were placed in distributed regions of a single association network, the frontoparietal control network (orange): PFC_{lp}, PGa, and PFC_{mp} (from Yeo et al. 2011). The anatomical tracings were from Selemon and Goldman-Rakic (1985): areas 9 and 10 (Case 1), area 7 (Case 11), and area 9 medial (Case 5), respectively. In Figure 2.14, the STS anatomical tracing estimate was from an injection in area 22 (Selemon and Goldman-Rakic 1985 Case 12) on the anterior superior temporal gyrus. Because the extent of the expansion of the superior temporal pole in humans is unknown, the corresponding human STS seed region (from

Yeo et al. 2011) was placed in the middle portion of the superior temporal sulcus that showed a similar pattern in the functional connectivity to the anatomy. The PGc injection was made in area 7a of the monkey (Cavada and Goldman-Rakic 1991 Case 2). The corresponding human seed region was placed in the inferior parietal lobule below the intraparietal sulcus, which is more likely to correspond to monkey area 7a or opt. The PCC and PFC_{md} injections were in area 23/PCC (Baleydier and Mauguiere 1980 Case 1) and area 32 (Yeterian and Pandya 1991 Case 2), respectively; the corresponding human seed regions were the same as those described for Figures 2.9 and 2.12, respectively. Finally, the frontal pole injection was in area 10o (Ferry et al. 2000 Case OM38). The human frontal pole seed region (PFC_a) was placed in the medial aspect of estimated area 10p (Öngür et al. 2003), anterior to the PFC_{md} seed region.

The cortical seed region (-40, 4, -2) used to create the fcMRI maps in Figure 2.10 was placed in the ventral attention network (violet) portion of the insula in the 7-network parcellation in order to illustrate the cortical signal bleeding into the striatum.

Distribution of Parcellations and Raw Data

A primary result of our analyses is the parcellation of the striatum into networks. The parcellations in FreeSurfer space are available (http://www.freesurfer.net/fswiki/StriatumParcellation_Choi2012). Movies of the region-based functional connectivity estimates can be downloaded from http://www.youtube.com/choiyeobuckner. The raw fMRI data from the 1,000 subjects in the functional connectivity analysis will be made openly available to researchers using the procedures established by the OASIS data releases (Marcus et al. 2007; 2010) and the 1,000 Functional Connectomes Project (Biswal et al. 2010).

Chapter 3:

Choi, E.Y., Buckner, R.L., and Badre D. (in preparation).

A Functional Hierarchy of Cortical Association Networks

Potentially Mediated by the Striatum.

Summary

Patient lesion and neuroimaging studies have identified a caudal to rostral functional hierarchy in the lateral frontal cortex corresponding to easy to demanding cognitive control. However, monkey tract-tracing studies show that the lateral frontal cortex is reciprocally connected with distributed regions of association cortex, forming multiple large-scale association networks. In this study, we investigated the link between the functional hierarchy localized in the lateral frontal cortex and large-scale, distributed association networks. An overlay of hierarchical cognitive control task activity (from Badre and D'Esposito 2007) with an estimate of human cortical networks (from Yeo et al. 2011) revealed the expected hierarchy in the lateral frontal cortex and a second hierarchy in the parietal cortex. Critically, activity in both hierarchies overlapped with the same association network in an order-specific manner. These results suggest a functional hierarchy of association networks underlying hierarchical cognitive control. We also investigated the possibility of corticostriatal connectivity supporting the functional hierarchy of the lateral frontal cortex. An fcMRI analysis revealed that the functional connectivity between the lateral frontal cortex and the striatum has a rostral to caudal correspondence, but was inconclusive in determining a hierarchical interaction via corticostriatal connections. Overall, our results show that hierarchical cognitive control is subserved, not by a functional hierarchy of local regions, but by a functional hierarchy of association networks; and that the striatum is functionally connected to these association networks, providing a potential means for their hierarchical interaction.

Introduction

Understanding the neural basis of cognitive functions has been challenging due to the complex nature of these functions and the connectivity that underlies them. Progress has been made, however, in the lateral frontal cortex, initially from patient lesion studies that identified its role in executive functions (Milner 1963) and later from neuroimaging studies that showed activation in the lateral frontal cortex during various executive control tasks (Duncan and Owen 2000). Further deconstruction was made from memory and cognitive control studies that identified a functional gradient in the lateral frontal cortex, with caudal regions processing simpler or more concrete cognitive functions and rostral regions processing more complex or abstract cognitive functions (Badre and D'Esposito 2007; Buckner 2003; Koechlin et al. 2003). These regions further appear to be hierarchically organized such that rostral, higher order regions influence the processing of caudal, lower order regions (Badre and D'Esposito 2009). In particular, a study of stroke patients with localized lesions in the lateral frontal cortex showed that patients were impaired in hierarchical cognitive control tasks at and above, but not below, a level corresponding to the lesion's caudo-rostral location (Badre et al. 2009).

Cognitive control studies have underscored the importance of regions in the lateral frontal cortex. However, the prefrontal cortex does not act alone, but rather in concert with other regions. The prefrontal cortex has widespread connections to distributed locations of the association cortex (Yeterian et al. 2012). Based on monkey tract-tracing studies, Goldman-Rakic (1988) suggested that the association cortex is divided into multiple networks, each with reciprocally connected regions in the lateral frontal cortex and other distributed parts of association cortex (Goldman-Rakic 1988; Selemon and Goldman-Rakic 1988). Thus, association

cortex is composed of parallel, distributed association networks with preferentially within-network connections. Supporting this organization, a network parcellation of the human cerebral cortex using intrinsic functional connectivity MRI (fcMRI) showed the presence of parallel association networks consisting of preferentially correlated regions distributed throughout the association cortex (Yeo et al. 2011). The parallel, distributed organization of association networks suggests that cognitive control, and cognitive functions more broadly, arises from the interactions of distributed regions of a network. However, this organization raises the question of how the functional hierarchy of regions in the lateral frontal cortex, discovered to underlie cognitive control, relates to these parallel, distributed association networks.

A second question concerns how the functional hierarchy in the lateral frontal cortex arises. In addition to potential direct cortico-cortical interaction, one way may be through hierarchical interactions between cortico-basal ganglia-thalamic circuits (henceforth called basal ganglia circuits). Animal tract-tracing studies have suggested that there are parallel basal ganglia circuits dedicated to motor, limbic, and cognitive functions (Alexander et al. 1986, 1990). In addition, these studies have shown that the striatum, the input structure of the basal ganglia, appears to receive projections from nearly all regions of the cerebral cortex (except primary visual cortex). This was seen to be true for the human striatum, as well (Choi et al. 2012), suggesting that there may be unique caudo-rostrally arranged basal ganglia circuits specific to higher and lower orders of the functional hierarchy. In addition, there is a great degree of overlap between projections in the striatum (Haber et al. 2006), a possible means for integration across basal ganglia circuits. Thus, hierarchical interactions between the lateral frontal cortex regions may arise from caudo-rostral, order-specific basal ganglia circuits interacting at the level of the striatum.

We addressed the questions above using a combined fMRI and fcMRI approach. fMRI provides an indirect measure of neural activity by measuring changes in the blood oxygenation level-dependent (BOLD) signal following neural activity (Kwong et al. 1992: Ogawa et al. 1992). fcMRI is an analysis method of fMRI data that measures the functional connectivity between brain regions based on their temporal correlation in spontaneous, low-frequency BOLD activity (Biswal et al. 1995; for review, see Fox and Raichle 2007). As an fMRI-based method, the functional connectivity detected by fcMRI is a measure of the functional co-activation of two regions, which is made possible by the polysynaptic anatomical connections between them. Thus fcMRI is a measure reflecting both anatomical connections and functional interactions. fcMRI has been used to identify whole networks in humans (Lee et al. 2012; Power et al. 2011; Yeo et al. 2011), including sensory networks, such as the motor network (Biswal et al. 1995), and distributed association networks (Greicius et al. 2003; Vincent et al. 2006).

In this study, we addressed two questions. Firstly, how does the functional hierarchy in the lateral frontal cortex relate to the parallel, distributed organization of association networks? To investigate this, we compared fMRI task activity from a hierarchical cognitive control study (from Badre and D'Esposito 2007) to a comprehensive estimate of human association networks in 1,000 human subjects using fcMRI (from Yeo et al. 2011). Secondly, does the functional hierarchy in the lateral frontal cortex arise from hierarchical interactions in the striatum between caudo-rostral, order-specific basal ganglia circuits? To address this, we examined the organization of corticostriatal functional connectivity from regions of the lateral frontal cortex hierarchy. We compared the connectivity patterns with two model predictions of their organization, one suggestive of hierarchical interactions and one that is ambiguous. Our goals were to reconcile an apparent conflict between the functional hierarchy of the lateral frontal

cortex and association network organization and to explore the possibility of a basal ganglia mechanism for establishing the functional hierarchy of the lateral frontal cortex.

Results

Cognitive control recruits distributed association regions

Thus far, cognitive control studies have focused on elucidating the role of the lateral frontal cortex in cognitive control. However, monkey tract-tracing studies indicate that the lateral frontal cortex is a part of association networks consisting of distributed regions across frontal, parietal, and temporal cortex (Goldman-Rakic 1988). This suggests that there are distributed regions across the cerebral cortex, not just in lateral frontal cortex, that are involved in cognitive control. In order to explore this possibility, we reexamined fMRI task activity from a hierarchical rule usage study conducted by Badre and D'Esposito (2007) that places strong demands on cognitive control. Briefly, hierarchical rules consist of higher order rules that specify the use of lower order rules. The basic logic of a hierarchical rule usage task is illustrated in Figure 3.1, which shows that the second order rule (cued by the presentation of a circle or triangle) indicates which first order rule to follow when a subject subsequently sees a tree or a house cue. In the study by Badre and D'Esposito (2007), participants completed four such independent rule usage tasks that ranged from a relatively easy first order task to a highly demanding fourth order task. Adding to prior reports of a functional gradient in the lateral frontal cortex underlying cognitive control, Badre and D'Esposito identified specific caudal-to-rostral regions in the lateral frontal cortex distinguished by activity specific to each order. However, like most prior studies, this study did not focus on regions beyond the lateral frontal cortex.

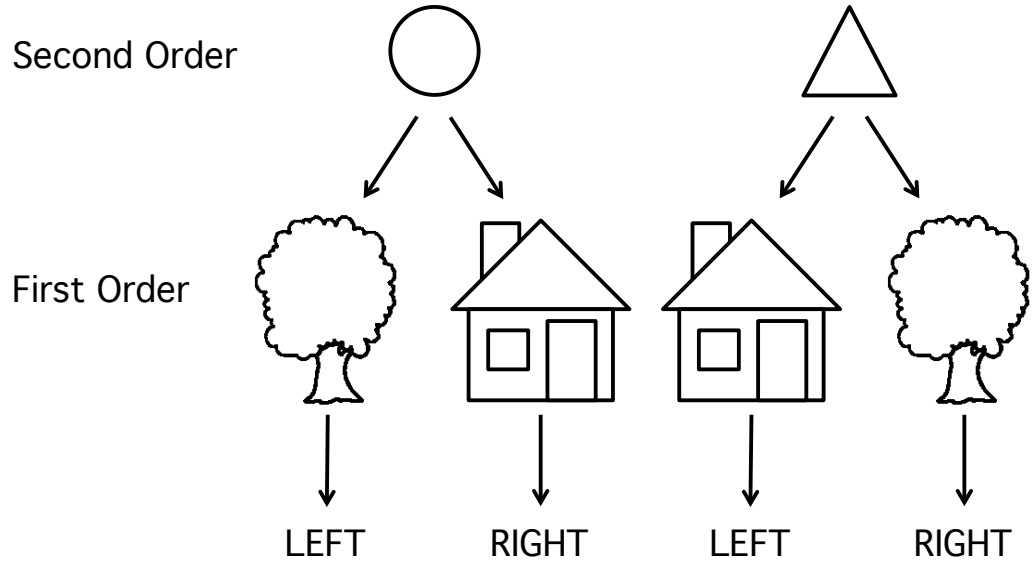

Figure 3.1 Hierarchical rule usage. This example schematic illustrates the basic concept of hierarchical rule usage. In a first order task, subjects press a left button if a tree is shown or a right button if a house is shown. In a second order task, subjects follow this rule if a circle is shown or the reverse rule if a triangle is shown preceding the stimulus. Similarly, higher order tasks contain higher order rules that constrain the use of lower order rules. Thus, hierarchical rule usage requires subjects to hold multiple contingent rules in memory and select the proper rule and action based on the context provided.

In the present study, we reexamined the task fMRI activity across the whole brain during the four independent rule usage tasks. Fig. 3.2 shows the whole-brain, order-specific group mean images of activity. The order-specific activity was obtained by identifying in each task the regions with activity that covaried with changes in rule competition (the number of available rules in a trial), which modulates the demand for cognitive control. The top, middle, and bottom rows show the lateral, dorsal, and medial views of the left cerebral cortex, respectively. Black lines denote network boundaries for the 17-network parcellation from 1,000 subjects (Yeo et al. 2011), as discussed in the next section. The smaller brains above show the 17-network parcellation corresponding to the black network boundaries.

An examination of the whole brain for the first order task revealed massive activity localized to the motor cortex, somatosensory cortex, and premotor regions (Fig. 3.2, first

column), as expected for a low-order task. However, higher order tasks showed involvement of distributed regions in the lateral and medial frontal, parietal, and temporal cortex (Fig. 3.2, second, third, fourth columns). As identified by Badre and D'Esposito (2007), the lateral frontal cortex contains activity in regions overlapping BA 44, 45, 47, and 10, as well as a second set of regions located more dorsally in and around dorsal Brodmann area (BA) 6 and caudal portions of BA 8 and 9. The medial frontal cortex contained activity in or near BA 6, 8, and dorsal portions of BA 32 and 24. The parietal cortex contained activity in and around the intraparietal sulcus, including BA 7 and 40. The temporal lobe contained activity in and around BA 37 and caudal portions of 21 and 22. As suggested by the anatomical connectivity of the lateral frontal cortex, these data reveal a distributed set of regions throughout association cortex underlying cognitive control.

Functional hierarchy in lateral frontal cortex

Having identified distributed regions of activity in hierarchical rule usage, we asked whether they are locally arranged in a functional hierarchy, as described for the lateral frontal cortex. An examination of the lateral frontal cortex revealed the expected caudal-to-rostral shift in task activity from the first to fourth orders (Fig. 3.2, top row) located in and around dorsal and ventral BA 6 (first order); dorsal BA 6, dorsal BA 44, and caudal BA 46 (second order); dorsal BA 6 and 44, caudal BA 46 and 9, dorsal BA 45, and parts of BA 10 (third order); and dorsal BA 44, caudal BA 46 and 9, dorsal BA 45, and BA 10 and 47 (fourth order). As reported by Badre and D'Esposito (2007), the regions of peak activity specific to the first through fourth orders are located in dorsal BA 6 (premotor dorsal; PMd), dorsal BA 44 (pre-premotor dorsal; prePMd), dorsal BA 45 (dorsolateral prefrontal cortex; DLPFC); and BA 10 (rostral lateral prefrontal

cortex; RLPFC), respectively. We note that although there is a general caudal-to-rostral trend in activity with increasing rule order, there is also overlap in active regions across the task orders. This is most salient for dorsal BA 6, which shows activity in the first, second, and third order tasks, as well as dorsal BA 44 region, which shows activity in the second, third, and fourth order tasks.

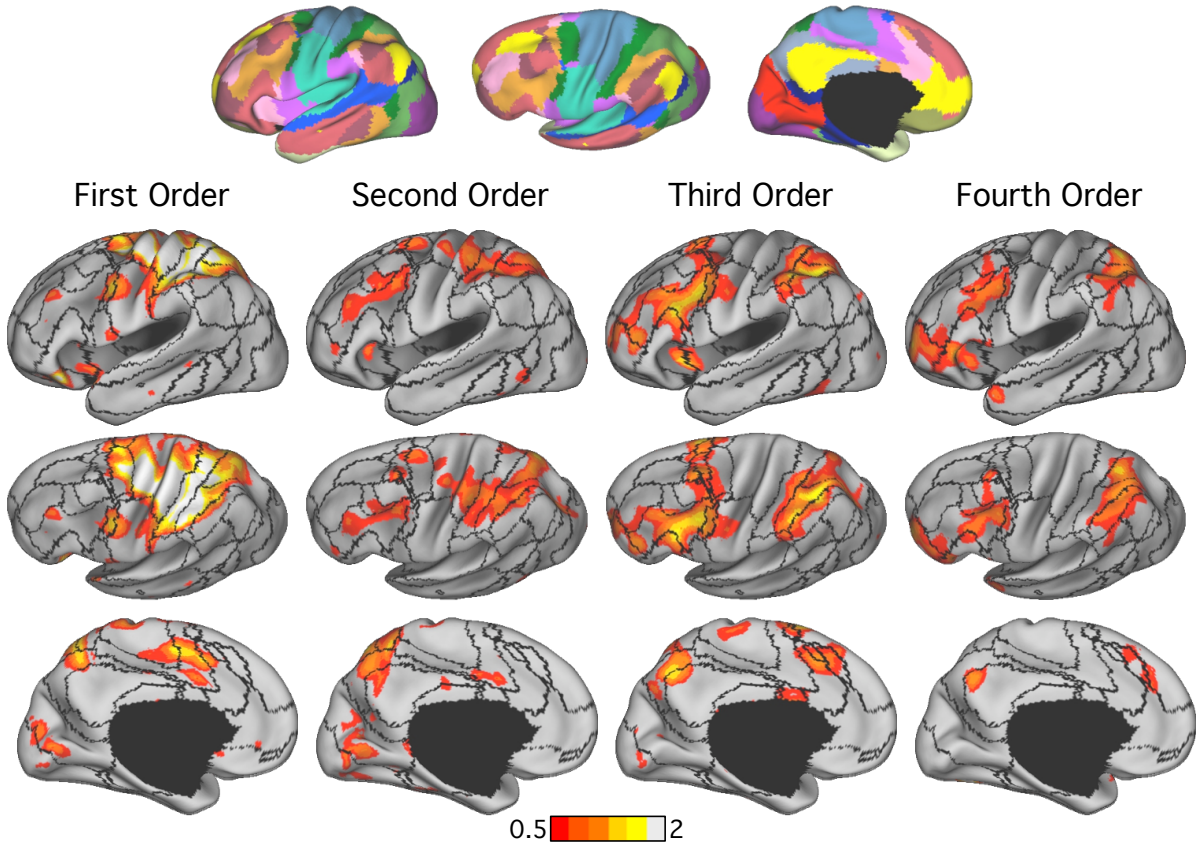

Figure 3.2 Order-specific task activity underlying hierarchical rule usage. Whole brain task activity (beta values) specific to four orders of rule usage (Badre and D'Esposito 2007) was projected onto the Caret cortical surface and overlaid with a 17-network estimate of human cortical networks based on resting-state fMRI in 1,000 subjects (Yeo et al. 2011; parcellation shown above). Black lines denote network boundaries. The top, middle, and bottom rows show the lateral, dorsal, and medial views of the left hemisphere. These results show activity localized to the sensorimotor cortex in the first order task, moving centrifugally with higher order tasks.

Functional hierarchy in parietal cortex

In addition to the lateral frontal cortex, we asked whether the activity in other distributed regions were also organized in functional hierarchies. An examination of parietal cortex revealed the presence of a functional hierarchy organized in a dorsorostral-to-ventrocaudal manner (Fig. 3.2, second row). There was order-specific activity for the first order task in somatosensory cortex, BA 5, and rostral BA 7; second order task in parts of BA 5 and in rostral BA 7; third order task in BA 7 and 40 in and around the inferior parietal sulcus; and fourth order task in BA 7 and 40 ventral to the inferior parietal sulcus. Thus there is a smaller and more overlapping but nonetheless distinct rostral-to-caudal functional hierarchy in parietal cortex mirroring the caudal-to-rostral functional hierarchy in the lateral frontal cortex. The global, whole brain pattern is one of localized activity in the sensorimotor cortex at lower levels of cognitive control, moving centrifugally as higher cognitive control is recruited.

Although we observed task activity in the temporal and medial frontal cortex, we did not see a similar shift in task activity from lower to higher order tasks as seen in the lateral frontal cortex and parietal cortex. This may be due to resolution limitations or the weak involvement of these regions in the hierarchical rule usage tasks we have analyzed.

Cognitive control recruits lower order and higher order association networks

Given the identification of multiple distributed association networks by monkey anatomical tract-tracing studies and human resting-state estimates of networks, we wondered whether the regions at each rule order comprising the functional hierarchies in the lateral frontal cortex and parietal cortex belonged to the same association networks. To address this, the task activity at each rule level was overlaid on the 17-network resting-state estimate of human

functional cortical networks derived from 1,000 subjects (Yeo et al. 2011; Fig. 3.2, network boundaries shown with black lines). In the lateral frontal cortex, the activity overlapped primarily with motor-related networks (green and blue) in the first order task, an association network (orange) in the second and third order tasks, and a second, separate association network (maroon) in the fourth order task. This is illustrated in Figure 3.3*A*, which shows the mean task activity at each rule order overlapping with three lateral frontal regions: a caudally-located region from a motor association network (green) and mid and rostral regions from the two association networks (called here association I and II networks) that overlap the observed functional hierarchy. Bars are colored from dark to light to indicate activity involved in lower to higher order rules. The black bars corresponding to the first order task show the greatest mean activity in the motor association region, which decreases progressively for the association I and II regions. The opposite pattern holds for the fourth order task activity shown in light blue bars, which is lowest for the motor association region and increases progressively for the mid and rostral association regions. The second and third order task activity show the greatest mean activity for the middle association I region and less activity for the motor association and association II regions. A repeated measures ANOVA with a Greenhouse-Geisser correction showed a significant order by ROI interaction effect ($F(2,36) = 4.82$, $p < 0.05$). A follow-up paired t-test of the first and fourth order activity showed significance for the motor association region ($p < 0.001$) but not for the association II region. The lack of significance in the association II region may be due to the greater individual subject variability during the first order task, which may reflect highly variable use of high order regions during low order tasks or signal loss in the rostral pole of the brain due to proximity to the nasal cavities.

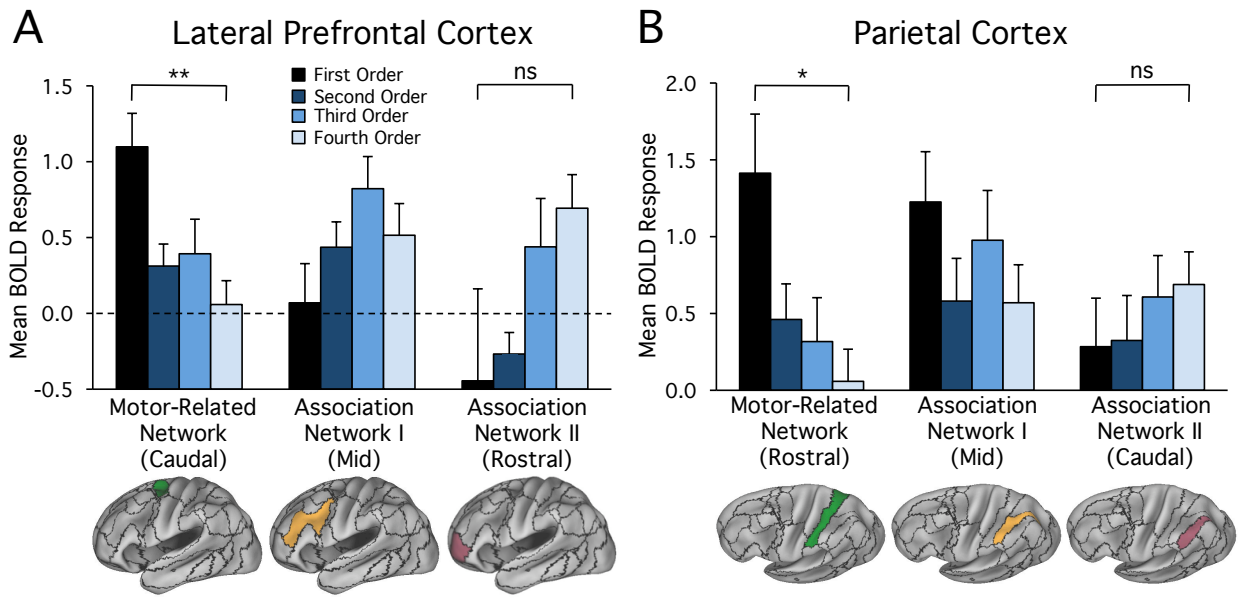

Figure 3.3 Quantification of task activity in motor and association networks. The mean overlap of order-specific task activity with regions of a motor association and two separate association networks (labeled association networks I and II) in the lateral frontal (A) and the parietal (B) cortex was quantified. Bars are colored dark to light shades indicating lower to higher order activity. The regions are highlighted below the bar graphs in their respective network colors (motor association: green; association network I: orange; association network II: maroon). An order by region repeated measures ANOVA showed an interaction effect ($F(2,36) = 4.82$, $p < 0.05$ for lateral frontal cortex; $F(6,108) = 9.74$, $p < 0.001$ for parietal cortex). Follow-up paired t-tests were performed for the first and fourth order activity for the motor network and association network II in both the lateral frontal and parietal cortex (* $p < 0.05$; ** $p < 0.001$; ns = not significant). These results show that as the rule order increases, there is a concurrent shift in task activity in the lateral frontal and parietal cortex from a motor association network to a lower order association network and finally to a higher order association network.

In order to test whether the same networks are involved in the functional hierarchy observed in the parietal cortex, the task activity at each rule order was quantified in three corresponding regions in parietal cortex (Fig. 3.3*B*, bottom). Unlike the frontal regions arranged caudo-rostrally, the corresponding parietal regions are located rostro-caudally from lower to higher orders of rules, in keeping with the centrifugal pattern of activity described above. Like the lateral frontal activity, the first order activity (black bars) is greatest in the motor association region (green) and decreases progressively in the mid (orange) and caudal (maroon) association I and II regions; the second and third order activity (medium shade blue bars) is greatest in the

association I region; and the fourth order activity (light blue bars) is low in the motor association region and increases progressively in the association I and II regions. A repeated measures ANOVA (no Greenhouse-Geisser correction) showed a significant order by ROI interaction effect ($F(6,108) = 9.74$, $p < 0.001$). A follow-up paired t-test of the first and fourth order activity showed significance for the motor association region ($p < 0.05$), but not for the association II region.

Altogether, these results show that the lateral frontal and parietal activities are preferentially modulated by rule order and overlap primarily with the same network, specifically a motor association network (green) at the first order, an association network (orange) at the second and third orders, and a separate association network (maroon) at the fourth order. This suggests that cognitive control is subserved, not by a set of regions in the lateral frontal cortex, but by association networks consisting of distributed regions. Furthermore, the association networks are preferentially active at different orders of cognitive control, suggesting that association networks are anatomically organized in parallel, but functionally organized in a hierarchy.

The majority of the striatum is functionally connected to association networks

We next turned to the question of whether or not the functional hierarchy of the lateral frontal cortex (and potentially of association networks, discussed below) arises from hierarchical interactions in the striatum between caudo-rostral basal ganglia circuits specific to the hierarchical regions of the lateral frontal cortex. However, before addressing this question, we first assessed the potential for the basal ganglia to be involved in cognition. Our knowledge of the basal ganglia, based on invasive animal studies, is primarily of its motor and reward-related

functions, leading to a dominant, but changing, view of the basal ganglia as a motor and/or limbic structure. The basal ganglia's role in cognition is far less understood.

Recently, studies using neuroimaging techniques have provided comprehensive functional and anatomical maps of the striatum in humans (Barnes et al. 2010; Choi et al. 2012; Cohen et al. 2008; Draganski et al. 2008; Tziortzi et al. 2013). These maps allow us to estimate for the first time the extent of the association, motor, and limbic territories in the striatum, thereby providing insight into the extent of the basal ganglia's roles in these functional domains. Figure 3.4 shows a quantification of association, sensory (premotor/ventral attention, motor, and visual), and limbic territories from our 7-network striatal parcellation map (Choi et al. 2012; Study 1) and a DTI anatomical map (Tziortzi et al. 2013). Both maps show that the majority of the striatum is primarily connected to association networks (fcMRI [left red bars]: 52%; DTI [right red bars]: 60%), while there is approximately one-half to one-third less territory primarily devoted to the motor (fcMRI [left blue bars]: 23%; DTI [left blue bars]: 13%) and limbic (fcMRI [left cream bars]: 13%; DTI [right cream bars]: 20%) networks. The presence of extensive association territory in the striatum suggests a strong involvement of the human basal ganglia in cognitive functions and challenges the view of the human basal ganglia as primarily motor and/or limbic in nature.

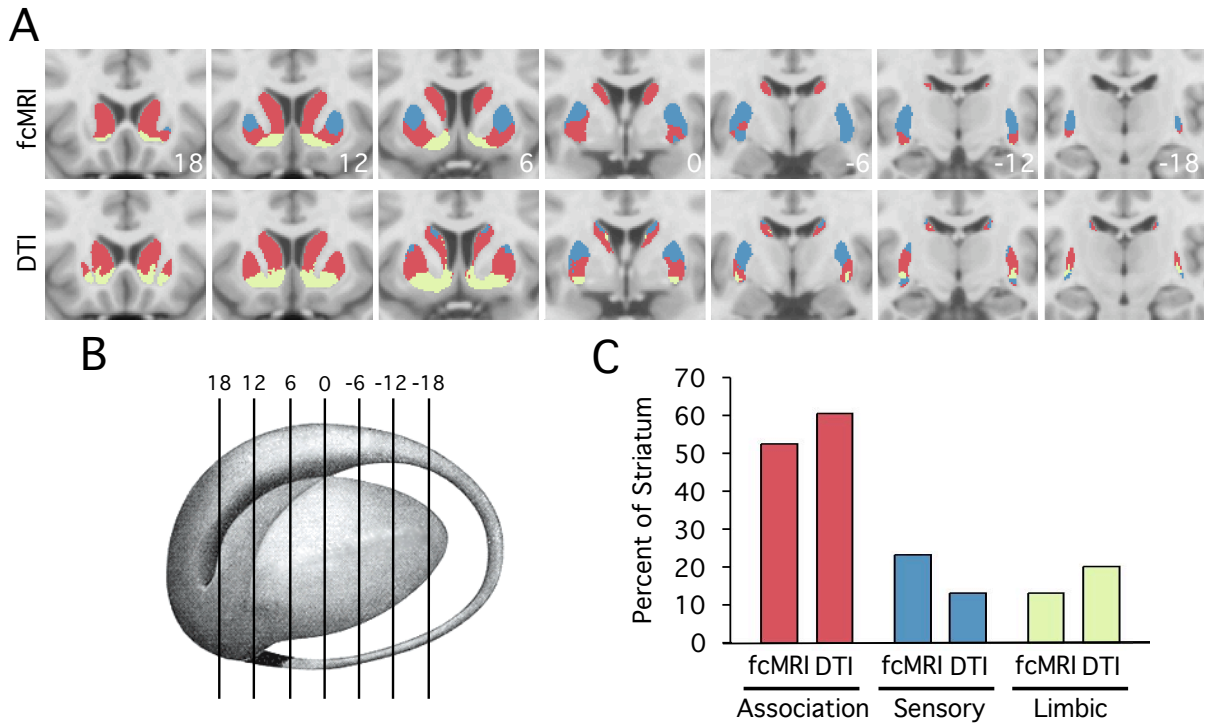

Figure 3.4 Spatial estimates of association, sensory, and limbic territories in striatum. The extent of association (red), sensory (blue), and limbic (cream) territories in the striatum was estimated from comprehensive, winner-take-all functional (resting-state fMRI) and anatomical (DTI) maps of the human striatum (Choi et al. 2012; Tziortzi et al. 2013). (A) The territories are shown in coronal slices through the striatum based on a classification of the functional divisions of the fcMRI (top) and DTI (bottom) maps as association, sensory, or limbic (B). (C) The percentages of striatal territory devoted primarily to association (fcMRI: 52%; DTI: 60%), sensory (fcMRI: 23%; DTI: 13%), or limbic (fcMRI: 13%; DTI: 20%) function were quantified. Both functional and anatomical maps reveal that the majority of the human striatum is primarily linked to association networks.

Two model predictions of the connectivity between lateral frontal cortex and striatum

We next addressed the question concerning the possibility of basal ganglia circuits underlying the functional hierarchy of the lateral frontal cortex. With fcMRI, we can gain insight into this question by examining the organization of the correlations from the cortical regions of the hierarchy. We first created two possible models of the organization, one that suggests hierarchical interaction and one that is ambiguous. The first model shows a simple hierarchical organization in which a higher order cortical region exerts its influence over lower order regions

via connections that overlap with those from lower order regions. Thus higher order regions have broader territories of correlation that overlap those of lower order regions. This nested organization provides a strong suggestion of the direction of influence. Figure 3.5*A* illustrates this organization using curves representing the connectivity through the rostro-caudal extent of the striatum.

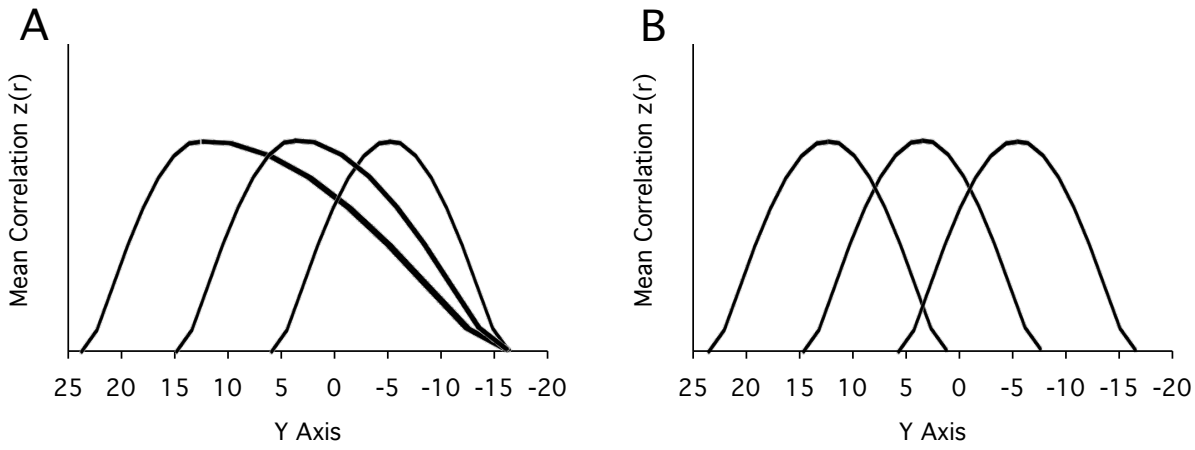

Figure 3.5 Models of lateral frontal-striatal connectivity. The functional hierarchy in the lateral frontal cortex may be mediated by an asymmetrically overlapping connectivity in which higher order regions have broader connections to the striatum and overlap with the narrower connections of lower order regions. (A) A model plot of correlations through the rostro-caudal extent of the striatum shows higher order correlation curves engulfing lower order correlation curves. (B) An ambiguous organization is also possible in which all cortical regions have identical correlation curves located rostro-caudally in the striatum. In such an organization, we are unable to determine if there is a hierarchical interaction of connections between the lateral frontal cortex and the striatum using fcMRI.

However, we might observe another organization (Fig. 3.5*B*) that could also support a hierarchical connectivity, but is ambiguous to determine from its organization. In this model, higher and lower order cortical regions have identical correlation curves. Although there is overlap between these curves, which could support hierarchical interaction, they do not suggest a direction of influence as the nested organization of the first model does. A hierarchy of interactions can exist with this organization of identical correlation curves, but we would not be

able to detect it using fcMRI. In the next section, we compared the correlation patterns from the hierarchical cortical regions to these two models.

The striatum is differentially coupled to hierarchical regions in the lateral frontal cortex

We computed the functional connectivity to the striatum from the four order-specific cortical regions mentioned above (PMd, prePMd, DLPFC, and RLPFC; see Fig. 3.8*A*, top). We first examined whether there is a distinct basal ganglia circuit for each of the regions of the hierarchy. The first order seed region (PMd) in dorsal BA 6 was primarily correlated with the putamen, not surprisingly given its functional proximity to the motor cortex. The second, third, and fourth order regions showed longitudinal correlations throughout the rostro-caudal extent of the striatum, with the strongest correlations in the caudate (Fig. 3.6). The correlation patterns are distinguished by the location of the peak correlation and the rostro-caudal breadth of the correlations. The fourth order map shows the broadest territory of correlations with a rostrally located peak of correlation. The third and second order maps show successively narrower territories and further caudal peaks of correlation. Thus, there is a rostral-to-caudal differential in the correlations of these maps that corresponds with the rostro-caudal locations of the cortical seed regions (e.g., rostral cortical regions are most strongly correlated with the rostral caudate). These results show that the striatum is differentially connected with the regions of the hierarchy, suggesting that there are distinct basal ganglia circuits for each order of cognitive control.

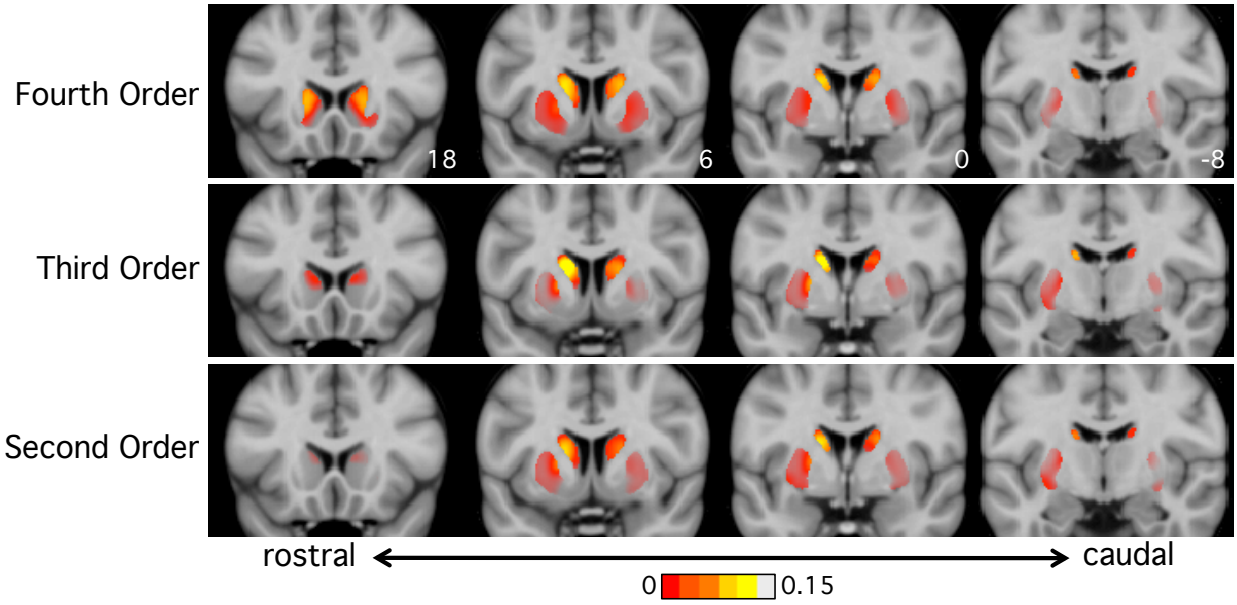

Figure 3.6 Lateral prefrontal-striatal connectivity assessed by fcMRI. Coronal slices display the striatal resting-state correlations of second, third, and fourth order-specific cortical regions identified from a hierarchical cognitive control study (Badre and D'Esposito 2007). The correlations span the rostro-caudal extent of the striatum (most strongly in the caudate) with the broadest extent for the fourth order correlations and increasingly narrower extents for the third and second order correlations. There is a rostral-to-caudal gradient in the location of the peak correlation from fourth order to second order, corresponding with the rostro-caudal location of the cortical regions.

The organization of correlations between the lateral frontal cortex and the striatum

We next compared the correlation patterns with the model predictions. In order to highlight the differences in functional connectivity patterns, for each order-specific connectivity map, the peak correlations for twenty-one evenly spaced coronal slices were plotted (Fig. 3.8*A*, bottom), allowing for a comprehensive view of the correlation patterns. Plots of the coordinates of the peak correlations show that they are all located closely together (Fig. 3.7), with the exception of those in the rostral slices of the fourth order map, which are located more medially (Fig. 3.7*B*). In agreement with the correlation maps shown in Figure 3.6, the corticostriatal connectivity plots show the broadest correlation curve for the fourth order cortical region and increasingly narrower correlation curves for the lower order regions. In addition, higher order

correlation curves overlap lower order curves (Fig. 3.8*A*, bottom). These results agree with the first model prediction, which is suggestive of hierarchical interactions via basal ganglia circuits at the level of the striatum.

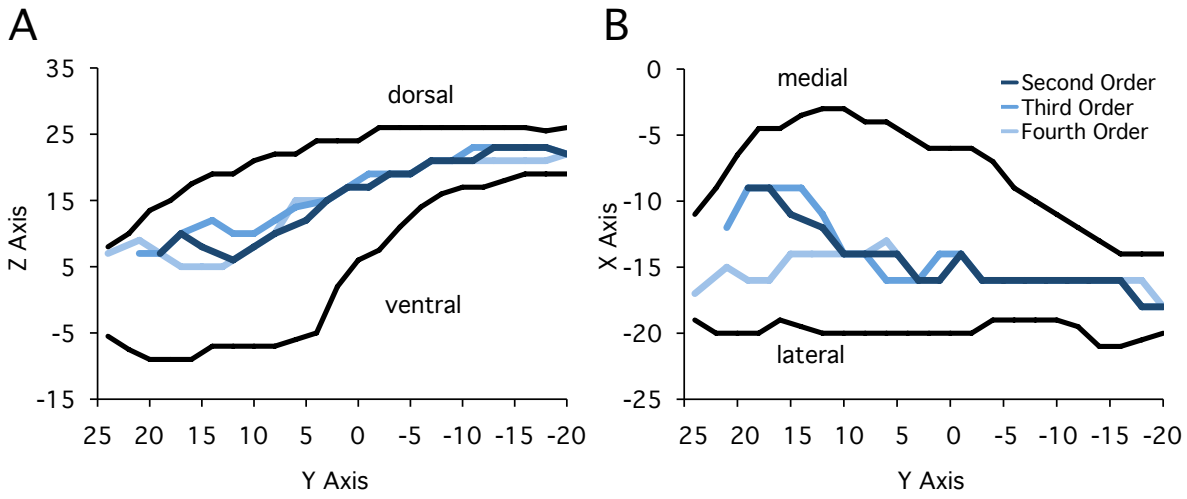

Figure 3.7 Coordinates of peak corticostriatal correlation voxels. In order to comprehensively assess multiple corticostriatal correlation maps, the peak correlations at 21 coronal slices for each order-specific correlation map (see Fig. 3.6) were viewed on a plot (see Fig. 3.8). The (A) Z and Y or (B) X and Y coordinates of the peak correlation voxels are plotted. These coordinates show that the peak voxel is the same or nearly the same across the different order-specific corticostriatal maps, located in the dorsal and lateral portion of the caudate. The exception is in the rostral caudate for the fourth order map, whose peak voxels are located more medially in the caudate than the others.

There is, however, a confound due to the locations of the cortical seed regions. The regions are near the borders of association networks where there is a blurring of different signals from neighboring networks (see Fig. 3.8*A*, top). This creates a confound in which we cannot determine whether the nested overlap of the striatal correlation curves (Fig. 3.8*A*, bottom) is due to a true hierarchical organization or to a mixture of cortical signals.

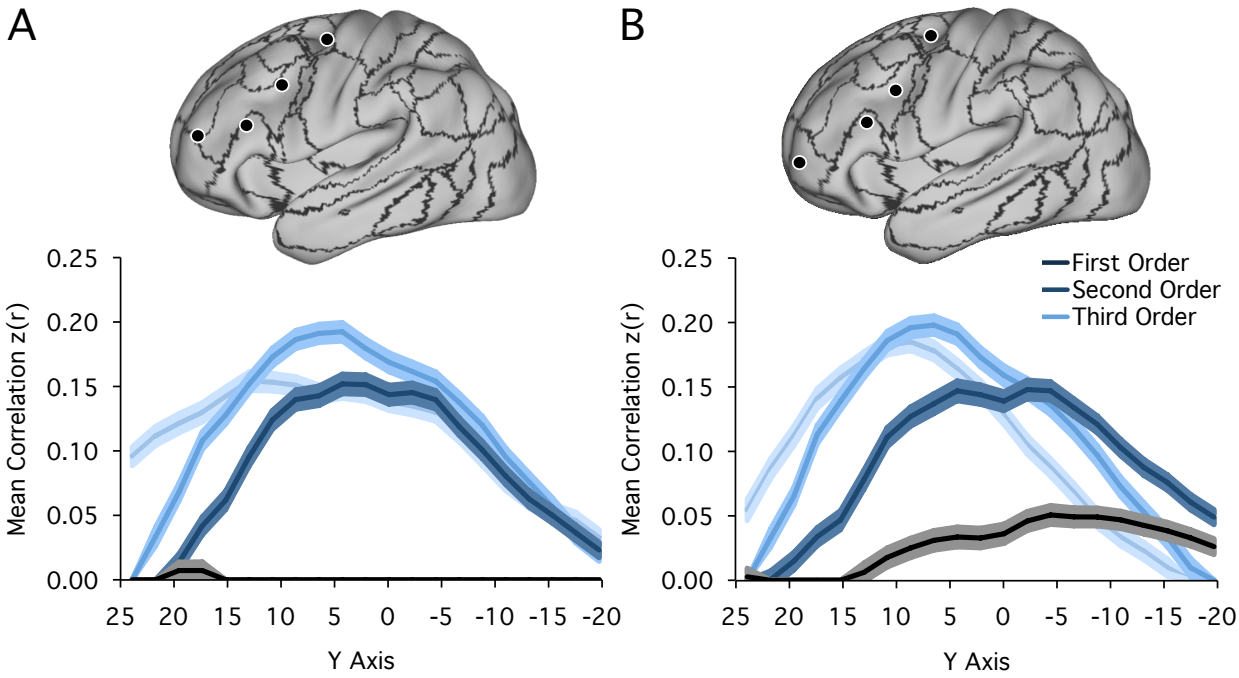

Figure 3.8 Order-specific corticostriatal correlation plots. Plots show the peak striatal correlations (darker centered lines) with the standard error values (surrounding lighter bands) for each order-specific cortical region at 21 coronal slices through the striatum. Cortical regions are indicated above the plots and overlaid with the network borders (black lines) of the 1,000 subject 17-network cortical parcellation (Yeo et al. 2011). (A) Task-specific cortical regions (most strongly correlated with rule competition in each hierarchical rule usage task) reveal a hierarchical connectivity with the striatum, in accordance with the first model prediction (see Fig. 3.5*A*). However, results are confounded by the locations of the cortical regions near network borders where there is a mix of different network signals. (B) Cortical regions adjusted to avoid network borders reveal an ambiguous connectivity structure resembling the second model prediction (see Fig. 3.5*B*).

To minimize signal contamination, a new set of cortical regions (Fig. 3.8*B*, top) were tested that were moved away from the network borders into high confidence regions based on the confidence map of the 17-network cortical parcellation (Yeo et al. 2011). We expected that if the hierarchical organization from the first set of cortical regions is true, the organization should be preserved after moving the cortical regions away from the network borders. Corticostriatal connectivity plots were created from functional connectivity maps computed using this second set of cortical regions (Fig. 3.8*B*, bottom). These plots reveal a rostro-caudal series of roughly

identical correlation curves for the second, third, and fourth order cortical regions, more resembling the second model prediction. Thus, it is likely that the overlap seen with the first set of cortical regions is a result of signal blurring at network boundaries. A hierarchical organization may in fact exist with this second organization of connectivity, but we are unable to determine this using fcMRI.

Discussion

The present study investigated the link between the functional hierarchy in the lateral frontal cortex underlying cognitive control and the parallel, distributed organization of association networks. The study also investigated the possibility of a basal ganglia mechanism giving rise to the functional hierarchy of the lateral frontal cortex. We found that in addition to the functional hierarchy in the lateral frontal cortex, there is a second functional hierarchy in the parietal cortex underlying hierarchical cognitive control. Critically, the activity from different task orders overlapped specifically with different association networks in both the lateral frontal and parietal cortices. These results suggest that hierarchical cognitive control, and cognitive behavior more generally, arises from the interactions between networks, rather than between regions localized in the lateral frontal cortex. These results also suggest a functional hierarchy of lower order and higher order association networks, which provides an explanation for how we accomplish hierarchical behaviors with anatomically parallel, distributed association networks. We also investigated whether the functional hierarchy of the lateral frontal cortex might arise from order-specific basal ganglia circuits that hierarchically interact at the level of the striatum. We first showed that the majority of the human striatum is association territory, while one half to one third as much territory is motor or limbic. We then examined the functional connectivity from the hierarchical regions of the lateral frontal cortex. We found a rostral-to-caudal correspondence in connectivity between regions of the lateral frontal cortex and their peak correlations in the striatum. However, the organization of the correlations was ambiguous in revealing whether or not there are hierarchical interactions. In the following sections, we discuss implications and caveats of these results.

A functional hierarchy of association networks

Our study provides the first identification of hierarchically organized networks, providing evidence for a model of hierarchical networks previously proposed by Joaquín Fuster (1995, 2003, 2008). In Fuster's model, there are dual hierarchies of information processing, one in the lateral frontal cortex for action and one in the parietal cortex for perception. Reciprocal levels of the dual hierarchies are suggested to connect via long-range projections (Pandya and Yeterian 1985) forming hierarchical networks. These networks are hypothesized to support continual perception-action cycles that allow for hierarchically organized behavior and rapid, dynamic interactions with the environment.

The evidence for the functional hierarchies in the lateral frontal and parietal cortices is extensive and has been described in depth by Fuster (1995, 2003, 2008). Briefly, there are functional, connectional, developmental, and evolutionary gradients of primary sensory cortex, to sensory association cortex, to presumably lower order association regions, and finally to presumably higher order association regions. In addition to the demonstration of unimodal sensory and heteromodal association cortex by functional studies, monkey anatomical studies have shown that there is a flow of feed-forward connections following this gradient (Amaral 1987; Jones and Powell 1970; Mesulam 1998). A similar gradient is seen in the growth of the brain during human development and over evolution. Axonal myelination, an approximate marker of neuronal maturation, occurs first perinatally for primary sensory cortices and then progressively to higher order association regions, some beginning as late as 1 month after birth and continuing until puberty (Flechsig 1901). Similarly, comparative studies of humans and other mammals show the presence of predominantly sensory regions in the simplest animals to the gradual expansion and development of association cortex in increasingly sophisticated

animals (Kaas 2006). A neuroimaging study by Hill et al. (2010) demonstrates these findings elegantly, showing the largely selective expansion of association cortex from human infancy to adulthood and between Rhesus macaque monkeys and humans. Thus, there is extensive evidence from multiple fields supporting the existence of higher and lower order regions in distributed parts of the association cortex.

The hypothesized order-specific connections between the lateral frontal and parietal hierarchies are based on the identification of anatomical connections between these two lobules (Pandya and Yeterian 1985); however, the actual order-specific connections have never been specified. Our finding that distributed task activity at a given order overlaps with a specific association network now provides evidence for order-specific functional interaction. In addition, the identification of specific association networks, including their constituent regions, now facilitates the identification of order-specific connections in monkeys.

Distributed functional hierarchies of association regions

In addition to the functional hierarchies in the lateral frontal cortex and parietal cortex, we also observed second, third, and fourth order task activity in the dorsal lateral frontal cortex, dorsomedial frontal cortex, and temporal cortex, coinciding with other distributed regions of the association I and II networks. While the task activity was not organized in a hierarchy, the 17-network cortical parcellation shows the same sequence of motor association, association I, and association II regions in these distributed locations as in the lateral frontal and parietal cortices, suggesting the presence of functional hierarchies in these locations, as well. Our lack of observation of functional hierarchies in these locations may be due to the smaller size of these regions than those of the lateral frontal and parietal cortices, or the lack of hierarchical activity in

these parts of association cortex during the tasks we have examined. The latter possibility will be discussed again below.

Although we did not observe a functional hierarchy of regions in all the distributed locations predicted by the cortical parcellation, evidence of other regional hierarchies have been seen in recent neuroimaging work. The most progress has been made in the dorsomedial PFC, which has been also shown to have a caudal-to-rostral functional hierarchy of lower to higher order cognitive control. Using a hierarchical motor sequence task, Koechlin and colleagues showed that there are caudal-to-rostrally arranged regions in the dorsomedial PFC that are preferentially active for the context of a trial (lower order contextual control) or of the entire block of trials (higher order episodic control; Kouneiher et al. 2009). Huettel and colleagues converged upon similar results after identifying caudal-to-rostral regions related to the cognitive control of response execution, choice selection, or strategy selection (Venkatraman et al. 2009). They later showed that there was a caudal-to-rostral correspondence in fcMRI correlations between the same dorsomedial PFC regions and the middle frontal gyrus of the lateral frontal cortex (Taren et al. 2011). The authors suggested that the functional hierarchy in the dorsomedial PFC processes motivational incentive or conflict monitoring during cognitive control, influencing processing in the lateral frontal cortex in an order-specific manner.

The presence of a distinct second functional hierarchy in the lateral frontal cortex has been suggested, located ventral to the well-known functional hierarchy occupying the inferior frontal sulcus and middle frontal gyrus. Koechlin and colleagues, using first and second order motor sequence tasks, found a functional hierarchy involving the anterior (BA 45) and posterior (BA 44) parts of Broca's area (Koechlin and Jubault 2006). The authors suggested that this ventral hierarchy is specialized in the completion of subgoals towards an overarching goal, in

contrast to the more dorsal hierarchy specializing in temporal information. Consistent with this finding, D'Esposito and colleagues reported a caudal-to-rostral gradient of functional connectivity between the dorsomedial PFC and two gradients of regions in the rostral middle frontal gyrus and the ventral inferior frontal gyrus, including Broca's area (Blumenfeld et al. 2012). These results suggest the presence of at least two functional hierarchies in the lateral frontal cortex, a topic we will return to below.

Finally, our study demonstrates for the first time a functional hierarchy in and around the intraparietal sulcus (IPS), discovered from examining regions parametrically correlated to task-related control for four orders of hierarchical rule use (Badre and D'Esposito 2007). Two prior studies have reported activity in the parietal cortex during hierarchical tasks, but without a hierarchical organization. Duncan and colleagues found distributed regions of activity within the frontoparietal control network, including in the lateral frontal cortex, dorsomedial PFC, and parietal cortex, during a hierarchical target detection and working memory task (Farooqui et al. 2012). However, they found that higher order conditions lead to stronger and broader activity in both the frontal and parietal cortices, rather than a hierarchical ordering of activity. Koechlin and colleagues, using the same hierarchical motor sequence tasks mentioned above, found no differences in the activity of parietal regions between the hierarchical and non-hierarchical conditions (Jubault et al. 2007).

Our detection of a functional hierarchy in the parietal cortex, in contrast to the other studies, may have been due to the greater demand of cognitive control placed on the subjects, who completed tasks with up to four orders of rules. The tasks used by Koechlin and colleagues are first and second order tasks, and the task from Duncan and colleagues appears to be second or possibly third order. However, another possibility is that while a functional hierarchy of

networks may exist with the architecture to support hierarchical activity in distributed parts of association cortex, these regional hierarchies may not always be active in a given task. They may become apparent when the task demands hierarchical activity for the particular function specialized by that part of association cortex. In this case, both studies from the Duncan and Koechlin groups independently investigated activity specifically underlying the cognitive control of completing steps towards a goal spanning multiple trials, which was not the case in the hierarchical rule tasks analyzed in this study. Similarly, a hierarchical cognitive control task strongly engaging the ventral visual pathway may yield the hierarchical activity in the temporal cortex that is predicted by the cortical parcellation.

Multiple functional hierarchies of association networks

In the discussion above of a potential second functional hierarchy in the ventrolateral PFC, it was mentioned as evidence that Blumenfeld et al. (2012) had discovered a dorsal (rostral middle frontal gyrus) and a ventral (ventral area 6 and anterior insula) caudal-to-rostral gradient of functional connectivity with the dorsomedial PFC. Interestingly, the 17-network cortical parcellation also predicts two functional hierarchies in the lateral frontal cortex, but in distinctly different locations. These hierarchies are located primarily in the lateral inferior frontal sulcus/middle frontal gyrus, as examined in the present study, and further dorsally in the caudal middle frontal gyrus/superior frontal sulcus. A comparison of the 17-network cortical parcellation with the whole-brain functional connectivity maps created by Blumenfeld et al. with dorsomedial PFC seed regions (see their Fig. 1) shows that their dorsal and ventral gradients overlap with regions of the violet and pink networks in the rostral middle frontal gyrus and in ventral area 6 and the anterior insula, respectively. Similarly, the seed regions of the dorsomedial

PFC used to create the maps lie within the dorsomedial PFC regions of the violet and pink networks in the cortical parcellation. There also appear to be additional gradients of correlation in the parietal and temporal cortices, again overlapping with violet and pink network regions. Thus, it appears that there are *two* sets of functional hierarchies of association networks, both demonstrated by hierarchical tasks and fcMRI. This is consistent with the lack of a functional hierarchy in the dorsomedial PFC in our hierarchical rule use tasks, but its presence in the hierarchical motivation and conflict-related tasks (Kouneiher et al. 2009; Venkatraman et al. 2009). Given the nature of the tasks and the functions ascribed to particular regions, the hierarchy of networks examined in the present study appears to be involved in external tasks with relatively little self-relevance. The second functional hierarchy of the violet- and pink-colored networks appears to process more motivation-, conflict-, bottom-up attention-, and/or motor-related information. Thus, it is possible that there are functional domain-specific hierarchies of networks. If this is true, we may observe other sets of hierarchically organized networks, such as perhaps the red- and yellow-colored networks comprising the default network that underlies internally-oriented, self-related thoughts.

The majority of the striatum is primarily linked to association networks

A quantification of the motor, limbic, and association territories from a functional connectivity and anatomical map of the human striatum revealed that the majority of the human striatum is connected with association cortex. While we did not quantify other comprehensive maps of the striatum (Barnes et al. 2011; Cohen et al. 2008; Draganski et al. 2008), they are qualitatively similar to the maps we have analyzed.

We are aware of only one prior quantification of striatal functional territories. Haber et al.

(2006) estimated 22% of the monkey striatum to be limbic (defined as having connections to the anterior cingulate and orbitofrontal cortex). This is similar to the limbic territory estimates we report here in humans (fcMRI: 13%; DTI: 20%). There have not been any reported quantifications of the association or motor territories of the striatum in animals, which would tell us if the striatal association territory has expanded concurrently with the association cortex over evolution. It is possible that studying the striatum in monkeys and rodents has lead to an underestimation of the involvement of the human striatum in cognitive functions.

Functional connectivity between lateral frontal cortex and striatum

The analysis of the functional connectivity between hierarchical regions of the lateral frontal cortex and the striatum revealed a promisingly hierarchical, but ultimately confounded organization of correlations and a non-confounded, but hierarchically ambiguous organization. However, one feature remained the same between these two results. There was a rostral-to-caudal correspondence between the locations of the cortical seed regions and their peak striatal voxels of correlation. This is consistent with DTI observations of a rostral-to-caudal correspondence in fibers from the lateral prefrontal cortex to the striatum (Draganski et al. 2008; Verstynen et al. 2012). This is also consistent with the current anatomical model of corticostriatal projections (Haber et al. 2006), which are longitudinal through the striatum (Goldman and Nauta 1977; Künzle 1975), but also most dense in the striatal region closest to the cortical region of origin (Kemp and Powell 1970). Thus, our otherwise null results agree that there are distinctly different basal ganglia circuits specific to each order of hierarchy. These basal ganglia circuits may well underlie hierarchical interactions, but we are unable to resolve this using fcMRI.

In this study, we more generally identified a functional hierarchy of association networks. Here, too, the basal ganglia is capable of supporting hierarchical interactions on a network-level. The results of Study 1 demonstrate in humans a principle originally discovered in monkeys: interconnected regions of an association network have overlapping connections in the striatum. Thus a given striatal region in association territory receives converging input from the distributed regions of an association network. Monkey anatomical studies have also shown that association projections have extensive overlap with other association projections beyond their converging regions. This is particularly the case for diffuse projections, which are much more expansive than the focal projections that comprise the stereotyped corticostriatal connectivity patterns (Haber et al. 2006). This may be the means for supporting hierarchical interactions between networks. We also know from Study 1 that the striatum is functionally coupled to all association networks, essentially the entire association cortex, in the 7-network cortical parcellation. Thus any between-network interactions have the chance of occurring in the basal ganglia.

In reality, there is integration occurring at all levels of cortico-basal ganglia-thalamic circuits, including in the progressively smaller structures of the basal ganglia, from reciprocal and non-reciprocal thalamo-cortical connections (McFarland and Haber 2002), and via direct cortico-cortical connections. Whether the functional hierarchy of association networks depends on all or select mechanisms of integration remains to be answered.

Caveats and limitations

As previously mentioned, fcMRI is a correlational measure of functional co-activation constrained by anatomical connections. As such, much like anatomical connectivity studies, we are limited to inferring functional mechanisms from the organization of the correlations. In the

first model prediction, the nested structure of the correlations allows us to infer hierarchical interactions. However, in the second model prediction, the similar overlap of identical sets of correlations is ambiguous of a hierarchy; a hierarchy may exist, but we cannot detect it with fcMRI. At this point, we have reached the limit of what fcMRI can tell us about functional mechanisms. Anatomical studies with the resolution to see synaptic terminals may reveal further clues on how the projections interact. Functional and behavioral animal studies using neurophysiological recordings, calcium imaging, or manipulations altering corticostriatal connections provide additional ways to clarify the organization of corticostriatal connectivity.

Another complication was recently brought to our attention by Yeo, Krienen, and Buckner, who investigated whether the organization of functional correlations is dependent on the task state of the subjects. They found that the frontoparietal control network expands when subjects are performing a semantic classification task (see Buckner et al. 2013, their Fig. 3). Furthermore, the expanded borders of the frontoparietal control network well encapsulated the task-related activity, which would have overlapped with multiple networks in the resting-state derived parcellation. This suggests that fcMRI results more reflective of the functional interactions during hierarchical cognitive control may be obtained by using fMRI data acquired during task performance. With this approach, we may find that the order-specific cortical seed regions of the first set are well within parcellation-derived network borders.

Conclusions

Cognitive control, and likely cognitive behaviors in general, are subserved by distributed association networks. Hierarchical cognitive control in particular is subserved by a lower order association network recruited during cognitively easier tasks and a higher order association

network recruited during cognitively demanding tasks. This suggests that association networks, while anatomically organized in parallel, are functionally organized in a hierarchy. The hierarchical interaction between association networks may arise from its connectivity with subcortical structures, such as the basal ganglia. Indeed, the majority of the human striatum is association territory, challenging the idea of the basal ganglia as primarily motor or limbic in nature. The functional connectivity between the hierarchical regions of the lateral frontal cortex and the striatum has a rostral-to-caudal correspondence, indicating distinct, order-specific cortico-basal ganglia-thalamic circuits, but its potentially hierarchical nature remains to be determined.

Experimental Procedures

Overview

The present study explored the relationship between the functional hierarchy of regions in the lateral frontal cortex identified through hierarchical cognitive control studies and parallel, distributed association networks involving the lateral frontal cortex. In addition the study investigated a potential corticostriatal mechanism for supporting the functional hierarchy of the lateral frontal cortex. The study consisted of two analyses. In the first analysis, we sought to determine how regions involved in hierarchical cognitive control overlap with association networks (Yeo et al. 2011). To this end, we examined the whole brain fMRI activity specific to four orders of hierarchical rules previously collected and reported by Badre and D'Esposito (2007; N = 19). Order-specific activity was obtained by finding the activity that parametrically covaried with rule competition (i.e., number of rules available to use) during the trials of each task, which modulates the demand on cognitive control. We projected the cortical activity of these four order-specific fMRI maps from the volume to the FreeSurfer surface space and overlaid them onto a 17-network parcellation of the cerebral cortex (N = 1,000) based on resting-state fMRI, as previously reported by Yeo et al. (2011). The overlap was quantified between functional activity from the task and network-defined regions belonging to three networks in the lateral frontal and the parietal cortices, which together overlapped with most of the functional activity.

In the second analysis, we sought to determine whether corticostriatal connections might be supporting the functional hierarchy identified in the lateral frontal cortex using resting-state fcMRI. We first created two model predictions of the corticostriatal correlations, one that was

suggestive and one that was ambiguous in indicating a functional hierarchy in corticostriatal connections using fcMRI. We then computed the resting-state correlations for the four order-specific cortical regions in a group of 500 subjects. To comprehensively assess the correlations, we plotted the peak correlation value at 21 coronal slices throughout the striatum for each corticostriatal correlation map. The results were compared to two model predictions of their organization.

Hierarchical Rule Study

The cognitive control task data analyzed in the present study was previously reported in a study by Badre and D'Esposito (2007) with the goal of identifying the regions of the lateral frontal cortex that are involved in four orders of rule usage. The relevant methods are described briefly here; see Badre and D'Esposito (2007) for further details.

Participants Subjects consisted of nineteen paid participants (10M), ages 18 to 31, clinically normal, native English speakers, right-handed, and with normal or corrected-to-normal vision. Two subjects were excluded due to incompletion of the study or significant artifacts in the MRI data. Participants were pre-screened for prior neurological or psychiatric illness, and MRI contraindications. Written informed consent was obtained in accordance with procedures set by the Committee for Protection of Human Subjects at the University of California, Berkeley.

Task Design Participants completed four independent rule usage tasks with one, two, three, or four orders of rule abstraction. In a single trial of each task, subjects were shown a visual cue and made a button press response according to rules with one, two, three, or four levels of instruction

depending on the task (see Badre and D'Esposito, their Fig. 2). In order to identify regions with activity specific to each order, trials had 1, 2, or 4 possible competing responses for the highest order of the task (see Badre and D'Esposito, their Fig. 1), which served as a parametric variable in the data analysis.

In the first order task ("Response Experiment"), the cues were squares of different colors (Badre and D'Esposito, their Fig. 1, *A* and *B*). The rule indicated which buttons to press given different colors. Hence, the rule is first order, indicating color-to-response mappings. Response competition varied with 8 8-trial blocks in which 4 colors mapped to one, two, or four button presses. For each block, subjects viewed an instruction screen for 10 sec, then a fixation screen for 8 seconds, followed by 8 trials consisting of a cue presentation of 1900 ms and a noise mask for 100 ms. Trials were jittered by a fixation screen for 0-6 sec.

In the second order task ("Feature Experiment"), the cues were colored squares containing an object with varying features of texture (mottled, smooth, bright, or dim) for half the subjects or orientation (up, down, left, or right) for the other half of subjects. The rule specified which button to press given different pairings of color and object texture or orientation (e.g., Press "1" if the red square contains a mottled object or press "2" if the red square contains a smooth object). Hence, the rule is second order, indicating color-to-feature-to-response mappings. Response competition varied with 8 8-trial blocks in which 4 colors mapped to one, two, or four textures or orientations. For each block, subjects viewed an instruction screen for 10 sec, then a fixation screen for 8 sec, followed by 8 trials consisting of a cue presentation of 3900 ms and a noise mask for 100 ms. Trials were jittered by a fixation screen for 0-4 sec.

In the third order task ("Dimension Experiment"), the cues were colored squares with two objects within. In this rule, color specified which dimension (texture, orientation, shape, or size) was relevant, and which buttons to press if the two objects were matching or non-matching in this feature. Hence, the rule is third order, indicating color-to-dimension-to-feature-to-response mappings. Response competition varied with 8 8-trial blocks in which 4 colors mapped to one, two, or four dimensions. For each block, subjects viewed an instruction screen for 10 sec, then a fixation screen for 8 sec, followed by 8 trials consisting of a cue presentation of 3900 ms and a noise mask for 100 ms. Trials were jittered by a fixation screen for 0-4 sec.

The fourth order task ("Context Experiment") was the same as the third order task, but certain colors indicated different dimensions across the entire task depending on the instructions (context) given to the subjects. Response competition varied with 6 8-trial blocks in which a given color mapped to a dimension for 25%, 50%, or 100% of blocks across the entire task. Hence, context is modulated across the entire task. The rule is fourth order, indicating context-to-color-to-dimension-to-feature-to-response mappings.

For the first, second, and third order tasks, blocks were separated by a 12 sec fixation period and fully counterbalanced for order. Block order was fixed in the fourth order task as part of the contextual information provided to the subjects. Color mappings were counterbalanced across subjects. Cue, response, feature, and dimension switches were controlled for frequency and repetition across blocks.

Experimental Procedure Data were collected over two sessions (separated by 1 day to 1 week) with two rule tasks completed during each session. Since the fourth order task had colors with multiple, precise mappings, this task was always completed first in the first session. Since the fourth and third order tasks were nearly the same, the third order task was always done in the second session and with different colors. The rest of the tasks were counterbalanced for order across the subjects. Prior to the scans, subjects were instructed on the rules and practiced the tasks both outside and inside the scanner. Visual stimuli were viewed on a screen through a mirror attached to the head coil.

MRI Data Acquisition The MRI data were collected on a 4T Varian/Inova (Palo Alto, CA) MRI system. Structural data included anatomical images acquired by a T1-weighted gradient-echo multislice sequence (GEMS) and a high-resolution T1-weighted MP-FLASH 3-D sequence. The functional imaging data were acquired using a two-shot gradient-echo echo-planar imaging (EPI) sequence sensitive to blood oxygenation level-dependent (BOLD) contrast. Functional imaging parameters were: TR = 2000 ms, TE = 28 ms, 3.5 x 3.5 x 5-mm, 18 axial slices (whole-brain coverage), and 0.5 mm interslice gap voxels.

Functional MRI Data Preprocessing Functional MRI data were corrected for slice-acquisition-dependent time shifts and interpolated to a 1 second resolution. Volumes that were large outliers in global signal were removed by replacing them with the global mean signal. Subsequent preprocessing using SPM2 (Wellcome Department of Cognitive Neurology, London, UK) included motion correction, normalization to the Colin brain in Montreal Neurological Institute (MNI) space using a 12-parameter affine transformation and a nonlinear transformation, and

resampling into 3 mm cubic voxels. Data were then spatially smoothed with an 8-mm full-width half-maximum (FWHM) Gaussian kernel.

Data Analysis Data for each task were independently analyzed in SPM2 at the subject level using a general linear model, which included a regressor for rule competition mentioned above. The resulting maps contained regions that are parametrically correlated with rule competition at each order. Statistical significance was assessed using a subject-specific fixed-effects model. Subject maps were entered into a group, second-level analysis that used a one-sample t-test against the null hypothesis of no activity at each voxel. Activity clusters in the group map consisting of at least 5 contiguous voxels exceeding an uncorrected threshold of $p < 0.001$ were considered reliable.

For the present study, unthresholded group and subject SPM contrast files were nonlinearly transformed from the Colin MNI space to FreeSurfer volumetric space and then projected to the FreeSurfer cortical surface for quantification of task activity. Cortical projection maps are displayed using Caret software (Van Essen 2005).

Quantification of Task Activity Task activity was quantified at the group and individual subject level for three regions in the lateral frontal cortex that together overlapped the functional hierarchy observed in the lateral frontal cortex. These regions belonged to the dorsal attention network (colored green in the parcellation) and two association networks covering the mid (orange) or rostral lateral (maroon) prefrontal cortex. To examine whether a functional gradient also exists in parietal cortex, task activity was also quantified in three parietal regions belonging

to the same networks. To determine the significance of the results, an Order by ROI (4 x 3) repeated measures ANOVA was performed for the lateral frontal cortex or parietal cortex. Paired t-tests were subsequently performed between the first and fourth orders for the motor association (green) or second association (maroon) network regions in the lateral frontal cortex or parietal cortex.

Resting-state Functional Connectivity Analysis

Participants Five hundred paid participants were ages 18 to 35, clinically normal, native English speakers, majority right-handed (91%), and with normal or corrected-to-normal vision (mean age = 21.3 yr, 42.6% male). This is the same dataset as the discovery sample set in previous papers (Buckner et al. 2011; Choi et al. 2012; Yeo et al. 2011). Subjects were excluded from the study if their slice-based fMRI SNR was low (< 100; Van Dijk et al. 2012) or artifacts were detected in the MRI data. Participants were pre-screened for prior neurological or psychiatric illness, psychoactive medications, and MRI contraindications. Written informed consent was obtained in accordance with procedures set by institutional review boards of Harvard University or Partners Healthcare.

MRI Data Acquisition The MRI data were collected on matched 3T Tim Trio scanners (Siemens, Erlangen, Germany) using the vendor-supplied 12-channel phased-array head coil. Structural data included a high-resolution multiecho T1-weighted magnetization-prepared gradient-echo image (multiecho MP-RAGE; van der Kouwe et al. 2008). Structural scan (multiecho MP-RAGE) parameters were: TR = 2200 ms, TI = 1100 ms, TE = 1.54 ms for image 1 to 7.01 ms for image 4, FA = 7º, 1.2 x 1.2 x 1.2-mm and FOV = 230. The functional imaging

data were acquired using a gradient-echo echo-planar imaging (EPI) sequence sensitive to BOLD contrast (Kwong et al. 1992; Ogawa et al. 1992). Functional imaging parameters were: TR = 3000 ms, TE = 30 ms, flip angle = 85º, 3 x 3 x 3-mm voxels, FOV = 216 and 47 slices aligned to the anterior commissure-posterior commissure plane (whole brain coverage; van der Kouwe et al. 2005). During the functional scans, subjects were instructed to stay still, stay awake, and keep their eyes open.

Functional MRI Data Preprocessing Functional imaging data were preprocessed as described in Yeo et al. (2011). Briefly, the first four volumes of each run were discarded, slice-acquisition-dependent time shifts were compensated per volume using SPM2, and head motion was corrected using rigid body translation and rotation using FMRIB Software Library (FSL; Jenkinson et al. 2002; Smith et al. 2004). The data underwent further preprocessing specific to resting-state functional connectivity analysis, including low-pass temporal filtering, head-motion regression, whole-brain signal regression, and ventricular and white matter signal regression (Van Dijk et al. 2010).

Structural MRI Data Preprocessing and Surface Functional-Structural Data Alignment Structural data preprocessing and functional-structural data alignment were the same as described in Yeo et al. (2011). Briefly, for each subject, the cerebral cortex was modeled as a two-dimensional surface and registered to a common spherical coordinate system using the FreeSurfer version 4.5.0 software package (http://surfer.nmr.mgh.harvard.edu). The structural and functional images were aligned (Study 1, Fig. 2.16) using the FsFast software package (http://surfer.nmr.mgh.harvard.edu/fswiki/FsFast). The resting-state BOLD fMRI data were then

aligned to the common spherical coordinate system. A 6-mm FWHM Gaussian smoothing kernel was applied to the fMRI data in the surface space and the data were downsampled to a 4-mm mesh. See Yeo et al. (2011) for further details.

Hybrid Surface- and Volume-Based Alignment, Mapping Between Surface- and Volume-Based Coordinates, and Visualization The surface and volume were aligned according to the procedure described in Choi et al. (2012) and Buckner et al. (2011). The striatum was modeled as a volume and aligned to the surface using a non-linear volumetric registration algorithm. The subject's fMRI data was transformed into the common FreeSurfer nonlinear volumetric space and smoothed with a 6-mm FWHM smoothing kernel. Spatial correspondence between the FreeSurfer surface and volumetric coordinate systems was established by averaging over 1,000 subjects the transformation from each subject's native space to the FreeSurfer surface space and the transformation from the FreeSurfer nonlinear volumetric space. For figure images, the normalized FreeSurfer nonlinear volumetric data were then transformed into FSL MNI space. The striatum was defined using a FreeSurfer template mask of the striatum (note: mask does not include the tail of the caudate because of resolution limitations). All analyses were performed in FreeSurfer surface and volumetric spaces. Results were displayed in MNI atlas space for the volume and the left and right inflated PALS cortical surfaces using Caret software (Van Essen 2005) for the surface. See Choi et al. (2012) and Buckner et al. (2011) for further details.

Regression of Cerebral Cortex Signal from Striatum In order to remove the cortical signal bleeding from adjacent cortex into the striatum, the mean cortical signal of cortical voxels adjacent to the left (within 4.0 voxels or 8 mm) or right (within 4.5 voxels or 9 mm) putamen

was regressed from the entire left or right striatum at the subject level. This regression revealed correlations to the motor network in the posterior putamen and association networks in the anterior putamen, as predicted by monkey anatomy. See Study 1, Figs. 2.10 and 2.11 for further details.

Selecting Cortical Regions for Functional Connectivity Analysis Functional connectivity was performed on two sets of cortical vertices. The first set consisted of the closest vertices to the regions that were most parametrically correlated to rule competition in the second, third, and fourth order hierarchical rule tasks. The MNI coordinates for these cortical regions are: -30, -10, 68 (first order; PMd); -38, 10, 34 (second order; prePMd); -50, 26, 24 (third order; DLPFC); and -36, 50, 6 (fourth order; RLPFC). The second set of cortical vertices was based on the first set, but moved away from cortical network boundaries as defined by the 1000 subject 17-network resting-state parcellation of the cerebral cortex (Yeo et al. 2011) to avoid signal mixing with neighboring networks. The MNI coordinates for these cortical regions are: -23, -10, 56 (first order); -38, 4, 29 (second order); -54, 19, 22 (third order); and -37, 59, -2 (fourth order).

Functional Connectivity Analysis Striatal fcMRI maps for specific cerebral seed regions were obtained by computing the Pearson's product moment correlation between the cortical region's resting-state fMRI time course and the time courses of striatal voxels. Each cortical region consisted of a single surface vertex (~4 x 4 mm), but should be considered spatially more extensive due to spatial smoothing. Group mean correlation *z*-maps were obtained by converting the correlation (*r*) maps of individual subjects to *z*-maps using Fisher's *r*-to-*z* transformation and then averaging across all subjects in the group. For subjects with multiple runs, the individual

subject *z*-maps were first averaged within subject and then submitted to the group average. An inverse Fisher's *r*-to-*z* transformation was then applied to the group-averaged correlation *z*-map, yielding a group mean correlation (*r*) map.

Corticostriatal Correlation Plots In order to comprehensively quantify the resting state fcMRI maps in the striatum, for each cortical region, the strongest correlation value at each of 21 coronal slices spanning the striatum was plotted to create corticostriatal correlation curves. Coronal slices were evenly spaced 2 mm apart throughout the striatum. Visual inspection showed that the correlation curves reflected the change in correlations through the striatum in the full correlation maps.

Quantification of Striatal Functional Territories Networks in the 7-network striatal parcellation (N = 1,000; Choi et al. 2012) were classified into association, sensory, or limbic territories as follows. Association: default (colored red in the striatal parcellation) and frontoparietal control (orange) networks. Sensory: sensorimotor (blue), dorsal attention (green), ventral attention (violet), and visual (purple) networks. Limbic: limbic (cream) network. The occupied territory was quantified as the percent of voxels within the territory of the total number of voxels in the striatum. DTI-based quantification of the striatum was based on results from a winner-take-all parcellation reported by Tziortzi et al. (2013; see their Table 2.1) in which each striatal voxel was assigned to the cortical target with the highest probability of connection. Their networks were classified into three broad territories as follows. Association territory: executive and parietal cortex. Sensory territory: rostral- and caudal-motor cortex. Limbic territory: limbic cortex.

Chapter 4:

General Discussion

Despite early views of the basal ganglia as a motor structure, progress over more than a century of research has shown that the basal ganglia process information from nearly the entire cerebral cortex and several subcortical structures. While animal research has been crucial in identifying connections and functional mechanisms, there is a limit to the information that animal studies can provide for humans, particularly for the association cortex, which is greatly expanded in humans relative to animals (Hill et al. 2010). In the two studies presented here, we begin to identify and characterize human basal ganglia circuits with a focus on those from association cortex.

One of the key pieces of information necessary in understanding the role of the striatum in humans is a map showing the topography of connections from the cerebral cortex to the striatum. Knowing the architecture of connections constrains the range of possible functional interactions and potentially provides insight into functional mechanisms. Study 1 addressed this need by using fcMRI to map the functional connections from the whole striatum to cortical networks covering the entire cerebral cortex. While this is not a map of direct anatomical connections, it does reflect functional interactions made possible by polysynaptic connections. In Study 1, we showed that fcMRI detects the inverted topography of connections from the motor cortex to the posterior putamen, as identified from monkey anatomy (Künzle 1975; Flaherty and Graybiel 1993). We also found a medial-to-lateral topography of SMA and motor correlations in the posterior putamen, also shown by monkey anatomy (Takada et al. 1998a) and by human DTI (Leh et al. 2007).

Encouraged by these results, we then created a striatal parcellation map assigning each striatal voxel to its most strongly correlated network. The results recapitulated the three broad motor, association, and limbic territories, as well as providing details of the organization from

specific cortical networks. We also found that the striatal correlation patterns from five functionally distinct motor, association, and limbic cortical regions largely agreed with the striatal projections from homologous monkey cortical regions. This demonstrates that fcMRI is capable of detecting functional connections from not only motor-related regions, but also from association and limbic regions.

We then further explored the organization of corticostriatal connectivity. We demonstrated evidence of the principle of interconnected cortical regions connecting to similar striatal regions. For two association networks (the frontoparietal control and default networks), the distributed cortical regions of each network correlate with similar striatal regions with a pattern unique to each network. We further showed similar connectivity patterns from homologous distributed monkey regions of both association networks. These results suggest that each striatal region in association territory receives information from an entire network.

Altogether, these results show many similarities between the human and monkey corticostriatal connectivity. However, there are parts of the human association cortex that are greatly expanded relative to those in monkey association cortex. The striatal parcellation provided by my work shows how these expanded cortical regions are functionally connected to the striatum. This information will serve as an important model with which to interpret human fMRI results or to create hypotheses for investigation, as we did in Study 2.

In Study 2, we examined corticostriatal connectivity from association cortex in greater detail. The parallel, distributed association network model based on anatomical connectivity proposes that association networks each consist of regions distributed throughout the lobes of the cerebral cortex, with regions of different networks adjacent to one another (Goldman-Rakic 1988; Fig. 4.1). This model naturally leads to the question of how do these networks interact to

form integrated, complex behavior. In Study 2, we found that fMRI activity in the lateral frontal and parietal cortices during hierarchical rule usage overlaps with the same association network. The network was specific to the order of rules in the task: the first order task activity overlapped a motor association network that includes premotor cortex; the second and third order task activity overlapped with an association network (called association I network); and the fourth order task overlapped with a separate association (called association II network). This shows that hierarchical cognitive control, and potentially cognitive functions in general, is subserved not by a set of localized regions, but by networks of multiple, distributed regions. Our findings also indicate that association networks, although anatomically organized in parallel, appear to be functionally organized in a hierarchy.

If a functional hierarchy between association networks exists, what is the connectivity underlying it? We explored whether there is a hierarchical organization to corticostriatal connectivity that could underlie the functional hierarchy. We found evidence of a rostral-to-caudal correspondence in functional connectivity between the hierarchical regions of the lateral frontal cortex and the caudate, which may support the hierarchical interactions of association networks. However, using fcMRI, the organization of the correlations was ambiguous in suggesting a hierarchical organization.

Altogether, the results of these two studies contribute human information to our knowledge of the basal ganglia. Below, I discuss several implications and caveats of the findings, as well as potential directions for future research.

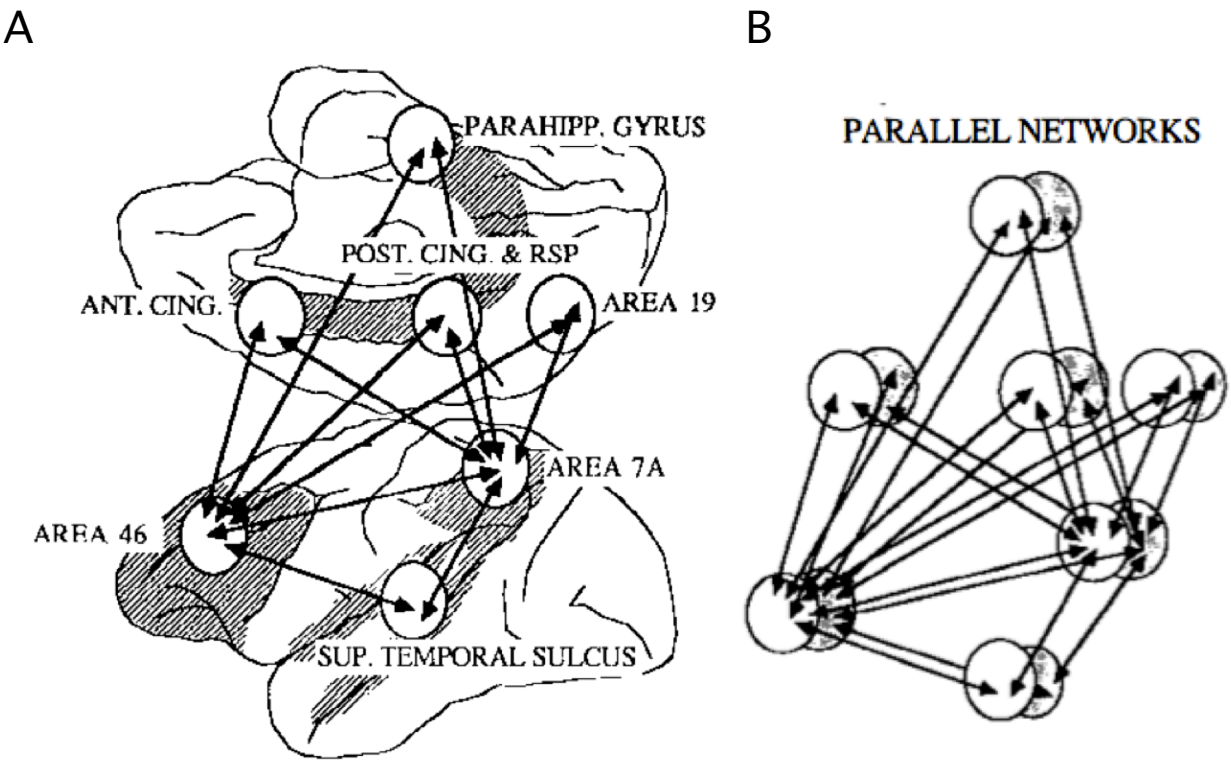

Figure 4.1 Parallel, distributed model of association networks. (A) Cartoon model illustrating the common cortical targets of area 46 in the prefrontal cortex and area 7A in the parietal cortex of the monkey. Note that targets are distributed across association cortex. (B) Schematic of two parallel association networks, each with a unique set of interconnected, distributed cortical regions. Adapted from Goldman-Rakic (1988) with permission from Annual Reviews, Inc.

Insights into striatal connectivity and function

The principle of interconnected cortical regions projecting to overlapping striatal regions was suggested previously by Yeterian and Van Hoesen (1978) and further investigated by Selemon and Goldman-Rakic (1985). Study 1 demonstrated that the human striatum is coupled to cortical networks, each with its distinct connectivity pattern in the striatum. We further demonstrated the similarity of these connectivity patterns to those from homologous monkey regions for the frontoparietal and default networks. In addition, as discussed in the Discussion of Study 1, there are other pieces of monkey anatomical evidence supporting this organization. Double-labeling studies by Selemon and Goldman-Rakic (1985) and Cavada and Goldman-

Rakic (1991) both showed that functionally distinct regions project to distinct regions of the striatum with an organization similar to that seen with human fcMRI. Retrograde injections of the striatum also show distributed patterns of labeling in the cortex, indicating that a single region of the striatum receives input from distributed cortical regions, potentially those comprising a network (Arikuni and Kubota 1986; McGeorge and Faull 1989; Rosell and Gimenez-Amaya 1999).

Thus, it seems likely that a single striatal region receives inputs from the distributed regions of a network. This suggests that the striatum is a place where distinct information from the different regions of a network converge and are integrated. In addition, while the broad organization of association, motor, and limbic territories is generally true, corticostriatal projections cross these boundaries (Haber et al. 2006), indicating that there is also integration across different functional networks.

While it appears that cortical regions within a network are connected to similar regions in the striatum, it does not appear that the amount of inputs is the same across cortical regions. There is significantly greater input from frontal than from non-frontal regions. An early anatomical study showed that there are greater anterior (anterior to and including somatomotor cortex) versus posterior (posterior to somatomotor cortex) projections to the striatum in rabbits (Carman et al. 1963). An anatomical tracing study of the cingulate cortex showed that the striatum receives much greater input from the anterior (area 24) than posterior (area 23) cingulate cortex (Baleydier and Mauguiere 1980). Human fcMRI also shows stronger correlations of the striatum with frontal regions than with parietal and occipital regions (personal observation). This asymmetry in connections can be observed from Figures 2.13 and 2.14 in Study 1. Figure 2.13, comparing corticostriatal connectivity of human and monkey regions in the frontoparietal control

network, shows weaker correlations from the parietal region (PGa) than from the frontal regions (PFC_{lp} and PFC_{mp}). Figure 2.14, showing an analogous comparison for the default network, shows the strongest correlation for the medial frontal region (PFCmd) and weaker correlations for non-frontal regions (STS, PGc, and PCC; Note: the anterior frontal region PFC_a is in a high MR susceptibility area, thus its weak striatal correlation is most likely due to signal loss).

The regions of non-frontal cortex are comprised mostly of sensory and sensory association regions. With the exception of the somatomotor cortex and the olfactory cortex, which are strongly connected to the posterior putamen (Künzle 1975, 1977) and ventral striatum (Heimer and Wilson 1975), respectively, the striatum receives relatively weak and/or limited projections from the auditory and visual association regions (Saint-Cyr et al. 1990; Webster et al. 1993; Yeterian and Pandya 1998), even fewer projections from the primary auditory cortex (Yeterian and Pandya 1998), and no projections from the primary visual cortex (Saint-Cyr et al. 1990). The same study showing limited projections from auditory regions also showed, in contrast, massive projections from a limbic rostral temporal region (Yeterian and Pandya 1998). Thus, it appears that the striatum is mostly concerned with frontal association, motor, and limbic regions. The striatum's function may be to assign a limbic label to cognitive information and couple it with an action or downstream influence on information processing. It does not appear to be highly concerned with sensory information, albeit more concerned with sensory association information.

This asymmetric connectivity is consistent with a dual cingulate model proposed by Baleydier and Mauguiere (1980), who found a differential in projections emanating from the posterior and anterior cingulate cortex in keeping with their functional duality of processing sensory association information and emotional and visceral information, respectively. The

posterior cingulate cortex (area 23) was found to be specifically connected with the associative regions of temporal cortex, the medial temporal and orbitofrontal cortices, and the medial pulvinar. In contrast, the anterior cingulate cortex (area 24) was preferentially connected to the nucleus accumbens; intralaminar, mediodorsal, and ventral anterior thalamic nuclei (output targets of the basal ganglia); and the amygdala. Hence, the preponderance of fronto-striatal connections is not unique to the striatum; it is also characteristic of other functionally related structures.

It is also interesting to note that the anterior striatum is much larger than the posterior striatum, particularly for the caudate. As Kemp and Powell (1970) initially showed and later observed by human DTI studies, corticostriatal connections have a greater amount of connectivity in the striatal regions closest to the cortical regions of origin (in addition to their longitudinal connectivity throughout the striatum). Thus, it is possible that the anterior striatum is larger due to the greater amount of projections incoming from the frontal cortex. These greater inputs from the frontal cortex may be due to the striatum's putative greater involvement in frontal cortical functions (e.g., reflected by preferential connectivity with the frontal cortex) or simply because there is more association territory in the frontal versus non-frontal cortex. It would be interesting to compare the volumetric ratio of the anterior versus posterior striatum to the spatial ratio of frontal versus non-frontal association territory and the density ratio of frontal versus non-frontal association connections to the striatum.

The parallel, distributed model of association networks

In 1988, Goldman-Rakic proposed the model of parallel and distributed association networks (Fig. 4.1), which was introduced in Study 2. The organization has two main features.

Firstly, an association network consists of regions in distributed parts of the association cortex that are interconnected with no apparent hierarchy (Fig. 4.1*A*). Secondly, there are multiple association networks in parallel, with regions of different networks adjacent to one another in the distributed parts of association cortex (Fig. 4.1*B*). Thus, a given region has stronger connections to distant regions within the same network than to neighboring regions of a different network. Goldman-Rakic provided two pieces of evidence to support this model. The first was that distinctly different regions of parietal cortex project to distinctly different regions of the prefrontal cortex, which demonstrates the parallel aspect of her model. The second was that double-labeling experiments with injections in the parietal and prefrontal cortices with two separate tracers lead to a convergence of tracers in about 15 distributed cortical regions. This supports the idea of interconnected, distributed regions comprising a network (Selemon and Goldman-Rakic 1988).

However, there are several limitations to the studies that need to be addressed. One limitation is the need to demonstrate actual synaptic terminations in the regions of interest, which was not possible with the tracers at the time. A second limitation is the large sizes of the tracer injections in the double-labeling experiments, which increase the chances of non-specific injections and incorrect conclusions. Figure 4.2 shows three examples of how large injections can lead to a false negative or a false positive conclusion.

Figure 4.2*A* shows three parallel association networks (black, white, gray) with distributed regions (circles). Black lines denote anatomical connections. Dashed ovals encircle regions that have been injected or labeled by a red or blue tracer. Large tracer injections can fail to detect parallel, distributed association networks if the injections label regions from different networks. For example, a large red tracer injection in the upper left cluster overlapping the white

and gray network regions (see arrow) and a large blue tracer in the upper right cluster overlapping the white and black network regions (see arrow) lead to incomplete convergence in the bottom cluster. This may lead to the failure to detect parallel, distributed networks. While this is not applicable to Goldman-Rakic's 1988 papers, a similar situation has had implications for the striatum. When testing the model of interconnected cortical regions projecting to similar striatal regions, Selemon and Goldman-Rakic (1985) used double-labeling cases with large injections in reciprocally connected cortical regions. This lead to projection patterns in the striatum with partial overlap. Although they concluded that this was not convergence, the large injection sites make it difficult to be certain of this.

More relevantly for the parallel, distributed association network model, large injections may lead to the conclusion of this model when, in fact, it is not true. Figure 4.2*B* shows a situation in which there are two distributed, but not fully interconnected association networks. A large blue tracer injection to the bottom regions (see arrow) and a large red tracer injection to the upper right regions (see arrow) leads to an overlap of both tracers on a white region in the upper left cluster, and two black regions in the upper right and bottom clusters. This could give the illusion of a parallel, distributed network when, in fact, they are regions from two, non-interconnecting networks.

More insidiously, Figure 4.2*C* shows a second example of a potential false positive. Here, there are two hierarchical pathways (white and black) with distributed regions that converge on the same region (gray) at the top of the pathways. Large tracer injections covering black and white regions in the upper left and upper right clusters would lead to a convergence on the gray region. This would give the illusion of a parallel, association network when, in fact, the underlying connectivity is actually hierarchical.

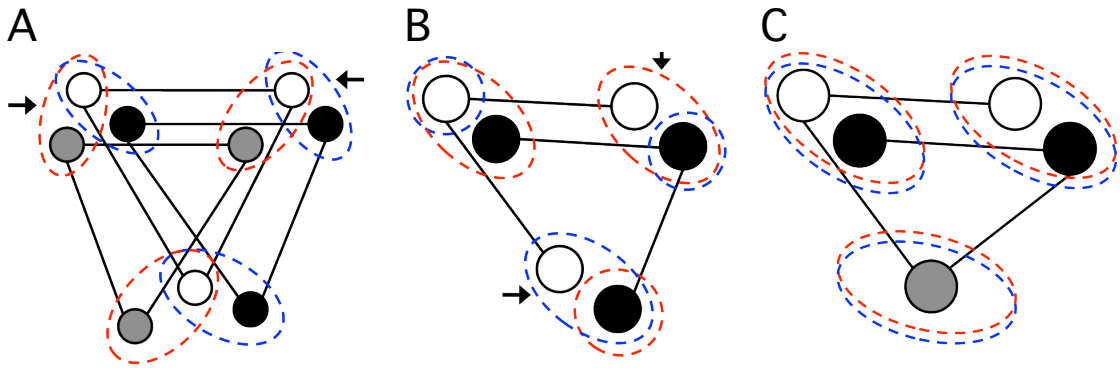

Figure 4.2 False negative and false positive examples from large tracer injections. Large injections have the potential for incorrect conclusions depending on where they are placed. (A) Given the presence of parallel, interconnected networks, a red tracer in the upper left cluster and a blue tracer in the upper right cluster (see arrows) may overlap regions of different networks, leading to minimal tracer overlap in the bottom cluster. This may lead to a false negative conclusion. (B) Given two distributed, but not fully interconnected association networks, a blue tracer injection in the bottom regions and a red tracer injection to the upper right regions (see arrows) lead to convergence of the tracers on a white network region in the upper left and two black network regions in the bottom and upper right clusters, leading to a false positive conclusion. (C) Given two hierarchical pathways (white and black) with distributed regions and convergence on a single region (gray) at the top of the hierarchy, large tracer injections in the upper left and upper right clusters lead to a convergence on the gray region. This may lead to a false positive conclusion. Circles represent distributed cortical regions. Circle colors represent different networks. Black lines represent anatomical connections. Red and blue dashed ovals indicate overall tracer results from an injection in any of the ovals. Arrows clarify tracer injection locations.

Our finding from Study 2 using fMRI task data of a functional hierarchy of association networks supports the model of parallel, distributed association networks. The co-activation of lateral frontal and parietal regions of the same network during a task, for three distinct networks, provides functional confirmation of the connectivity-based model. Our evidence from Study 1 for the model of interconnected cortical regions connecting to similar striatal regions is suggestive, but not strong, of a parallel, distributed organization, adding to the fcMRI evidence from Yeo et al. (2011). However, the methods of both studies do not tell us whether within-network regions are fully interconnected, as suggested by Goldman-Rakic.

Fortunately, advances in tracers have been made since 1988, allowing the limitations above to be addressed. Fluorescent tracers have higher specificity and resolution, allowing us to verify terminal synapses in target regions. In addition, neuroimaging is now available and used to identify the precise location to place small injections, allowing for greater specificity. A re-investigation with modern methods would bring new information to the parallel, distributed association networks model, which has not been investigated since it was proposed in 1988.

Functional hierarchy of association networks

From the human cortical parcellation (Yeo et al. 2011) and the observation of activity in lower and higher order association networks in Study 2, it appears to be true that association networks are at least functionally parallel and distributed, even if not all of the constituent regions are anatomically connected to one another. The presence of parallel networks naturally leads to the question of how they interact to form complex, integrated behavior.

The interaction of networks is an understudied area with few existing models. One of these is a model proposed by Fuster (1995, 2003, 2008) consisting of a functional hierarchy of association networks.[1] The model essentially says that the parietal cortex processes perception and the frontal cortex processes action via a hierarchy of simple to complex processing. These dual hierarchies are connected by long-distance projections, creating higher and lower order networks. Fuster's model beautifully predicts the results of Study 2, which provide the first identification of networks organized in a functional hierarchy. This result indicates that

[1] In addition to the functional hierarchy model, another model of network interactions suggested by Posner and Petersen (1990; Petersen and Posner 2012) consists of a superordinate attention network(s) that allows focal, selected attention to stimuli detected by subordinate attention networks. A third, emotion regulation model consists of a "cold" control network that includes the dorsolateral prefrontal cortex and regulates a "hot" emotion network (Ochsner et al. 2012).

association networks are anatomically organized in parallel, as described by Goldman-Rakic, but functionally organized in a hierarchy. This explains how we can have hierarchically structured behaviors with parallel, preferentially self-connected networks. This insight into how association networks interact may potentially facilitate a broader, network perspective of behavior. For the cognitive control field alone, our identification of the specific hierarchical networks involved urges a network, not regional, perspective.

However, further work needs to be done to establish a functional hierarchy of association networks. This includes identification of the anatomical connections underlying this functional hierarchy and then their manipulation in animal neurophysiological recording or calcium imaging studies. Anatomical connectivity supporting a functional hierarchy between association networks could arise from hierarchical cortico-cortical and/or cortico-subcortical connectivity. In Study 2, we could not determine whether hierarchical corticostriatal connectivity exists using fcMRI, underscoring the need for anatomical studies. A functional hierarchy may also arise from hierarchical corticothalamic connections. As shown by McFarland and Haber (2002), corticothalamic connections exist reciprocally between specific cortical and thalamic regions and exist broadly and non-reciprocally from both directions. An anatomical study is much needed to investigate the potential connections underlying a functional hierarchy of association networks, which could then be tested in animal functional studies.

Evolutionary implications

The presence of lower versus higher order networks suggests that, over evolution, new association cortex develops as distributed networks. This is corroborated by the demonstration of distributed regions of expansion between human and monkey cerebral cortex and the later

development of distributed regions from human infancy to adulthood (Hill et al. 2010). Comparative studies also show that the neocortex has expanded much more quickly over evolution than has the striatum (Finlay and Darlington 1995). How, then, have the new neocortical networks mapped onto the striatum over evolution?

Given that the corticostriatal connectivity patterns between the monkey and human appear highly similar and the association I and II networks both have the same broad correlation pattern in the striatum, it seems likely that the projections from newer association networks converged upon those of older networks of similar function. In addition, the general similarity of the cytoarchitecture of the human, monkey, rat, and cat striata (Graybiel and Ragsdale 1978; Holt et al. 1997) suggests that the basal ganglia have not developed new mechanisms over evolution. Thus, it appears that human abilities are expansions based on primitive ones that exist in monkeys, rather than new abilities that formed over evolution, and processed by the basal ganglia with similar, although perhaps elaborated, mechanisms as those in the monkey.

Conclusion

In light of the century-long process of understanding the basal ganglia, a process advanced by developments of new technology, these studies are among the first to use neuroimaging to investigate the human basal ganglia. The first study provides an in-depth link of the prior knowledge based on animal studies to human results. The second study explores association networks and their functional connectivity to the striatum, a topic that receives limited insight from animal studies. Like any other technique, fcMRI has limitations, but its strengths in identifying functional connections throughout the brain contribute to a more global understanding of the striatum. As illustrated by a juxtaposition of the cortical, cerebellar, and

striatal 7-network parcellations (Fig. 4.3), the basal ganglia are a part of large-scale networks spanning not only the cerebral cortex, as discussed at length here, but also the cerebellum and likely nearly all other structures of the brain.

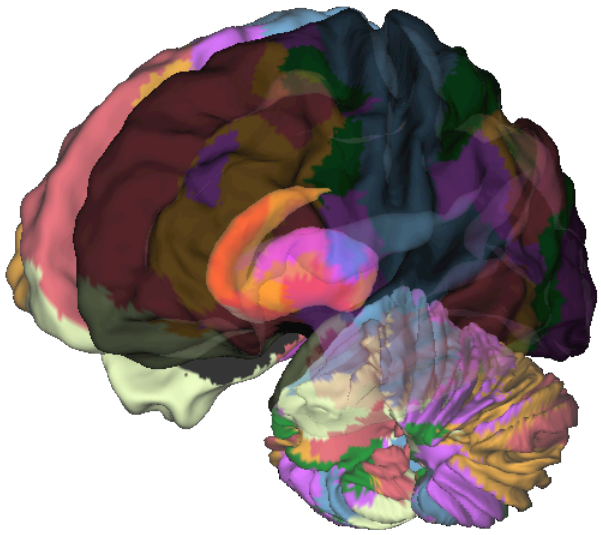

Figure 4.3 Seven-network parcellation maps of cerebral cortex, cerebellum, and striatum. An antero-lateral view of the 7-network parcellations of the cerebral cortex, cerebellum, and striatum are displayed together in one brain. The left hemisphere is darkened and translucent to allow the striatum to be visible. Behavior arises from the coordinated interactions of networks spanning the entire brain. Cortical and cerebellar parcellations from Yeo et al. (2011) and Buckner et al. (2011).

References

Adrian ED. Afferent areas in the cerebellum connected with the limbs. *Brain* 66: 289-315, 1943.

Albin RL, Young AB, and Penney JB. The functional anatomy of basal ganglia disorders. *Trends Neurosci* 12: 366-375, 1989.

Alexander GE, Crutcher MD, and DeLong MR. Basal ganglia-thalamocortical circuits: parallel substrates for motor, oculomotor, "prefrontal" and "limbic" functions. *Prog Brain Res* 85: 119-146, 1990.

Alexander GE, and DeLong MR. Microstimulation of the primate neostriatum. II. Somatotopic organization of striatal microexcitable zones and their relation to neuronal response properties. *J Neurophysiol* 53: 1417-1430, 1985.

Alexander GE, DeLong MR, and Strick PL. Parallel organization of functionally segregated circuits linking basal ganglia and cortex. *Annu Rev Neurosci* 9: 357-381, 1986.

Amaral D. Memory: Anatomical organization of candidate brain regions. In: *Handbook of Physiology; The Nervous System, Vol 5: Higher Functions of the Brain, Part 1*, edited by Plum F. Bethesda, MD: American Physiological Society, 1987.

Andersen RA, Asanuma C, Essick G, and Siegel RM. Corticocortical connections of anatomically and physiologically defined subdivisions within the inferior parietal lobule. *J Comp Neurol* 296: 65-113, 1990.

Andrews-Hanna JR, Snyder AZ, Vincent JL, Lustig C, Head D, Raichle ME, and Buckner RL. Disruption of large-scale brain systems in advanced aging. *Neuron* 56: 924-935, 2007.

Arikuni T, and Kubota K. The organization of prefrontocaudate projections and their laminar origin in the macaque monkey: a retrograde study using HRP-gel. *J Comp Neurol* 244: 492-510, 1986.

Badre D, and D'Esposito M. Functional magnetic resonance imaging evidence for a

hierarchical organization of the prefrontal cortex. *J Cogn Neurosci* 19: 2082-2099, 2007.

Badre D, and D'Esposito M. Is the rostro-caudal axis of the frontal lobe hierarchical? *Nat Rev Neurosci* 10: 659-669, 2009.

Badre D, Hoffman J, Cooney JW, and D'Esposito M. Hierarchical cognitive control deficits following damage to the human frontal lobe. *Nat Neurosci* 12: 515-522, 2009.

Baker JT, Holmes AJ, Masters G, Buckner RL, and Öngür D. Disruption of frontoparietal control network in schizophrenia and psychotic bipolar disorder. *Arch Gen Psychiatry*, in press.

Baleydier C, and Mauguiere F. The duality of the cingulate gyrus in monkey. Neuroanatomical study and functional hypothesis. *Brain* 103: 525-554, 1980.

Bandettini PA, Wong EC, Hinks RS, Tikofsky RS, and Hyde JS. Time course EPI of human brain function during task activation. *Magn Reson Med* 25: 390-397, 1992.

Barnes CL, and Pandya DN. Efferent cortical connections of multimodal cortex of the superior temporal sulcus in the rhesus monkey. *J Comp Neurol* 318: 222-244, 1992.

Barnes KA, Cohen AL, Power JD, Nelson SM, Dosenbach YB, Miezin FM, Petersen SE, and Schlaggar BL. Identifying basal ganglia divisions in individuals using resting-state functional connectivity MRI. *Front Syst Neurosci* 4: 18, 2010.

Basser PJ, Mattiello J, and Le Bihan D. Estimation of the effective self-diffusion tensor from the NMR spin echo. *J Magn Reson Ser B* 103: 247-254, 1994.

Belliveau JW, Kennedy DN, Jr., McKinstry RC, Buchbinder BR, Weisskoff RM, Cohen MS, Vevea JM, Brady TJ, and Rosen BR. Functional mapping of the human visual cortex by magnetic resonance imaging. *Science* 254: 716-719, 1991.

Bhatia KP, and Marsden CD. The behavioural and motor consequences of focal lesions of the basal ganglia in man. *Brain* 117 (Pt 4): 859-876, 1994.

Biswal B, Yetkin FZ, Haughton VM, and Hyde JS. Functional connectivity in the motor cortex of resting human brain using echo-planar MRI. *Magn Reson Med* 34: 537-541, 1995.

Biswal BB, Mennes M, Zuo XN, Gohel S, Kelly C, Smith SM, Beckmann CF, Adelstein JS, Buckner RL, Colcombe S, Dogonowski AM, Ernst M, Fair D, Hampson M, Hoptman MJ, Hyde JS, Kiviniemi VJ, Kotter R, Li SJ, Lin CP, Lowe MJ, Mackay C, Madden DJ, Madsen KH, Margulies DS, Mayberg HS, McMahon K, Monk CS, Mostofsky SH, Nagel BJ, Pekar JJ, Peltier SJ, Petersen SE, Riedl V, Rombouts SA, Rypma B, Schlaggar BL, Schmidt S, Seidler RD, Siegle GJ, Sorg C, Teng GJ, Veijola J, Villringer A, Walter M, Wang L, Weng XC, Whitfield-Gabrieli S, Williamson P, Windischberger C, Zang YF, Zhang HY, Castellanos FX, and Milham MP. Toward discovery science of human brain function. *Proc Natl Acad Sci USA* 107: 4734-4739, 2010.

Blinder P, Tsai PS, Kaufhold JP, Knutsen PM, Suhl H, and Kleinfeld D. The cortical angiome: an interconnected vascular network with noncolumnar patterns of blood flow. *Nat Neurosci* 16: 889-897, 2013.

Blumenfeld RS, Nomura EM, Gratton C, and D'Esposito M. Lateral prefrontal cortex is organized into parallel dorsal and ventral streams along the rostro-caudal axis. *Cereb Cortex* 2012.

Bohanna I, Georgiou-Karistianis N, and Egan GF. Connectivity-based segmentation of the striatum in Huntington's disease: vulnerability of motor pathways. *Neurobiol Dis* 42: 475-481, 2011.

Buckner RL. Functional-anatomic correlates of control processes in memory. *J Neurosci* 23: 3999-4004, 2003.

Buckner RL. Human functional connectivity: new tools, unresolved questions. *Proc Natl Acad*

Sci USA 107: 10769-10770, 2010.

Buckner RL, Andrews-Hanna JR, and Schacter DL. The brain's default network: anatomy, function, and relevance to disease. *Ann N Y Acad Sci* 1124: 1-38, 2008.

Buckner RL, Krienen FM, Castellanos A, Diaz JC, and Yeo BTT. The organization of the human cerebellum revealed by intrinsic functional connectivity. *J Neurophysiol* 2011.

Buckner RL, Krienen FM, and Yeo BTT. Opportunities and limitations of intrinsic functional connectivity MRI. *Nat Neurosci* 16: 832-837, 2013.

Caine ED, and Shoulson I. Psychiatric syndromes in Huntington's disease. *Am J Psychiatry* 140: 728-733, 1983.

Calzavara R, Mailly P, and Haber SN. Relationship between the corticostriatal terminals from areas 9 and 46, and those from area 8A, dorsal and rostral premotor cortex and area 24c: an anatomical substrate for cognition to action. *Eur J Neurosci* 26: 2005-2024, 2007.

Carman J, Cowan W, and Powell T. The organization of cortico-striate connexions in the rabbit. *Brain* 86: 525-562, 1963.

Carpenter MB, Nakano K, and Kim R. Nigrothalamic projections in the monkey demonstrated by autoradiographic technics. *J Comp Neurol* 165: 401-415, 1976.

Caspers S, Geyer S, Schleicher A, Mohlberg H, Amunts K, and Zilles K. The human inferior parietal cortex: cytoarchitectonic parcellation and interindividual variability. *Neuroimage* 33: 430-448, 2006.

Cavada C, and Goldman-Rakic PS. Posterior parietal cortex in rhesus monkey: I. Parcellation of areas based on distinctive limbic and sensory corticocortical connections. *J Comp Neurol* 287: 393-421, 1989.

Cavada C, and Goldman-Rakic PS. Topographic segregation of corticostriatal projections

from posterior parietal subdivisions in the macaque monkey. *Neuroscience* 42: 683-696, 1991.

Chevalier G, and Deniau JM. Disinhibition as a basic process in the expression of striatal functions. *Trends Neurosci* 13: 277-280, 1990.

Choi EY, Yeo BTT, and Buckner RL. The organization of the human striatum estimated by intrinsic functional connectivity. *J Neurophysiol* 108: 2242-2263, 2012.

Cohen MX, Lombardo MV, and Blumenfeld RS. Covariance-based subdivision of the human striatum using T1-weighted MRI. *Eur J Neurosci* 27: 1534-1546, 2008.

Cohen MX, Schoene-Bake JC, Elger CE, and Weber B. Connectivity-based segregation of the human striatum predicts personality characteristics. *Nat Neurosci* 12: 32-34, 2009.

Crittenden JR, and Graybiel AM. Basal ganglia disorders associated with imbalances in the striatal striosome and matrix compartments. *Front Neuroanat* 5: 59, 2011.

Cummings JL. Frontal-subcortical circuits and human behavior. *Arch Neurol* 50: 873-880, 1993.

Dale AM, Fischl B, and Sereno MI. Cortical surface-based analysis. I. Segmentation and surface reconstruction. *Neuroimage* 9: 179-194, 1999.

Damasio H, Grabowski T, Frank R, Galaburda AM, and Damasio AR. The return of Phineas Gage: clues about the brain from the skull of a famous patient. *Science* 264: 1102-1105, 1994.

DeLong MR. Primate models of movement disorders of basal ganglia origin. *Trends Neurosci* 13: 281-285, 1990.

DeLong MR, and Georgopoulos A. Motor functions of the basal ganglia. In: *Handbook of Physiology: The Nervous System, Motor Control*. Bethesda, MD: Am Physiol Soc, 1981, sect. 1, vol. II, part 2.

DeVito JL, and Smith OA, Jr. Subcortical projections of the prefrontal lobe of the monkey. *J Comp Neurol* 123: 413-423, 1964.

Di Martino A, Scheres A, Margulies DS, Kelly AM, Uddin LQ, Shehzad Z, Biswal B, Walters JR, Castellanos FX, and Milham MP. Functional connectivity of human striatum: a resting state FMRI study. *Cereb Cortex* 18: 2735-2747, 2008.

Draganski B, Kherif F, Kloppel S, Cook PA, Alexander DC, Parker GJ, Deichmann R, Ashburner J, and Frackowiak RS. Evidence for segregated and integrative connectivity patterns in the human basal ganglia. *J Neurosci* 28: 7143-7152, 2008.

Duncan J, and Owen AM. Common regions of the human frontal lobe recruited by diverse cognitive demands. *Trends Neurosci* 23: 475-483, 2000.

Eblen F, and Graybiel AM. Highly restricted origin of prefrontal cortical inputs to striosomes in the macaque monkey. *J Neurosci* 15: 5999-6013, 1995.

Ehringer H, and Hornykiewicz O. Verteilung von noradrenalin and dopamin (3-hydroxytyramin) im gehirn des menschen und ihr verhalten bei erkrankungen des extrapyramidalen systems. *Klin Wochenschr* 38: 1236-1239, 1960.

Evans AC, Collins DL, Mills SR, Brown ED, Kelly RL, Peters TM. 3D statistical neuroanatomical models from 305 MRI volumes. *Proceedings IEEE Nuclear Science Symposium and Medical Imaging Conference.* London: MTP, 1993, vol. 95, p. 1813-1817.

Evarts EV, and Thach WT. Motor mechanisms of the CNS: cerebrocerebellar interrelations. *Annu Rev Physiol* 31: 451-498, 1969.

Farooqui AA, Mitchell D, Thompson R, and Duncan J. Hierarchical organization of cognition reflected in distributed frontoparietal activity. *J Neurosci* 32: 17373-17381, 2012.

Ferrier D. *The Functions of the Brain*. London: Smith, Elder, & Co., 1876.

Ferry AT, Öngür D, An X, and Price JL. Prefrontal cortical projections to the striatum in macaque monkeys: evidence for an organization related to prefrontal networks. *J Comp Neurol* 425: 447-470, 2000.

Finlay BL, and Darlington RB. Linked regularities in the development and evolution of mammalian brains. *Science* 268: 1578-1584, 1995.

Fischl B, Liu A, and Dale AM. Automated manifold surgery: constructing geometrically accurate and topologically correct models of the human cerebral cortex. *IEEE Trans Med Imaging* 20: 70-80, 2001.

Fischl B, Rajendran N, Busa E, Augustinack J, Hinds O, Yeo BTT, Mohlberg H, Amunts K, and Zilles K. Cortical folding patterns and predicting cytoarchitecture. *Cereb Cortex* 18: 1973-1980, 2008.

Fischl B, Salat DH, Busa E, Albert M, Dieterich M, Haselgrove C, van der Kouwe AJW, Killiany R, Kennedy D, Klaveness S, Montillo A, Makris N, Rosen B, and Dale AM. Whole brain segmentation: automated labeling of neuroanatomical structures in the human brain. *Neuron* 33: 341-355, 2002.

Fischl B, Sereno MI, and Dale AM. Cortical surface-based analysis. II: Inflation, flattening, and a surface-based coordinate system. *Neuroimage* 9: 195-207, 1999a.

Fischl B, Sereno MI, Tootell RB, and Dale AM. High-resolution intersubject averaging and a coordinate system for the cortical surface. *Hum Brain Mapp* 8: 272-284, 1999b.

Fischl B, van der Kouwe AJW, Destrieux C, Halgren E, Ségonne F, Salat DH, Busa E, Seidman LJ, Goldstein J, Kennedy D, Caviness V, Makris N, Rosen B, and Dale AM. Automatically parcellating the human cerebral cortex. *Cereb Cortex* 14: 11-22, 2004.

Fitzgerald PB, Laird AR, Maller J, and Daskalakis ZJ. A meta-analytic study of changes in

brain activation in depression. *Hum Brain Mapp* 29: 683-695, 2008.

Flaherty AW, and Graybiel AM. Corticostriatal transformations in the primate somatosensory system. Projections from physiologically mapped body-part representations. *J Neurophysiol* 66: 1249-1263, 1991.

Flaherty AW, and Graybiel AM. Two input systems for body representations in the primate striatal matrix: experimental evidence in the squirrel monkey. *J Neurosci* 13: 1120-1137, 1993.

Flaherty AW, and Graybiel AM. Input-output organization of the sensorimotor striatum in the squirrel monkey. *J Neurosci* 14: 599-610, 1994.

Flechsig P. Developmental (myelogenetic) localisation of the cerebral cortex in the human subject. *The Lancet* 2: 1027-1029, 1901.

Fonov V, Evans AC, Botteron K, Almli CR, McKinstry RC, and Collins DL. Unbiased average age-appropriate atlases for pediatric studies. *Neuroimage* 54: 313-327, 2011.

Fornito A, and Bullmore ET. What can spontaneous fluctuations of the blood oxygenation-level-dependent signal tell us about psychiatric disorders? *Curr Opin Psychiatry* 23: 239-249, 2010.

Fox MD, and Raichle ME. Spontaneous fluctuations in brain activity observed with functional magnetic resonance imaging. *Nat Rev Neurosci* 8: 700-711, 2007.

Fox PT, Miezin FM, Allman JM, Van Essen DC, and Raichle ME. Retinotopic organization of human visual cortex mapped with positron-emission tomography. *J Neurosci* 7: 913-922, 1987.

Fox PT, Mintun MA, Raichle ME, Miezin FM, Allman JM, and Van Essen DC. Mapping human visual cortex with positron emission tomography. *Nature* 323: 806-809, 1986.

Fudge JL, Breitbart MA, and McClain C. Amygdaloid inputs define a caudal component of

the ventral striatum in primates. *J Comp Neurol* 476: 330-347, 2004.

Fudge JL, Kunishio K, Walsh P, Richard C, and Haber SN. Amygdaloid projections to ventromedial striatal subterritories in the primate. *Neuroscience* 110: 257-275, 2002.

Fuster J. *Memory in the Cerebral Cortex*. The MIT Press, 1995.

Fuster J. *Cortex and the Mind*. New York: Oxford University Press, 2003.

Fuster J. *The Prefrontal Cortex, Fourth Edition*. Elsevier, Inc., 2008.

Gerfen CR. The neostriatal mosaic: compartmentalization of corticostriatal input and striatonigral output systems. *Nature* 311: 461-464, 1984.

Gerfen CR. The neostriatal mosaic: multiple levels of compartmental organization. *Trends Neurosci* 15: 133-139, 1992.

Geyer S. The microstructural border between the motor and the cognitive domain in the human cerebral cortex. *Adv Anat Embryol Cell Biol* 174: 1-89, 2004.

Geyer S, Ledberg A, Schleicher A, Kinomura S, Schormann T, Burgel U, Klingberg T, Larsson J, Zilles K, and Roland PE. Two different areas within the primary motor cortex of man. *Nature* 382: 805-807, 1996.

Glees P. The anatomical basis of cortico-striate connexions. *J Anat* 78: 47-51, 1944.

Golanov EV, Yamamoto S, and Reis DJ. Spontaneous waves of cerebral blood flow associated with a pattern of electrocortical activity. *Am J Physiol Regul Integr Comp Physiol* 266: R204-R214, 1994.

Goldman PS, and Nauta WJH. An intricately patterned prefronto-caudate projection in the rhesus monkey. *J Comp Neurol* 72: 369-386, 1977.

Goldman-Rakic PS. Topography of cognition: parallel distributed networks in primate association cortex. *Annu Rev Neurosci* 11: 137-156, 1988.

Graveland GA, Williams RS, and DiFiglia M. Evidence for degenerative and regenerative changes in neostriatal spiny neurons in Huntington's disease. *Science* 227: 770-773, 1985.

Graybiel AM. Neurotransmitters and neuromodulators in the basal ganglia. *Trends Neurosci* 13: 244-254, 1990.

Graybiel AM, and Ragsdale CW, Jr. Histochemically distinct compartments in the striatum of human, monkeys, and cat demonstrated by acetylthiocholinesterase staining. *Proc Natl Acad Sci USA* 75: 5723-5726, 1978.

Grefkes C, Geyer S, Schormann T, Roland P, and Zilles K. Human somatosensory area 2: observer-independent cytoarchitectonic mapping, interindividual variability, and population map. *Neuroimage* 14: 617-631, 2001.

Greicius MD, Krasnow B, Reiss AL, and Menon V. Functional connectivity in the resting brain: a network analysis of the default mode hypothesis. *Proc Natl Acad Sci USA* 100: 253-258, 2003.

Greve DN, and Fischl B. Accurate and robust brain image alignment using boundary-based registration. *Neuroimage* 48: 63-72, 2009.

Haber SN. The primate basal ganglia: parallel and integrative networks. *J Chem Neuroanat* 26: 317-330, 2003.

Haber SN, Adler A, and Bergman H. The Basal Ganglia. In: *The Human Nervous System, Third Edition*, edited by Mai JK, and Paxinos G. Amsterdam: Elsevier Academic, 2011.

Haber SN, Fudge JL, and McFarland NR. Striatonigrostriatal pathways in primates form an ascending spiral from the shell to the dorsolateral striatum. *J Neurosci* 20: 2369-2382, 2000.

Haber SN, and Gdowski MJ. The Basal Ganglia. In: *The Human Nervous System, Second Edition*, edited by Paxinos G, and Mai JK. Amsterdam: Elsevier Academic, 2004.

Haber SN, Kim KS, Mailly P, and Calzavara R. Reward-related cortical inputs define a large striatal region in primates that interface with associative cortical connections, providing a substrate for incentive-based learning. *J Neurosci* 26: 8368-8376, 2006.

Haber SN, Lynd E, Klein C, and Groenewegen HJ. Topographic organization of the ventral striatal efferent projections in the rhesus monkey: an anterograde tracing study. *J Comp Neurol* 293: 282-298, 1990.

Haber SN, Lynd-Balta E, and Spooren WP. Integrative aspects of basal ganglia circuitry. In: *Basal Ganglia IV*, edited by Percheron G, McKenzie JS, and Féger J. New York: Plenum, 1994.

Harrison BJ, Pujol J, Ortiz H, Fornito A, Pantelis C, and Yucel M. Modulation of brain resting-state networks by sad mood induction. *PLoS One* 3: e1794, 2008.

Harrison BJ, Soriano-Mas C, Pujol J, Ortiz H, Lopez-Sola M, Hernandez-Ribas R, Deus J, Alonso P, Yucel M, Pantelis C, Menchon JM, and Cardoner N. Altered corticostriatal functional connectivity in obsessive-compulsive disorder. *Arch Gen Psychiatry* 66: 1189-1200, 2009.

Heimer L. The olfactory cortex and the ventral striatum. In: *Limbic Mechanisms: The Continuing Evolution of the Limbic System Concept*, edited by Livingston K, and Hornykiewicz O. New York: Plenum, 1978.

Heimer L, and Wilson R. The subcortical projections of the allocortex: similarities in the neural associations of the hippocampus, the piriform cortex, and the neocortex. In: *Golgi Centennial Symposium*, edited by Santini M. Raven Press, 1975.

Hill J, Inder T, Neil J, Dierker D, Harwell J, and Van Essen DC. Similar patterns of cortical expansion during human development and evolution. *Proc Natl Acad Sci USA* 107: 13135-13140, 2010.

Holt DJ, Graybiel AM, and Saper CB. Neurochemical architecture of the human striatum. *J Comp Neurol* 384: 1-25, 1997.

Hoshi E, Tremblay L, Féger J, Carras PL, and Strick PL. The cerebellum communicates with the basal ganglia. *Nat Neurosci* 8: 1491-1493, 2005.

Inase M, Sakai ST, and Tanji J. Overlapping corticostriatal projections from the supplementary motor area and the primary motor cortex in the macaque monkey: an anterograde double labeling study. *J Comp Neurol* 373: 283-296, 1996.

Inase M, Tokuno H, Nambu A, Akazawa T, and Takada M. Corticostriatal and corticosubthalamic input zones from the presupplementary motor area in the macaque monkey: comparison with the input zones from the supplementary motor area. *Brain Res* 833: 191-201, 1999.

Jenkinson M, Bannister P, Brady M, and Smith S. Improved optimization for the robust and accurate linear registration and motion correction of brain images. *Neuroimage* 17: 825-841, 2002.

Johnson TN, Rosvold HE, and Mishkin M. Projections from behaviorally-defined sectors of the prefrontal cortex to the basal ganglia, septum, and diencephalon of the monkey. *Exp Neurol* 21: 20-34, 1968.

Johnston JM, Vaishnavi SN, Smyth MD, Zhang D, He BJ, Zempel JM, Shimony JS, Snyder AZ, and Raichle ME. Loss of resting interhemispheric functional connectivity after complete section of the corpus callosum. *J Neurosci* 28: 6453-6458, 2008.

Jones DK. Studying connections in the living human brain with diffusion MRI. *Cortex* 44: 936-952, 2008.

Jones EG, and Powell TPS. An anatomical study of converging sensory pathways within the

cerebral cortex of the monkey. *Brain* 93: 793-820, 1970.

Jubault T, Ody C, and Koechlin E. Serial organization of human behavior in the inferior parietal cortex. *J Neurosci* 27: 11028-11036, 2007.

Kaas JH. Evolution of the neocortex. *Curr Biol* 16: R910-R914, 2006.

Kelly C, de Zubicaray G, Di Martino A, Copland DA, Reiss PT, Klein DF, Castellanos FX, Milham MP, and McMahon K. L-dopa modulates functional connectivity in striatal cognitive and motor networks: a double-blind placebo-controlled study. *J Neurosci* 29: 7364-7378, 2009.

Kelly RM, and Strick PL. Cerebellar loops with motor cortex and prefrontal cortex of a nonhuman primate. *J Neurosci* 23: 8432-8444, 2003.

Kelly RM, and Strick PL. Macro-architecture of basal ganglia loops with the cerebral cortex: use of rabies virus to reveal multisynaptic circuits. *Prog Brain Res* 143: 449-459, 2004.

Kemp JM, and Powell TPS. The cortico-striate projection in the monkey. *Brain* 93: 525-546, 1970.

Kemp JM, and Powell TPS. The connexions of the striatum and globus pallidus: synthesis and speculation. *Philos Trans R Soc Lond B Biol Sci* 262: 441-457, 1971.

Kim R, Nakano K, Jayaraman A, and Carpenter MB. Projections of the globus pallidus and adjacent structures: an autoradiographic study in the monkey. *J Comp Neurol* 169: 263-290, 1976.

Koechlin E, and Jubault T. Broca's area and the hierarchical organization of human behavior. *Neuron* 50: 963-974, 2006.

Koechlin E, Ody C, and Kouneiher F. The architecture of cognitive control in the human prefrontal cortex. *Science* 302: 1181-1185, 2003.

Kouneiher F, Charron S, and Koechlin E. Motivation and cognitive control in the human

prefrontal cortex. *Nat Neurosci* 12: 939-945, 2009.

Krienen FM, and Buckner RL. Segregated fronto-cerebellar circuits revealed by intrinsic functional connectivity. *Cereb Cortex* 19: 2485-2497, 2009.

Künzle H. Bilateral projections from precentral motor cortex to the putamen and other parts of the basal ganglia. An autoradiographic study in Macaca fascicularis. *Brain Res* 88: 195-209, 1975.

Künzle H. Projections from the primary somatosensory cortex to basal ganglia and thalamus in the monkey. *Exp Brain Res* 30: 481-492, 1977.

Künzle H, Akert K. Efferent connections of cortical, area 8 (frontal eye field) in Macaca fascicularis. A reinvestigation using the autoradiographic technique. *J Comp Neurol* 173: 147-164, 1977.

Kwong KK, Belliveau JW, Chesler DA, Goldberg IE, Weisskoff RM, Poncelet BP, Kennedy DN, Hoppel BE, Cohen MS, Turner R, Cheng HM, Brady TJ, and Rosen BR. Dynamic magnetic resonance imaging of human brain activity during primary sensory stimulation. *Proc Natl Acad Sci USA* 89: 5675-5679, 1992.

Lancaster JL, Tordesillas-Gutierrez D, Martinez M, Salinas F, Evans A, Zilles K, Mazziotta JC, and Fox P. Bias between MNI and Talairach coordinates analyzed using the ICBM-152 brain template. *Hum Brain Mapp* 28: 1194-1205, 2007.

Larson-Prior LJ, Power JD, Vincent JL, Nolan TS, Coalson RS, Zempel J, Snyder AZ, Schlaggar BL, Raichle ME, and Petersen SE. Modulation of the brain's functional network architecture in the transition from wake to sleep. *Prog Brain Res* 193: 277-294, 2011.

Lauterbur PC. Image formation by induced local interactions - examples employing nuclear magnetic-resonance. *Nature* 242: 190-191, 1973.

Le Bihan D, and Breton E. Imagerie de diffusion in vivo par resonance magnetique nucleaire.

Compte Rendus de l'Academie de Sciences Paris 301: 1109-1112, 1985.

Lee MH, Hacker CD, Snyder AZ, Corbetta M, Zhang D, Leuthardt EC, and Shimony JS. Clustering of resting state networks. *PLoS One* 7: e40370, 2012.

Leh SE, Ptito A, Chakravarty MM, and Strafella AP. Fronto-striatal connections in the human brain: a probabilistic diffusion tractography study. *Neurosci Lett* 419: 113-118, 2007.

Lehéricy S, Ducros M, Van de Moortele P-F, Francois C, Thivard L, Poupon C, Swindale N, Ugurbil K, and Kim DS. Diffusion tensor fiber tracking shows distinct corticostriatal circuits in humans. *Ann Neurol* 55: 522-529, 2004.

Liles SL, and Updyke BV. Projection of the digit and wrist area of precentral gyrus to the putamen: relation between topography and physiological properties of neurons in the putamen. *Brain Res* 339: 245-255, 1985.

Lu J, Liu H, Zhang M, Wang D, Cao Y, Ma Q, Rong D, Wang X, Buckner RL, and Li K. Focal pontine lesions provide evidence that intrinsic functional connectivity reflects polysynaptic anatomical pathways. *J Neurosci* 31: 15065-15071, 2011.

MacLean PD. Cerebral evolution and emotional processes: new findings on the striatal complex. *Ann N Y Acad Sci* 193: 137-149, 1972.

Marcus DS, Fotenos AF, Csernansky JG, Morris JC, and Buckner RL. Open access series of imaging studies: longitudinal MRI data in nondemented and demented older adults. *J Cogn Neurosci* 22: 2677-2684, 2010.

Marcus DS, Wang TH, Parker J, Csernansky JG, Morris JC, and Buckner RL. Open Access Series of Imaging Studies (OASIS): cross-sectional MRI data in young, middle aged, nondemented, and demented older adults. *J Cogn Neurosci* 19: 1498-1507, 2007.

Marrakchi-Kacem L, Delmaire C, Guevara P, Poupon F, Lecomte S, Tucholka A, Roca P,

Yelnik J, Durr A, Mangin JF, Lehéricy S, and Poupon C. Mapping cortico-striatal connectivity onto the cortical surface: a new tractography-based approach to study Huntington disease. *PLoS One* 8: e53135, 2013.

Maunsell JHR, Van Essen DC. The connections of the middle temporal visual area (MT) and their relationship to a cortical hierarchy in the macaque monkey. *J Neurosci* 3: 2563-2586, 1983.

McFarland NR, and Haber SN. Thalamic relay nuclei of the basal ganglia form both reciprocal and nonreciprocal cortical connections, linking multiple frontal cortical areas. *J Neurosci* 22: 8117-8132, 2002.

McGeorge AJ, and Faull RL. The organization of the projection from the cerebral cortex to the striatum in the rat. *Neuroscience* 29: 503-537, 1989.

Mendez MF, Adams NL, and Lewandowski KS. Neurobehavioral changes associated with caudate lesions. *Neurology* 39: 349-354, 1989.

Merboldt KD, Hanicke W, and Frahm J. Self-diffusion NMR imaging using stimulated echoes. *J Magn Reson* 64: 479-486, 1985.

Mesulam MM. Frontal cortex and behavior. *Ann Neurol* 19: 320-325, 1986.

Mesulam MM. From sensation to cognition. *Brain* 121 (Pt 6): 1013-1052, 1998.

Mesulam MM, Van Hoesen GW, Pandya DN, and Geschwind N. Limbic and sensory connections of the inferior parietal lobule (area PG) in the rhesus monkey: a study with a new method for horseradish peroxidase histochemistry. *Brain Res* 136: 393-414, 1977.

Middleton FA, and Strick PL. Anatomical evidence for cerebellar and basal ganglia involvement in higher cognitive function. *Science* 266: 458-461, 1994.

Middleton FA, and Strick PL. Basal ganglia output and cognition: evidence from anatomical, behavioral, and clinical studies. *Brain and Cognition* 42: 183-200, 2000.

Middleton FA, and Strick PL. Basal-ganglia 'projections' to the prefrontal cortex of the primate. *Cereb Cortex* 12: 926-935, 2002.

Milner B. Effects of different brain lesions on card sorting. *Arch Neurol* 9: 100-110, 1963.

Mink JW. The basal ganglia: focused selection and inhibition of competing motor programs. *Prog Neurobiol* 50: 381-425, 1996.

Moseley ME, Cohen Y, Kucharczyk J, Mintorovitch J, Asgari HS, Wendland MF, Tsuruda J, and Norman D. Diffusion-weighted MR imaging of anisotropic water diffusion in cat central nervous system. *Radiology* 176: 439-445, 1990.

Mueller S, Wang D, Fox MD, Yeo BTT, Sepulcre J, Sabuncu MR, Shafee R, Lu J, and Liu H. Individual variability in functional connectivity architecture of the human brain. *Neuron* 77: 586-595, 2013.

Nauta WJH, and Mehler WR. Projections of the lentiform nucleus in the monkey. *Brain Res* 1: 3-42, 1966.

Nauta WJH, and Whitlock DG. Subcortical projections from the temporal neocortex in Macaca mulatta. *J Comp Neurol* 106: 183-212, 1956.

Ochsner KN, Silvers JA, and Buhle JT. Functional imaging studies of emotion regulation: a synthetic review and evolving model of the cognitive control of emotion. *Ann N Y Acad Sci* 1251: E1-24, 2012.

Ogawa S, Lee TM, Kay AR, and Tank DW. Brain magnetic resonance imaging with contrast dependent on blood oxygenation. *Proc Natl Acad Sci USA* 87: 9868-9872, 1990a.

Ogawa S, Lee TM, Nayak AS, and Glynn P. Oxygenation-sensitive contrast in magnetic resonance image of rodent brain at high magnetic fields. *Magn Reson Med* 14: 68-78, 1990b.

Ogawa S, Menon RS, Tank DW, Kim SG, Merkle H, Ellermann JM, and Ugurbil K.

Functional brain mapping by blood oxygenation level-dependent contrast magnetic resonance imaging. A comparison of signal characteristics with a biophysical model. *Biophys J* 64: 803-812, 1993.

Ogawa S, Tank DW, Menon R, Ellermann JM, Kim SG, Merkle H, and Ugurbil K. Intrinsic signal changes accompanying sensory stimulation: functional brain mapping with magnetic resonance imaging. *Proc Natl Acad Sci USA* 89: 5951-5955, 1992.

Öngür D, Ferry AT, and Price JL. Architectonic subdivision of the human orbital and medial prefrontal cortex. *J Comp Neurol* 460: 425-449, 2003.

Pandya DN, and Yeterian EH. Architecture and connections of cortical association areas. In: *Cerebral Cortex, Vol 4*, edited by Peters A, and Jones E. New York: Plenum Press, 1985.

Parent A. Extrinsic connections of the basal ganglia. *Trends Neurosci* 13: 254-258, 1990.

Parent A, and Hazrati LN. Functional anatomy of the basal ganglia. I. The cortico-basal ganglia-thalamo-cortical loop. *Brain Res Rev* 20: 91-127, 1995.

Parthasarathy HB, Schall JD, and Graybiel AM. Distributed but convergent ordering of corticostriatal projections: analysis of the frontal eye field and the supplementary eye field in the macaque monkey. *J Neurosci* 12: 4468-4488, 1992.

Pauling L, and Coryell CD. The magnetic properties and structure of hemoglobin, oxyhemoglobin and carbonmonoxyhemoglobin. *Proc Natl Acad Sci USA* 22: 210-216, 1936.

Penney JB, Jr., and Young AB. Speculations on the functional anatomy of basal ganglia disorders. *Annu Rev Neurosci* 6: 73-94, 1983.

Petersen SE, and Posner MI. The attention system of the human brain: 20 years after. *Annu Rev Neurosci* 35: 73-89, 2012.

Petrides M, and Pandya DN. Dorsolateral prefrontal cortex: comparative cytoarchitectonic

analysis in the human and the macaque brain and corticocortical connection patterns. *Eur J Neurosci* 11: 1011-1036, 1999.

Picard N, and Strick PL. Motor areas of the medial wall: a review of their location and functional activation. *Cereb Cortex* 6: 342-353, 1996.

Posner MI, and Petersen SE. The attention system of the human brain. *Annu Rev Neurosci* 13: 25-42, 1990.

Postuma RB, and Dagher A. Basal ganglia functional connectivity based on a meta-analysis of 126 positron emission tomography and functional magnetic resonance imaging publications. *Cereb Cortex* 16: 1508-1521, 2006.

Powell EW. The cingulate bridge between allocortex, isocortex and thalamus. *Anat Rec* 190: 783-793, 1978.

Power JD, Cohen AL, Nelson SM, Wig GS, Barnes KA, Church JA, Vogel AC, Laumann TO, Miezin FM, Schlaggar BL, and Petersen SE. Functional network organization of the human brain. *Neuron* 72: 665-678, 2011.

Power JD, Fair DA, Schlaggar BL, and Petersen SE. The development of human functional brain networks. *Neuron* 67: 735-748, 2010.

Ragsdale CW, Jr., and Graybiel AM. A simple ordering of neocortical areas established by the compartmental organization of their striatal projections. *Proc Natl Acad Sci USA* 87: 6196-6199, 1990.

Raskin SA, Borod JC, and Tweedy J. Neuropsychological aspects of Parkinson's disease. *Neuropsychol Rev* 1: 185-221, 1990.

Rosell A, and Gimenez-Amaya JM. Anatomical re-evaluation of the corticostriatal projections to the caudate nucleus: a retrograde labeling study in the cat. *Neurosci Res* 34: 257-269, 1999.

Roy AK, Shehzad Z, Margulies DS, Kelly AMC, Uddin LQ, Gotimer K, Biswal BB, Castellanos FX, and Milham MP. Functional connectivity of the human amygdala using resting state fMRI. *Neuroimage* 45: 614-626, 2009.

Russchen FT, Bakst I, Amaral DG, and Price JL. The amygdalostriatal projections in the monkey. An anterograde tracing study. *Brain Res* 329: 241-257, 1985.

Saint-Cyr JA, Ungerleider LG, and Desimone R. Organization of visual cortical inputs to the striatum and subsequent outputs to the pallido-nigral complex in the monkey. *J Comp Neurol* 298: 129-156, 1990.

Ségonne F, Dale AM, Busa E, Glessner M, Salat D, Hahn HK, and Fischl B. A hybrid approach to the skull stripping problem in MRI. *Neuroimage* 22: 1060-1075, 2004.

Ségonne F, Pacheco J, and Fischl B. Geometrically accurate topology-correction of cortical surfaces using nonseparating loops. *IEEE Trans Med Imaging* 26: 518-529, 2007.

Selemon LD, and Goldman-Rakic PS. Longitudinal topography and interdigitation of corticostriatal projections in the rhesus monkey. *J Neurosci* 5: 776-794, 1985.

Selemon LD, and Goldman-Rakic PS. Common cortical and subcortical targets of the dorsolateral prefrontal and posterior parietal cortices in the rhesus monkey: evidence for a distributed neural network subserving spatially guided behavior. *J Neurosci* 8: 4049-4068, 1988.

Shirer WR, Ryali S, Rykhlevskaia E, Menon V, and Greicius MD. Decoding subject-driven cognitive states with whole-brain connectivity patterns. *Cereb Cortex* 22: 158-165, 2012.

Smith SM, Jenkinson M, Woolrich M, Beckmann C, Behrens T, Johansen-Berg H, Bannister P, De Luca M, Drobnjak I, and Flitney D. Advances in functional and structural MR image analysis and implementation as FSL. *Neuroimage* 23: S208-S219, 2004.

Stanton GB, Goldberg ME, and Bruce CJ. Frontal eye field efferents in the macaque monkey:

I. Subcortical pathways and topography of striatal and thalamic terminal fields. *J Comp Neurol* 271: 473-492, 1988.

Stejskal EO, and Tanner JE. Spin diffusion measurements: spin echoes in the presence of a time-dependent field gradient. *J Chem Phys* 42: 288-292, 1965.

Stevens WD, Buckner RL, and Schacter DL. Correlated low-frequency BOLD fluctuations in the resting human brain are modulated by recent experience in category-preferential visual regions. *Cereb Cortex* 20: 1997-2006, 2010.

Strick PL, Dum RP, Mushiake H. Basal ganglia 'loops' with the cerebral cortex. In: *Functions of the Cortico-Basal Ganglia Loop*, edited by Graybiel AM, Kimura M. Tokyo: Springer-Verlag, 1995.

Szabo J. Topical distribution of the striatal efferents in the monkey. *Exp Neurol* 5: 21-36, 1962.

Szabo J. The efferent projections of the putamen in the monkey. *Exp Neurol* 19: 463-476, 1967.

Szabo J. Projections from the body of the caudate nucleus in the rhesus monkey. *Exp Neurol* 27: 1-15, 1970.

Takada M, Tokuno H, Hamada I, Inase M, Ito Y, Imanishi M, Hasegawa N, Akazawa T, Hatanaka N, and Nambu A. Organization of inputs from cingulate motor areas to basal ganglia in macaque monkey. *Eur J Neurosci* 14: 1633-1650, 2001.

Takada M, Tokuno H, Nambu A, and Inase M. Corticostriatal input zones from the supplementary motor area overlap those from the contra- rather than ipsilateral primary motor cortex. *Brain Res* 791: 335-340, 1998a.

Takada M, Tokuno H, Nambu A, and Inase M. Corticostriatal projections from the somatic motor areas of the frontal cortex in the macaque monkey: segregation versus overlap of input zones from the primary motor cortex, the supplementary motor area, and the premotor cortex. *Exp Brain Res* 120: 114-128, 1998b.

Talairach J, and Tournoux P. *Co-planar Stereotaxic Atlas of the Human Brain: 3-Dimensional Proportional System: an Approach to Cerebral Imaging*. New York: Thieme Medical Publishers, 1988.

Taren AA, Venkatraman V, and Huettel SA. A parallel functional topography between medial and lateral prefrontal cortex: evidence and implications for cognitive control. *J Neurosci* 31: 5026-5031, 2011.

Taylor DG, and Bushell MC. The spatial-mapping of translational diffusion-coefficients by the NMR imaging technique. *Phys Med Biol* 30: 345-349, 1985.

Tu PC, Hsieh JC, Li CT, Bai YM, and Su TP. Cortico-striatal disconnection within the cingulo-opercular network in schizophrenia revealed by intrinsic functional connectivity analysis: a resting fMRI study. *Neuroimage* 59: 238-247, 2012.

Tziortzi AC, Haber SN, Searle GE, Tsoumpas C, Long CJ, Shotbolt P, Douaud G, Jbabdi S, Behrens TE, Rabiner EA, Jenkinson M, and Gunn RN. Connectivity-based functional analysis of dopamine release in the striatum using diffusion-weighted MRI and positron emission tomography. *Cereb Cortex* 2013.

Ungerleider LG, Desimone R, Galkin TW, Mishkin M. Subcortical projections of area MT in the macaque. *J Comp Neurol* 223: 368-386, 1984.

van der Kouwe AJW, Benner T, Fischl B, Schmitt F, Salat DH, Harder M, Sorensen AG, and Dale AM. On-line automatic slice positioning for brain MR imaging. *Neuroimage* 27: 222-230, 2005.

van der Kouwe AJW, Benner T, Salat DH, and Fischl B. Brain morphometry with multiecho MPRAGE. *Neuroimage* 40: 559-569, 2008.

Van Dijk KRA, Sabuncu M, and Buckner R. The influence of head motion on intrinsic

functional connectivity MRI. *Neuroimage* 59: 431-438, 2012.

Van Dijk KRA, Hedden T, Venkataraman A, Evans KC, Lazar SW, and Buckner RL. Intrinsic functional connectivity as a tool for human connectomics: theory, properties, and optimization. *J Neurophysiol* 103: 297-321, 2010.

Van Essen DC. A Population-Average, Landmark-and Surface-based (PALS) atlas of human cerebral cortex. *Neuroimage* 28: 635-662, 2005.

Van Essen DC, and Dierker DL. Surface-based and probabilistic atlases of primate cerebral cortex. *Neuron* 56: 209-225, 2007.

Van Hoesen GW, Yeterian EH, and Lavizzo-Mourey R. Widespread corticostriate projections from temporal cortex of the rhesus monkey. *J Comp Neurol* 199: 205-219, 1981.

Venkatraman V, Rosati AG, Taren AA, and Huettel SA. Resolving response, decision, and strategic control: evidence for a functional topography in dorsomedial prefrontal cortex. *J Neurosci* 29: 13158-13164, 2009.

Verstynen TD, Badre D, Jarbo K, and Schneider W. Microstructural organizational patterns in the human corticostriatal system. *J Neurophysiol* 107: 2984-2995, 2012.

Vincent JL, Kahn I, Snyder AZ, Raichle ME, and Buckner RL. Evidence for a frontoparietal control system revealed by intrinsic functional connectivity. *J Neurophysiol* 100: 3328-3342, 2008.

Vincent JL, Patel GH, Fox MD, Snyder AZ, Baker JT, Van Essen DC, Zempel JM, Snyder LH, Corbetta M, and Raichle ME. Intrinsic functional architecture in the anaesthetized monkey brain. *Nature* 447: 83-86, 2007.

Vincent JL, Snyder AZ, Fox MD, Shannon BJ, Andrews JR, Raichle ME, and Buckner RL. Coherent spontaneous activity identifies a hippocampal-parietal memory network. *J*

Neurophysiol 96: 3517-3531, 2006.

Voorn P, Vanderschuren LJ, Groenewegen HJ, Robbins TW, and Pennartz CM. Putting a spin on the dorsal-ventral divide of the striatum. *Trends Neurosci* 27: 468-474, 2004.

Weber JT, and Yin TC. Subcortical projections of the inferior parietal cortex (area 7) in the stump-tailed monkey. *J Comp Neurol* 224: 206-230, 1984.

Webster KE. Cortico-striate interrelations in the albino rat. *J Anat* 95: 532-544, 1961.

Webster KE. The cortico-striatal projection in the cat. *J Anat* 99: 329-337, 1965.

Webster MJ, Bachevalier J, and Ungerleider LG. Subcortical connections of inferior temporal areas TE and TEO in macaque monkeys. *J Comp Neurol* 335: 73-91, 1993.

Wilson SAK. Progressive lenticular degeneration. *Brain* 34: 295-509, 1912.

Wilson SAK. An experimental research into the anatomy and physiology of the corpus striatum. *Brain* 36: 427-492, 1914.

Yeo BTT, Krienen FM, Sepulcre J, Sabuncu MR, Lashkari D, Hollinshead M, Roffman JL, Smoller JW, Zollei L, Polimeni JR, Fischl B, Liu H, and Buckner RL. The organization of the human cerebral cortex estimated by intrinsic functional connectivity. *J Neurophysiol* 106: 1125-1165, 2011.

Yeterian EH, and Pandya DN. Prefrontostriatal connections in relation to cortical architectonic organization in rhesus monkeys. *J Comp Neurol* 312: 43-67, 1991.

Yeterian EH, and Pandya DN. Striatal connections of the parietal association cortices in rhesus monkeys. *J Comp Neurol* 332: 175-197, 1993.

Yeterian EH, and Pandya DN. Corticostriatal connections of the superior temporal region in rhesus monkeys. *J Comp Neurol* 399: 384-402, 1998.

Yeterian EH, Pandya DN, Tomaiuolo F, and Petrides M. The cortical connectivity of the

prefrontal cortex in the monkey brain. *Cortex* 48: 58-81, 2012.

Yeterian EH, and Van Hoesen GW. Cortico-striate projections in the rhesus monkey: the organization of certain cortico-caudate connections. *Brain Res* 139: 43-63, 1978.

Ystad M, Hodneland E, Adolfsdottir S, Haasz J, Lundervold AJ, Eichele T, and Lundervold A. Cortico-striatal connectivity and cognition in normal aging: a combined DTI and resting state fMRI study. *Neuroimage* 55: 24-31, 2011.

Zhang D, Snyder AZ, Fox MD, Sansbury MW, Shimony JS, and Raichle ME. Intrinsic functional relations between human cerebral cortex and thalamus. *J Neurophysiol* 100: 1740-1748, 2008.